SYNTHESIS AND CHARACTERIZATION OF DRUG LOADED ALBUMIN MESOSPHERES FOR INTRATUMORAL CHEMOTHERAPY

By

SHEMA TAIAN FREEMAN

A DISSERTATION PRESENTED TO THE GRADUATE SCHOOL
OF THE UNIVERSITY OF FLORIDA IN PARTIAL FULFILLMENT
OF THE REQUIREMENTS FOR THE DEGREE OF
DOCTOR OF PHILOSOPHY

UNIVERSITY OF FLORIDA

2008

To my parents, Kenneth and Vanessa Ashley for their unwavering, unconditional love and support throughout my academic career

ACKNOWLEDGMENTS

I would like to thank my advisor and committee chairman Dr. Eugene P. Goldberg, for his knowledge, support, and incredible patience. I would also like to thank my committee cochair, Dr. Anthony Brennan for his support and mentorship. His words of advice and encouragement were invaluable. I would also like to thank my committee members: Dr. Christopher Batich, Dr. Amelia Dempere, and Dr. Wolfgang Streit. I would also like to thank Drs. Amelia Dempere and Jean Andino for being great role models for minority women in engineering. A special thank you is extend to Dr. Jonathan F.K. Earle for seeing potential in me and for cultivating a dream I never knew I had. From my undergraduate studies through my graduate studies he guided my career and was my spiritual rock.

I wish to acknowledge the following colleagues: Dr. Ahmad Hadba, Dr. Brian Ceuvas, and Dr. Joshua Stopek for setting a great example; Dr. Brett Almond for taking me under his wing and for countless hours of entertainment down the hill in Animal Care Services; Dr. Leslie Wilson for help in the lab and for attempting to make me a chemist; Dr. Michelle Carman and Paul Martin for their knowledge and advice in my cell culture studies; Dr. Iris V. Enriquez Schumacher for her advice, friendship, love, support, and infectious laughter.

Special appreciation is extended to my colleagues for their assistance and entertainment both in and out of the lab. These colleagues include but are not limited to Samesha Barnes, Amin Elachabi, Lynn Peck, Jim Schumacher, Cliff Wilson, Jim Seliga, and Ken Chung.

Finally, I would like to thank my family and friends too numerous to name for their love and support throughout my years here at the University of Florida. Special thanks go to my parents, Ken and Vanessa Ashley for their unconditional love and for always keeping grounded.

TABLE OF CONTENTS

page

LIST OF TABLES

LIST OF FIGURES

LIST OF ABBREVIATIONS

ACS	American Cancer Society
ACS	Animal Care Services
BSA	bovine serum albumin
CAB	cellulose acetate butyrate
CDDP	cisplatin
CTX	cyclophosphamide
DCE	1, 2 Dichloroethane
DMSO	dimethyl sulfoxide
EDTA	ethylenediame tetracetic acid
GEN	genipin
GTA	glutaraldehyde
HBV	hepatitis B virus
HIV	human immunodeficiency virus
HPV	human papillomavirus
IACUC	Institutional Animal Care and Use Committee
IT	intratumoral
LDH	lactate dehydrogenase
MS	mesosphere
MTD	maximum tolerated dose
NBP	4-(4-nitrobenzyl) pyridine
PBS	phosphate buffered saline
PERC	Particle Engineering Research Center
PSA	prostate specific antigen
PVP	poly vinyl pyrrolidone

SEM	scanning electron microscopy
TCA	trichloroacetic acid

Abstract of Dissertation Presented to the Graduate School
of the University of Florida in Partial Fulfillment of the
Requirements for the Degree of Doctor of Philosophy

SYNTHESIS AND CHARACTERIZATION OF DRUG LOADED ALBUMIN MESOSPHERES FOR INTRATUMORAL CHEMOTHERAPY

By

Shema Taian Freeman

May 2008

Chair: Eugene P. Goldberg
Cochair: Anthony Brennan
Major: Materials Science and Engineering

Conventional chemotherapy is problematic due to toxic complications. Intratumoral (IT) drug delivery, offers a new, less toxic, potentially more effective treatment concept.

The objectives of this research encompassed (1) an investigation of the synthesis of BSA mesospheres (MS) employing genipin (GEN) as a novel crosslinking agent, (2) comparison with glutaraldehyde (GTA) crosslinked mesosphere, (3) a study of process parameters to define conditions for the synthesis of 1-10μm drug loaded mesospheres, and (4) investigation of the drug delivery properties of such mesospheres for IT chemotherapy.

Smooth, spherical BSA-MS, crosslinked with glutaraldehyde and genipin, were prepared in a dry particle size range of 1μm to 10μm. It was shown that increasing dispersion stirring rate, crosslinking time and GEN/BSA ratio led to a decrease in particle size and a narrower particle distribution. It was also shown that increasing crosslinking time, GEN/BSA ratio, BSA concentrations, GEN concentration slowed enzymatic degradation.

Post-loading and *in situ* drug loading methods were studied for the incorporation of cyclophosphamide and cisplatin into mesospheres. Maximum post loading of cisplatin was 3.2% (w/w) and 2.6% (w/w) with GEN and with GTA crosslinking. For cyclophosphamide 8.2%

(w/w) and 7.1% (w/w) loading was achieved with GEN and GTA respectively. *In situ* drug loaded MS genipin and glutaraldehyde crosslinked mesospheres were also synthesized with 1.8% (w/w) cisplatin (using GEN) and 1.2% (w/w) (using GTA). Maximum loading of 13.3% (w/w) was achieved for cyclophosphamide in genipin crosslinked mesospheres.

The cytotoxicity of *in situ* loaded genipin and glutaraldehyde crosslinked cisplatin mesospheres was evaluated using a murine Lewis lung model. Both genipin and glutaraldehyde crosslinked BSA-cisplatin mesospheres proved to be cytotoxic during a 48 hour test.

Ultimately a standard set of processing parameters (BSA concentration, CAB concentration, GEN concentration, GEN/BSA ratio, stabilization stirring rate and crosslinking time) were defined to produce both GEN and GTA crosslinked cisplatin and cyclophosphamide BSA mesospheres. *In vitro* analysis confirmed the utility of mesosphere bound drug.

In several related studies, (1) IT delivered dispersions of mitoxantrone loaded albumin microspheres were shown to afford an effective treatment, with significantly prolonging animal survival and (2) genipin and gadolinium crosslinked MS were prepared from HA and BSA/HA.

CHAPTER 1
INTRODUCTION

Overview

Surgery followed by radiation or chemotherapy have remained the standard of treatment for solid tumors (brain, breast, lung and colorectal) from the early 1900s through the present. The effectiveness of radiation and chemotherapies are limited by systemic toxicities. Non systemic regional chemotherapy has been introduced as an alternative to systemic chemotherapy. A 2002 review compared conventional systemic therapies to non-systemic therapies and described the evolution of intratumoral chemotherapy.[1] Nano and microsphere drug delivery systems have been studied since the 1960s. Nanoparticles where first developed for vaccines and anticancer drugs. Nanoparticles are easily taken up by the vascular system which inhibits tumor uptake and sustainability. Larger size microspheres (50nm-2mm) have been developed that are less likely to move through the vascular system.[2]

The objective of the research presented here was to build on the work of Drs. Hadba,[3] Almond[4] and Cuevas[5]. Hadba found that glutaraldehyde crosslinked albumin microspheres particle size range 4μm to 40μm could be synthesized using suspension crosslinking. Furthermore it was reported that mean particle size was affected by varying processing parameters. Almond found microspheres of 5μm to 10μm released drug faster and to a greater extent than microspheres of 20μm to 40μm in size. In pre-clinical animal studies produced a distinction in the effectiveness of intratumoral treatment due to particle size where the smaller size range of microspheres resulted in a higher percentage survival for a longer length of time. Cuevas found that genipin crosslinked gelatin microspheres particle size range 0.04μm to 20μm. These microspheres were found to be an inefficient method of intratumoral delivery during pre-clinical animal studies because the severe swelling of particles in medium clogged the injection

needle making consistent dosing difficult. Swelling to such great degree was not seen with glutaraldehyde crosslinked microspheres. The goal of the research reported here was to develop a standard set of processing parameters that would produce particles in the most effective mesosphere size range that would swell minimally and deliver a high volume of drug bridging all of the best aspects of the previous work.

Summary of Specific Aims

The overall purpose of this research was to investigate the feasibility and optimization of the preparation of drug loaded glutaraldehyde and genipin crosslinked bovine serum albumin mesospheres as an intratumoral drug delivery device. The specific aims where as follows:

Aim I: Synthesized and characterized Genipin Crosslinked Bovine Serum Albumin (BSA) Mesospheres

Using suspension dispersion crosslinking bovine serum albumin mesospheres were synthesized where cellulose acetate butyrate was the dispersion agent and genipin was the crosslinking agent. Particle size was used as the numeric outcome to determine how varying processing conditions (protein concentration, dispersion agent concentration, crosslinker, protein/crosslinker ratio, dispersion stirring speed and crosslinking time) affected particle size and particle size distribution. Successful formulations were in the particle size range of 1μm-10μm, where at least 50% of particles are larger than 1μm and 90% of particles are smaller than 10μm. Morphology was evaluated using scanning electron microscopy.

Aim II: Evaluated Degradation Kinetics of Genipin Crosslinked BSA Mesospheres

Swollen ratio (a comparison of dry to wet mesosphere particle size) data for mesospheres synthesized in Aim I was used as a predictor of rate of mesosphere degradation. Low swollen ratios indicated a highly crosslinked matrix and slower degradation rate. Mesospheres were subjected to enzymatic degradation using a protease buffer. Solublized protein concentrations

were quantified using colorimetric BioRad protein assay. Degradation was reported as percent unsolublized protein remaining versus time. Crosslinking time and crosslink density proved to have the greatest affect on mesosphere degradation. Longer crosslinking times and higher crosslink densities provided slower degradation than did shorter crosslinking periods and lower crosslink densities.

Aim III: Synthesized and Characterized Drug Loaded Genipin (GEN) and Glutaraldehyde (GTA) Crosslinked BSA Mesospheres

Genipin and glutaraldehyde crosslinked mesospheres will be synthesized using a standard set of processing parameters determined from the Aims I and II. These blank mesospheres were soaked in cisplatin or cyclophosphamide drug solution for 36 hours on a rotator. Particle size and morphology was evaluated using similar methods described in Aim I for non drug loaded mesospheres. Drug loading was quantified by depletion assay. These tools were used to evaluate the affects of varying drug solution concentrations on particle size, particle size distribution and drug loading. Post loading of drugs resulted in a multimodal particle size distribution and particle size range of 1μm to 200μm. Drug entrapment for mesospheres with cisplatin was at least 1%(w/w) and with cyclophosphamide was at least 10% (w/w). *In situ* loading of drugs resulted in normal particle size distribution and particle size range of 1μm-10μm. Drug entrapment for mesospheres with cisplatin was at least 5% (w/w) and with cyclophosphamide was at least 10% (w/w). Due to the unstable nature of cisplatin in aqueous solution higher drug loading could not be achieved.

Aim V: Evaluate *In Vitro* Drug Release Properties of Drug Loaded GEN and GTA Crosslinked BSA Mesospheres.

In situ drug loaded mesospheres synthesized in Aim IV. Using the minimal sink model mesospheres were incubated in an enzyme buffer at 37ºC and aliquots were taken at various time points and drug concentration will be quantified. Release curve profiles were presented as the

percentage of total drug loading released versus time. The most successful formulation of mesospheres resulted in 80% of total encapsulated cisplatin release over a 24 hour period.

Aim VI: Evaluate Cytotoxicity of Cisplatin Loaded GEN and GTA Crosslinked BSA Mesospheres

Cytotoxicity of in sit loaded genipin and glutaraldehyde crosslinked cisplatin mesospheres will be evaluated using Cyto Tox 96 colorimetric cytotoxicity assay, which measures the concentration lactate dehydrogenase (LDH) in solution. LDH a stable cytosolic enzyme is only released upon cell lysis so an increase in absorbance corresponds with a greater volume of dead cells. Murine Lewis lung cells will be grown in a 37ºC, 5% CO2 environment and exposed to various free drug and mesosphere treatments. Cell death were measured a predetermined time points that coincided with drug release profile created in Aim V and a % cytotoxicity versus time plot was created. Mesosphere bound drug preformed as well or better than equivalent free drug doses.

CHAPTER 2
BACKGROUND

Introduction

Cancer is the second leading cause of death in the United States. Although anyone can develop cancer the majority (76%) of diagnosed cases are individuals 55 years and older. In 2006 more than 1500 people a day are expected to have died from cancer, over half a million Americans or approximately 1 in 4 deaths. Development of cancer can result from external influences such as tobacco, radiation, and infectious organisms or from internal influences such as inherited genetic mutations, hormones and immune conditions.[6] Little innovation has advanced the treatment of cancer. Though effective conventional treatment methods: surgery, radiation and chemotherapy are not very efficient and are associated with serious side effects and dose limiting toxicities. Presented in this chapter is a discussion of cancer and its treatment, albumin microspheres, and pharmacological properties of cisplatin and cyclophosphamide.

Cancer Prevalence and Classification

The word “cancer” was first used by Hippocrates to describe a family of diseases where tissues grew and spread unrestrained throughout the body.

Many factors are attributed as possible causes of cancer. Some are external factors like tobacco use, chemical or radiation exposure or infectious organisms. Others are internal factors like inherited mutations, hormones immune conditions or mutations that occur from metabolism. All of these factors may act in tandem to initiate or promote carcinogenesis. Many years, ten or more, may pass between exposure to external factors and detectable cancer. The American Chemical Society (ACS) estimates that 170,000 cancer deaths in 2006 will be attributed to tobacco use while 188,000 will be attributed to nutrition, physical activity or obesity. Another significant portion of cancer deaths will be attributed to infectious agents such as hepatitis B

virus (HBV), human papillomavirus (HPV), human immunodeficiency virus (HIV) or helicobacter. When added together approximately 70% of cancer deaths can be prevented by lifestyle choices. Regular screening examinations result in early detection of breast, colorectal, cervical, prostate oral cavity and skin cancers. Everyone is at risk of developing cancer. In the United States men have slightly less than a 50% lifetime risk and women slightly more than a 33% lifetime risk of developing cancer.[6]

Cancers are categorized and staged by their primary location in the body and degree of spread to other locations. The broadest categorization of tumors is either benign or malignant. Benign tumors typically grow to a confined local area where as malignant tumors can invade surrounding tissues, enter the bloodstream and spread to various other body parts. The major difference between the two is that benign tumors are not usually life threatening while malignant tumors are most often life threatening. Benign and malignant tumors are further characterized as classified as 'well', 'moderately' or 'poorly' differentiated. Well differentiated tumors are typically less aggressive than poorly differentiated tumors and are referred to as low grade. Low grade tumors more closely resemble normal parent tissue than do high grade poorly differentiated tumors. Tumor grade is used as a prognostic indicator where low grade tumors are associated with longer survival.[7]

Table 2-1. Cancer types characterized by origination site

Cancer Type	Origination Site
Carcinoma	Arise from epithelial cells that form covering layers over external and internal body surfaces
Sarcoma	Arise in supporting tissues such as bone, cartilage, blood vessels, fat, fibrous tissue and muscle
Lymphoma	Arise in white blood cells and grow primarily as solid masses of tissue
Leukemia	Arise in the bloodstream

Cancer Types

Breast Cancer

Breast cancer is the most frequently diagnosed caner in women with approximately 212,920 estimated cases for 2006. Breast cancer incidence has increased greatly due to increased use of mammography. Approximately 1,720 cases of breast cancer are expected in men during 2006. Approximately 42,430 persons (40,970 women, 460 men) are expected to have died from breast cancer in 2006. Breast cancer death rates declined by an average of 2.3% per year from 1990 to 2002, with larger decreases in younger women (< 50 years). This decrease is mostly attributed to better detection modalities of mammography which can detect an abnormality before it can be felt. Large tumors become more evident as a breast lump, thickening, swelling, distortion, tenderness, skin irritation, dimpling, nipple pain, scaliness ulceration, retraction or spontaneous discharge.

Being female followed by age are the greatest risk factors affecting breast cancer risk. Risk is also increased by the inherited genetic mutations (BRCA1 and BRCA2), a family history and high breast tissue density. Other factors include reproductive factors including menstrual periods that start early and/or end late in life, never having children, recent use of oral contraceptive, and having the first child after the age of 30.

Surgery (lumpectomy or mastectomy) is the first course of treatment. Surgery is usually followed by radiation therapy, chemotherapy or hormone therapy. The exact staging of treatment will be dependent on tumor size, cancer stage and patient preference. The five year survival for localized breast cancer is 98%, for cancer that has spread to the lymph nodes is 81% and for cancer that has distant metastases is 26%.[6]

Colorectal Cancer

The third most commonly diagnosed cancer among both men and women is colorectal cancer. Approximately 106,680 cases of colon and 41,930 cases of rectal are expected to occur in 2006. The incidence rates has decreased by an average of 1.8% per year from 1998-2002. This decrease is primarily due to increased screening for polyps. Rectal bleeding, blood in stool, a change in bowel habits and cramping pains in the lower abdomen are all symptoms of advanced stages of colorectal cancer. Approximately 10% of all death deaths will be attributed to colorectal cancers.

The greatest risk of colorectal cancer is age. 90% of all diagnosed cases occur in older persons (> 50 years). Having the genetic mutations FAP and HNPCC or a family history of polyps will also increase risk of colorectal cancer. Surgery is the primary treatment modality. If the cancer has not spread then surgery is curative. Chemotherapy and radiation therapy also employed before and after surgery for those persons whose cancer has invaded the bowel wall or lymph nodes. When colorectal cancer is detected in the early stage the 5 year survival rate is 90%, however only approximately 39% of colorectal cancers are diagnosed at the early stage. The 5 year survival rate of patients whose cancer has spread to the lymph node is 68% and for those with distant metastases the 5 year survival rate drops to just 10%.[6]

Lung and Bronchial Cancer

Lung and bronchial cancer will account for approximately 12% of all diagnosed cancer cases. The incidence rate of lung cancer in men has continually decreased from 1984 to 2002 while the rate in women has remained steady since 1998 after many years of continual increase. Lung cancer is the most commonly diagnosed cancer for both men and women. Approximately 162,460 or 29% of all cancer deaths in 2006 are expected to be due to lung cancer. Though breast cancer is the most commonly diagnosed cancer in women more women die from lung

cancer. Common symptoms include persistent cough, sputum streaked with blood, chest pain, voice change and recurrent pneumonia or bronchitis.

Cigarette smoking and other tobacco uses are the greatest risk factors in developing lung cancer. Other factors include second smoke, occupation or environmental exposures to radon, asbestos, some heavy metals, some organic chemicals and radiation, air pollutions and tuberculosis. Thus far early detection efforts have not improved the mortality rate due to lung cancer. Chest x-ray, cell biopsy of sputum and fiber optic examination of bronchial passages showed limited effectiveness in improving survival rates. Effective early detection methods are limited by the risks of lung biopsy.

Treatment modalities are determined by whether the diagnosed cancer is classified as small or non small cell carcinoma. For localized cancers surgery is the primary treatment. Chemotherapy and radiation will follow for those patients whose cancer has spread. Small cell carcinoma can be treated with chemotherapy alone or in combination with radiation resulting in long lasting remission. Biological therapies like gefitinib are used in rare cases. The 1 year survival rate for lung cancer has increased from 37% in 1975 to 42% in 1999-2001, however the 5 year survival rate is only about 15%. A 50% survival rate can be achieved for those cancers detected when still localized but this accounts for only 16% of diagnosed lung cancers.[6]

Prostate

Prostate cancer is the most frequently diagnosed form of cancer for men. Approximately 234,460 cases are expected to be diagnosed in 2006. A higher rate of incidence occurs in African American men than in white men. The incidence rate of prostate cancer increased greatly from 1988 to 1992 then declined sharply from 1992 to 1995 and has increased modestly since 1995. The modest increase is a result of the use of prostate specific antigen (PSA) blood testing.

Prostate cancer is also the leading cause of cancer death in men however the death rate continues to decrease each year.

There are no symptoms of early prostate cancer. Men with more advanced stages of prostate caner may experience weak or interrupted urine flow, inability to urinate or difficulty starting or stopping the urine flow, the need to urinate frequently, blood in urine, or pain or burning during urination. Symptoms of metastatic disease include continual pain in the lower back, pelvis or upper thigh. The greatest risk factors affecting prostate cancer are age, ethnicity and a family history of the disease.

Early detection methods include PSA blood testing and digital rectal examination. Treatment of prostate cancer is patient specific and will depend on the patient's age and medical condition. Early stage disease can be treated with surgery and external beam radiation or brachytherapy. Hormone therapy, chemotherapy and radiation therapy are used to treat more advanced metastatic stages of prostate cancer. More than 90% of prostate cancers are diagnosed in the local or regional stages. The 5 year survival rate for prostate cancer is close to 100%. This improvement is attributed to earlier diagnosis and better treatment modalities.[6]

Cancer Treatment

The efficacy of cancer treatment (tumor regression) is dependent on tumor responsiveness and heterogeneity. Tumor responsiveness is related to cell proliferation or doubling time of the tumor. High proliferative cancer cells are more susceptible to the cytotoxic actions of anticancer drugs. Secondly proliferative index can be used as a prognostic indicator. High levels of proliferation typically indicate poorer survival. Tumors are collections of cell populations which may have different genetic stabilities with different susceptibilities to genetic mutations. These factors contribute lead to the development of cancer drug sensitivities. Effective treatments must be able to combat both problems of cell growth and drug resistance.[7, 8]

The cell cycle is the basis of tumor growth. Proliferating cells will travel through many functional states during replication. The cell first enters gap phase one (G_1) where normal cellular growth and accumulation of DNA synthesis metabolites occurs. This is considered the critical control point in cell development because cells either enter a proliferative quiescent state until cell cycle conditions are appropriate or a decycle phase state that leads to terminal differentiation and cell death. The cell then enters a synthetic phase and where its genetic material is doubled during DNA synthesis. A second gap phase (G_2), premitotic phase, during which validation of chromosomal duplication occurs. Finally the cell enters the mitosis phase (M). The entire cycle can take hours or days depending on the location and type of cancer cell. These individual cells will duplicate and grow into colonies of cells. Not all cells will be proliferating at the same time. Tumors will consist of static, proliferating and necrotic cells.[7]

Tumor growth was described by Skipper in "Laboratory models: the historical perspective." Skipper's first law states doubling time of tumor cells is independent of tumor size. However tumors contain both proliferating and non proliferating cells so Gompertzian growth better describes tumor growth. Initially growth is exponential where tumor volume every unit of time. Eventually the tumor will reach critical mass and a growth plateau. This is a result of a decreased ratio of the number of dividing cells to the total tumor volume. Skipper's second law states that cell death follows first order kinetics meaning that the total number of cells killed by a particular drug dose is independent of cell number. This second law helped establish the two primary principals of chemotherapy: the maximum tolerated dose (MTD) of a drug should be used to achieve the greatest tumor kill possible and multiples single dose treatments may be more effective than single treatments giving in increasing doses.[9]

There are three primary methods of treating cancer: surgery, radiation, and chemotherapy. Surgery is the oldest approach to curing cancer and can be used to treat almost every organ in the body. If you cancer is diagnosed before the tumor metastasizes surgical removal will generally cure the disease. However most cancers have already spread before they are diagnosed so surgical treatment is followed by radiation and chemotherapy.

Radiation therapy uses high energy x-rays to kill cancer cells. Radiation kills cells through DNA damage resulting in cell suicide (apoptotic death) or chromosomal damage that prevents the cell from moving through mitosis (mitotic death). The success of radiation therapy is dependent on the difference in survival rates of normal versus cancer cells. In the case where a single large dose is administered and he survival rate between normal and cancer cells is small there would be a high chance of destroying a tumor but at the expense of a great deal of damage to normal tissue. Now if that same large dose is administered as a series of low dose and the difference in survival rates remains small the treatment effectiveness is magnified. Large percentage of cancer cells is destroyed while maintaining a healthy volume of normal cells. The multiple dose method of radiation therapy is the most common method of treatment.[8]

The third method of treating cancer called chemotherapy. Chemotherapy is useful in treating cancers that have already metastasized because it circulates through the bloodstream to reach cancer cells wherever they have spread. Many chemotherapy drugs are available for use in treatment of a variety of cancers and is the most commonly used in combination with surgery or radiation. Chemotherapy drugs are divided into two broad categories of those that are cell cycle phase-specific or those that attack all proliferative cells. Cell cycle specific are further categorized as antimetabolites, antimitotic, antitumor antibiotics, alkylating agents and platinum containing compounds. Antimetabolites can act as as analogues of nucleic acid precursors and

replace small molecules during DNA duplication. They may also bind with vital enzymes and inhibit biological function. Antitumor antibiotics are derived from *Steptomyces* species and cause DNA unwinding through intercalation. Alkylating agents covalently bond to intracellular molecules such as DNA. Platinum containing compounds become positively charged inside the cell and are highly reactive with DNA forming interstrand guanine-guanine crosslinks. Chemotherapy treatments are inhibited by the cancer cell's ability to mutant and develop a resistance to cytotoxic effect of drugs.[7]

Both radiation and chemotherapy are associated with toxic side effects that limit their effectiveness. Most anticancer drugs are most active against highly proliferating cell populations so normal, rapidly dividing cells and tissues are also susceptible to these drugs. The most dangerous problems involve the gastrointestinal tract and bone marrow and dictate dose limiting toxicities of many treatment regimens. Damage to these tissues causes nausea, vomiting, diarrhea, anemia, defective blood clotting, and immune deficiency. Another possible side effect of chemotherapy is anticancer drug resistance.

The concept of neoadjuvant, meaning chemotherapy given prior to surgery began to surface in the late 1970s and early 1980s. Until this point local surgery was considered the adjavant and few major drugs could be considered in treating cancers. These drugs included fluorouracil, methotrexate, cyclophosphamide, doxorubicin and cisplatin. In most recent years research as turned to investigating biological therapies.[6-8, 10, 11]

Mesosphere Synthesis

Mesosphere technology offers an innovative solution to dose limiting toxicity problem of traditional chemotherapy treatment. A 1989 review examines experimental and clinical uses of albumin microspheres, specifically, mobility and toxicity. Generally Gupta reports particles smaller than 1μm are easily taken up by the vascular system ultimately resulting in a treatment

methodology with the same dose limiting problems. Most of the remaining studies focused on particles in the range of 7-70μm summarizing that increasing particle size results in higher deliverable dose. The final few studies suggested that particles in the 1-10μm range would be of sufficient size to maintain residence in tumor tissue while allowing for a very high deliverable dose. Many factors including drug concentration, protein concentration, surfactant concentration, degree of ultrasonication during emulsification, degree of carrier stabilization, degree of agitation during carrier stabilization, design of apparatus, and type of oil will affect particles size and particle distribution.[12, 13] This research investigated synthesis of particles in this mesosphere range by standard glutaraldehyde crosslinking and genipin crosslinking. The following is a discussion of the history of these two crosslinking agents.

Glutaraldehyde Crosslinking

Glutaraldehyde is traditionally used as a tissue fixation agent. Glutaraldehyde crosslinking of albumin has been extensively studied. Glutaraldehyde or 1,5-pentanedial is a common dialdehyde used in fixation of tissue. The aldehyde groups react with primary amine groups of proteins through a Schiff base reaction Figure 2.1. Glutaraldehyde is not stable for long a period of time in aqueous media. Through aldol condensation cyclic hemiacetals are formed and they further react to form quaternary pyridinium crosslinks between aldehyde groups essentially forming poly glutaraldehyde.[14]

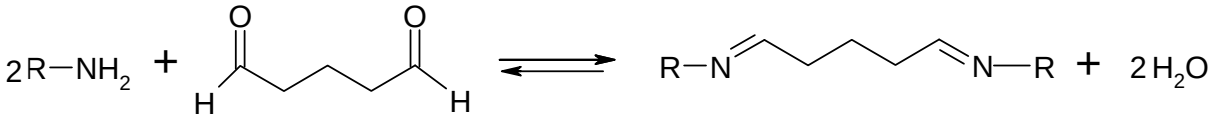

Figure 2-1. Schiff base reaction of glutaraldehyde and a primary amine.

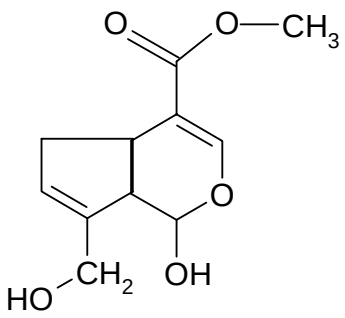

Figure 2-2. Structure of genipin

Genipin Crosslinking

Gelatin microspheres crosslinked by genipin was investigated by Cuevas. [5] Problems during in vivo studies resulted when microspheres swelled and were no longer injectable. Genipin is a hydrolytic product of geniposide. Geniposide is harvested from the fruit of

Genipa americana and Randia spinosa found in tropical Central and South America [15-18] Gardenia jaminoides Ellis found in East Asia from Viet Nam to southern Japan [15, 19-21] and Rothmannia urelliformis found in East Africa.[22] Typically the crystalline yield of genipin extracted from the seed and connective tissue of ripe fruit is 1%. Methanol extraction of ripe fruit produces geniposide. After some time exposure to air will cause the fruit to turn bluish-purple and a second methanol extraction produces genipin. Specifically the hydrolysis of geniposide with β-glucosidase produces genipin.[15, 18, 23, 24] In enzymatic genipin synthesis β-glucosidase also reacts with genipin to form geniposidic acid, a blue colored contaminant. To produce high purity genipin covalent bond formation between the enzyme and genipin must be controlled. Suppression is achieved by running hydrolysis for a short time with an immobilized enzyme of high activity. Fujukawa found using this method produced a genipin product of 100% purity which hydrolysis with native β-glucosidase produced a genipin product of dark blue color and 90% purity. Crystalline yield of genipin was also higher using an immobilized enzyme.[23, 25] Buechi has also produced an optically inactive synthesis genipin.[26] In the 1960's Djerassi was

the first to outline the structure of genipin (Figure 2-2). The empirical formula of genipin is $C_{11}H_{14}O_5$ and the structural formula bicyclic with of both primary and secondary carbomethoxy groups and an ether linkage where the ether oxygen is involved in one of the rings. The hydroxyl groups react spontaneously with amino acids to form a blue pigment.[18, 27-33] This blue pigment is very stable with respect to pH, temperature of light.[28] Genipin has long been used as folklore medicine as the cure all for inflammation, jaundice, headache, edema, fever, diarrhea and hepatic disorders and hypertension.[23, 34-37] Genipin is also thought to exhibit antitumor activity [15, 38, 39] and immunosuppressive nature.[40]

Commercially genipin is used as a blue food pigment.[30] Knowledge of the blue pigment formed with the reaction of genipin and amino acids led researchers to investigate the use of genipin in colorimetric determination of amino acids. Traditionally ninhydrin is used in this practice however Lee et al found that molar absorptivity ranged from 2-14 times higher than with ninhydrin. A linear increase of absorption with amino acid concentration increase means genipin can also be useful in quantification of amino acid.[41] Though genipin itself is colorless a dark bluish-purple stain is produced when genipin comes in contact with skin[18, 27] which has led investigators to look at genipin as a reagent for latent fingerprints.[42]

In the field of biomaterials genipin is known as a tissue fixation and crosslinking agent. Glutaraldehyde, formaldehyde and epoxy compounds have traditionally been used as fixation and crosslinking agents in biological applications. The cytotoxic nature of these compounds researchers have had a growing interest in genipin as a natural crosslinker in the fixation of biological tissues.[43-47] Genipin has been shown as a valid crosslinking agent of biological tissues exhibiting less toxicity than glutaraldehyde, formaldehyde and epoxy.[31, 48-59] Genipin has

also been investigated as a crosslinking agent in poly ethylene glycol[60, 61], chitosan[62-67], alginate[68-70] and gelatin[44, 58, 71-77] hydrogels and microspheres.

The crosslinking mechanism for crosslinking biopolymers such as chitosan, glucosamine or BSA is not fully understood (Figure 2-3). Literature supports two schemes to explain the crosslinking process. Both reaction sequences are required to form a single crosslink and are depicted in (Figure 2-3). One half of the crosslink is formed by way of nucleophilic attack of genipin at carbon C3 by a primary amine group to form an intermediate aldehyde group. Attack by the secondary amine group formed in the first step on the aldehyde group also formed in the first step opens the dihydropyran ring producing a heterocyclic compound of genipin containing primary amine groups. The second half of the crosslink is formed by SN2 nucleophilic substitution replacing the ester group on genipin with a secondary amide linkage. Polymerization

Reaction 1

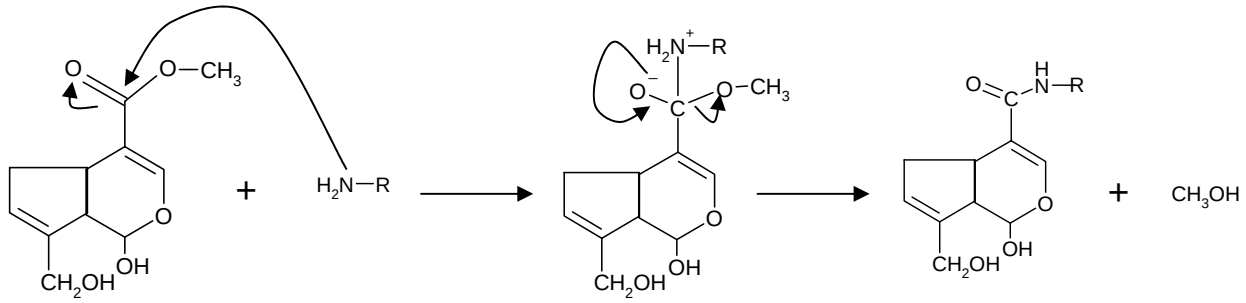

Reaction 2

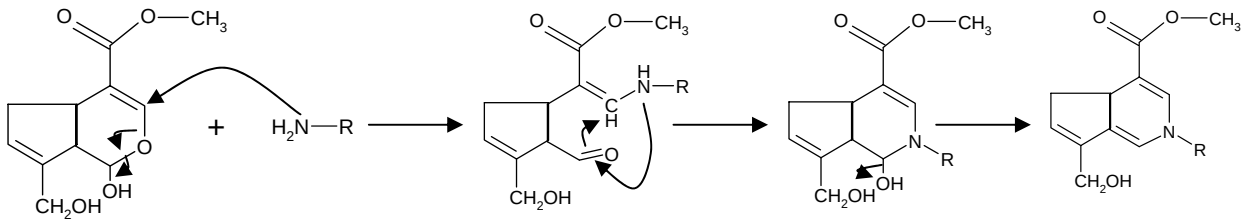

Figure 2-3. Possible crosslinking mechanism for genipin and amine groups

of genipin occurs in the presence of oxygen can also occur once crosslinks are formed. It is important to mention that secondary and tertiary structure play a role in determining the availability of crosslinking sites.[78, 79]

Chemotherapy Drugs

There are several families of chemotherapeutic drugs: alkylating agents, antitumor antibiotics, antimitotic agents, antimetabolites, hormone and enzyme therapies and biologic response modifiers. The first development of anticancer drugs was based on mustard gas reaseach during World War II. These compounds were known as alkylating agents.[9, 11] The list of the most widely used chemotherapeutics includes cyclophosphamide, methotrexate, fluorouracil, doxorubin, thiotepa, mitomycin, vinblastine, vincristine, prednisone, paclitaxel, epirubicin, mitoxantrone, ifosfamide, cisplatin, etoposide, docetaxel, vinorelbine, gemcitabine, and edatrexate. Specific treatment regimines will vary from patient to patient and will involve scheduled combination dosing of the afore mentioned drugs.[80] The discussion to follow focuses on the use of cisplatin and cyclophosphamide.

Cisplatin

The inhibition of Escherichia coli cell division when exposed to electrolysis products from a platinum electrode led to investigating the antitumor activities of platinum complexed with chlorine and ammonia groups. Cisplatin was identified as the most active and its structure

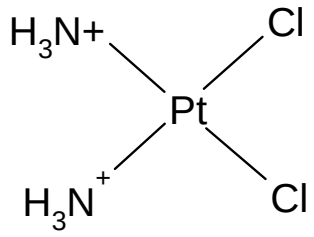

Figure 2-4. Structure of cisplatin

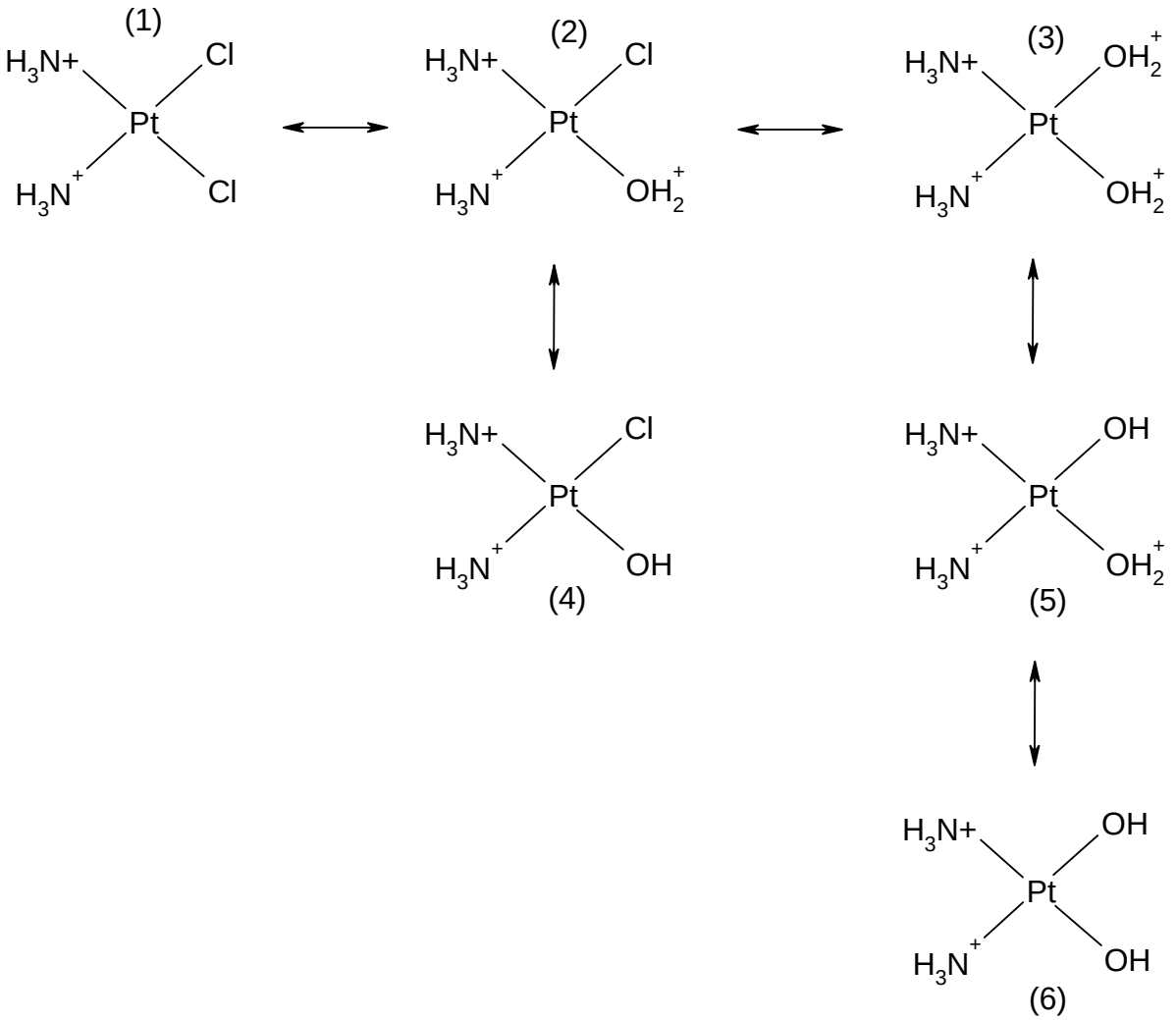

Figure 2-5. Cisplatin hydrolysis

consists of a square planar complex coordinated by a central platinum atom (Figure 2-4). Cisplatin is biologically unreactive because it does not react directly with molecules that ordinarily bound with platinum through nitrogen or oxygen. Therefore cisplatin must first undergo hydrolysis before it is the reactive. The chlorine atoms of cisplatin are susceptible to chemical displacement by water (Figure 2-5). The chlorine atom is systematically replaced by water creating first cis-$[PtCl(H_2O)(NH_3)_2]^+$ (2) and then cis-$[PtCl(H_2O)_2(NH_3)_2]^{2+}$ (3). The water molecules may also deprotonate forming hydroxo complexes 4, 5, 6 in Figure 2-5. The Pt-OH_2 is more reactive than the Pt-Cl bond and will react with nucleobases of DNA.[81]

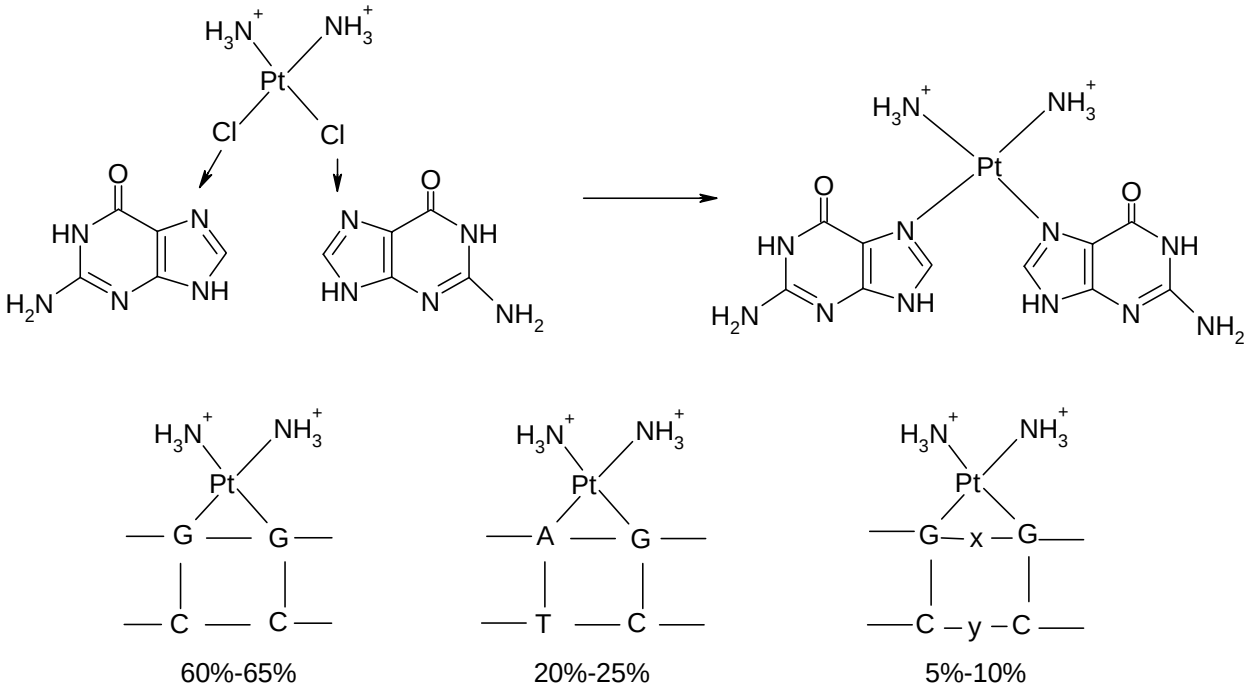

Figure 2-6. Cisplatin DNA adducts

The details of it's mechanism of action for cisplatin are not understood. Some cancers such as ovarian are highly sensitive where as others like pancreatic are only mildly responsive. Most of what is known about the mechanism of action is extrapolated from research performed using carboplatin a second generation platinum containing compound and cousin of cisplatin. DNA seems to be the most important target of cisplatin. Cisplatin interferes with DNA replication without affecting normal RNA and protein synthesis. Cisplatin preferably binds to the N^7 positions of quinine and adenine of DNA to form intrastrand crosslinks (Figure 2-6). This produces a local kinking and unwinding of the double helix.[9] Various formulations of cisplatin microspheres have been investigated since the late1980s.[82-88]

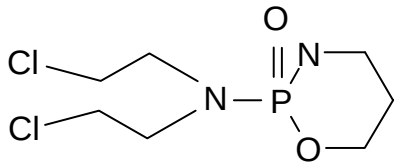

Figure 2-7. Structure of cyclophosphamide

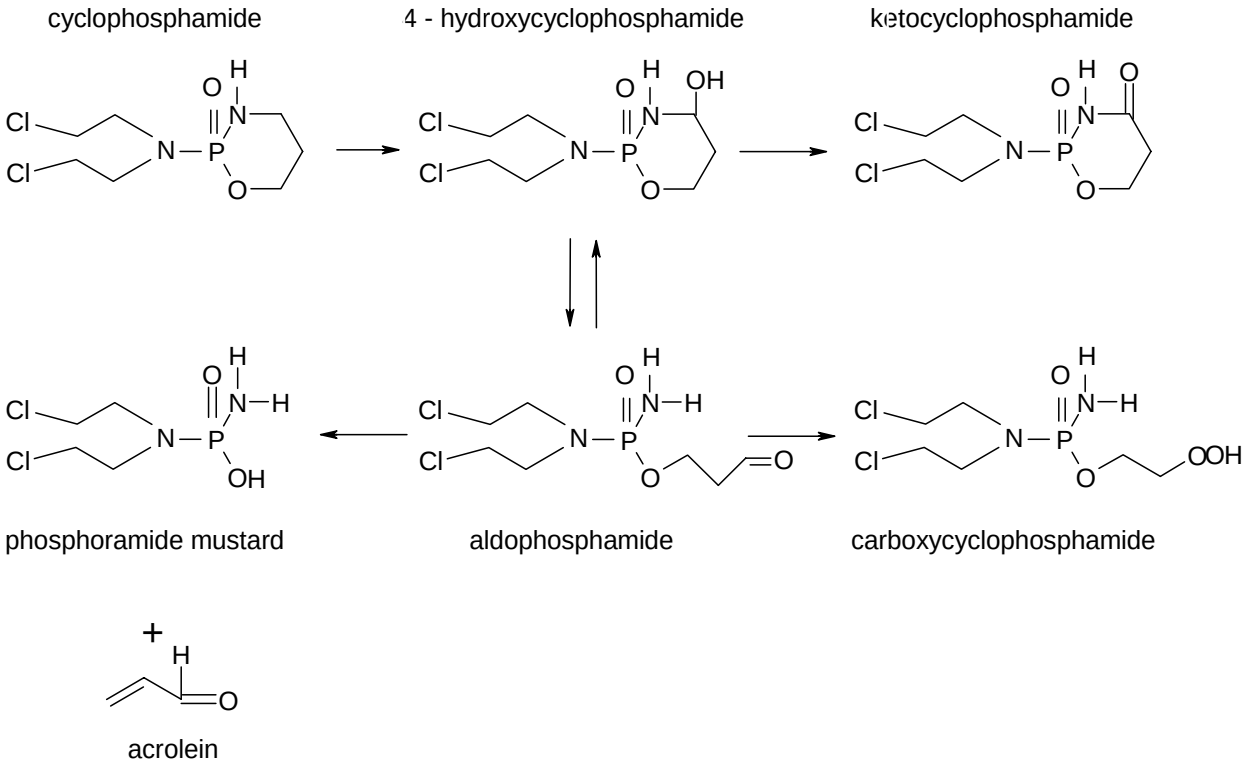

Figure 2-8. Cyclophospamide metabolic pathway

Cyclophosphamide

Cyclophosphamide belongs to a group of cancer drugs called alkylating agents and was the first of the nitrogen mustard class to be developed. Alkylating agents are highly reactive electrophiles that can covalently interact with a number of nucleophillic groups including amine, carboxyl, phosphate and sulfhydryl groups. The rational of its use was based on the observation of high levels of phosphoraamidases. Cyclophosphamide is not directly cytotoxic and requires hepatic activation. It undergoes a cytochrome P450 oxidation to 4-hydroxyclophosphamide. Four-hydroxyclophosphamide can then either be oxidized to 4-ketocyclophosphamide or tautomerized to aldophosphamide. Aldophosphamide is either deactivated by aldehyde dehydrogenase to form ammonia groups. Cyclophosphamide was identified as the most active and its structure carboxyphosphamide or undergoes spontaneous β elimination to yield acrolein

and phosphoramide mustard (Figure 2-8). Acrolein and phosphoramide are the active compounds, and slow the growth of cancer cells by interfering with the actions DNA.

The elimination half-life varies greatly, but the mean value of 7 hours with a range of 108 to 960 minutes. This half-life is shorter in children than in adults. Thus far investigations have found no linear relationship between dose and half-life. Cyclophosphamide is readily absorbed from the gastrointestinal tract. Metabolic rates and pathways may differ between oral and intravenous administration. The volume distribution is 0.7l/kg of total body water. Renal clearance is approximately 10ml/min. Total renal excretion is low with approximately 5-25% of an administered dose being recovered in urine.[9, 89]

Cyclophosphamide nano[90] and microspheres have been briefly investigated as targeted drug delivery devices in the treatment of rheumatoid arthritis[91] and cancer.[92, 93]

CHAPTER 3
SYNTHESIS OF GENIPIN CROSSLINKED BOVINE SERUM ALBUMIN MESOSPHERES: A MULTIPARAMETER STUDY OF FACTORS THAT AFFECT PARTICLE SIZE AND PARTICLE SIZE DISTRIBUTION

Introduction

A major aspect of this research was to establish the role processing conditions in controlling particles size and particle size distribution in the synthesis of protein mesospheres used in delivery of chemotherapy agents for localized intratumoral (IT) therapies. The goal was to produce spherical bovine serum albumin (BSA) mesospheres using suspension crosslinking with dry particle size range of 1-10μm. It was regarded as important to conduct a multiparameter statistical study of processing conditions based on previous microsphere work completed by Hadba[3] and Cuevas[5]. The effects of processing factors: dispersion stirring rate, BSA concentration, CAB concentration, genipin concentration, crosslinking time and GEN/BSA ratio were investigated. The measurable outcome of particle size provided a macroscopic evaluation of the varying process parameters. Several parameter combinations were further investigated for macroscopic mesosphere degradation and are discussed in Chapter 4.

Materials and Methods

Materials

Bovine serum albumin (BSA) and cellulose acetate butyrate (CAB) were purchased from Sigma-Aldrich. 1, 2 Dichloroethane (DCE) and acetone were purchased from Fisher Scientific. Genipin (GEN) was produced by Wacko Company and purchased from City Chemical. Ultrapure water was prepared in the laboratory using a Barnstead NANOpure.

Methods

Solution preparations

Bovine serum albumin is water soluble so BSA solutions were prepared in ultrapure water. The appropriate mass of BSA was weighted out in a 50ml centrifuge tube and dissolved in water. The true concentration was measured gravimetrically and the density of the solution was determined. Approximately 1 ml of BSA solution was dried at 130ºC on a Mettler LJ16 Moisture Analyzer to determine the dry weight per volume percent. Concentration was adjusted until true concentration was achieved within 2.5% of 20%(w/v).

Cellulose acetate butyrate solutions were prepared by dissolving the appropriate mass in DCE to a final concentration of 3% (w/v) or 5% (w/v).

Genipin solutions were prepared by dissolving the appropriate mass in acetone to a final concentration of 30mg/ml or 60mg/ml.

Mesosphere synthesis

A multiparameter study was designed to investigate the affect of BSA concentration, genipin concentration, CAB concentration and GEN/BSA ratio on genipin crosslinked BSA mesospheres. Stirring rate during emulsion stabilization and crosslink time were investigated as secondary factors effecting particle size. Mesospheres were prepared using a "water-in-oil" emulsion suspension crosslinking. In a typical preparation 5ml of BSA solution was added to a 300mL Labonco lyophilization flask containing 45ml of CAB solution.(Figure 3-1) The mixture was stirred for 20 minutes at a speed range of 800rpm to 1500rpm on either a Lightnin (model #L1V08), Caframo (model #BDC6015), or Caframo (model #BDC1850) high speed mixer. The crosslinking agent, genipin was added to the reaction vessel and stirring rate reduced to 600rpm. The crosslinking reaction continued for 6 to 24 hours; acetone was added to the reaction vessel and stirring continued for one additional hour. Particles were collected by centrifugation on a

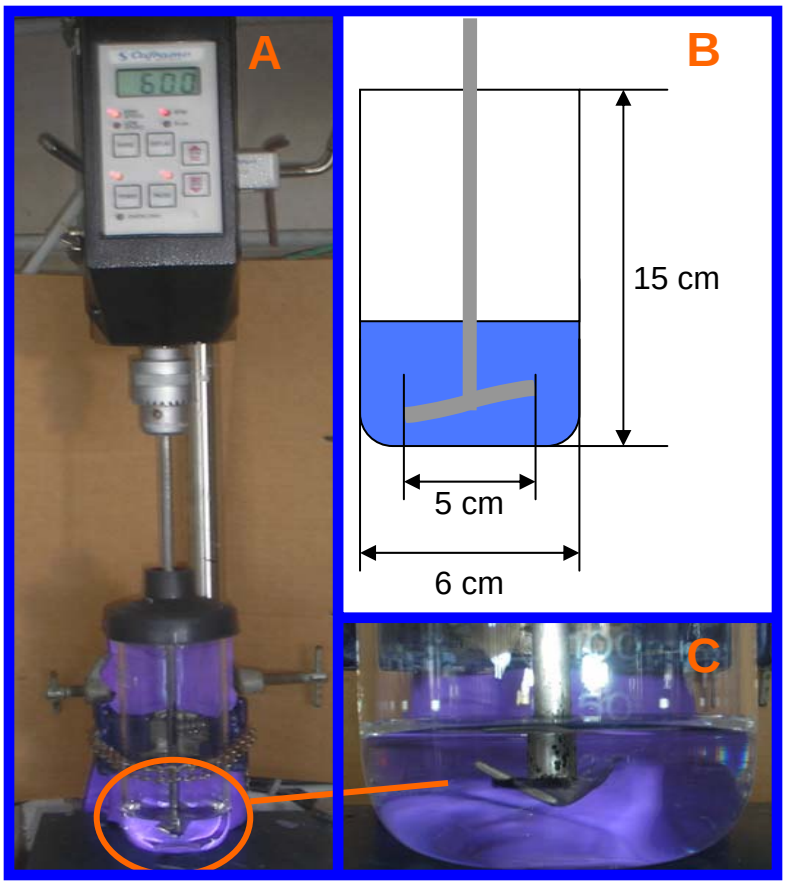

Figure 3-1. Mesosphere synthesis mixer setup: A) Full mixer setup placement B) Setup schematic C) Close up of blade placement

Dynac II benchtop (Clay Adams) by transferring approximately 25mL of solution to each of four 50mL centrifuge tubes, adding acetone to the 40mL mark and centrifuging for 5 minutes at 2000 rpm. The supernant CAB/acetone mixture was decanted; the mesosphere pellet was resuspended in acetone and centrifuged for 10 minutes at 2000 rpm for three additional washes. Particles were then air dried. Each condition was prepared in triplicate, one batch on each of the three mesosphere synthesis stations in the laboratory.

Scanning electron microscopy

Field emission scanning electron microscopy was used to examine the morphology of synthesized mesospheres. Dry mesospheres were mounted on carbon tape on an aluminum SEM stub. Stubs were sputter coated with a gold/palladium alloy using a Technix Hummer V Sputter

Table 3-1. Processing conditions varying BSA concentration

Processing Condition	Level
BSA Concentration (% w/v)	10, 20, 30
CAB Concentration (%w/v)	5
Aqueous Phase Volume (mL)	5
Organic Phase Volume (mL)	45
D/C Ratio	11.1
Genipin Concentration (mg/mL)	30
GEN/BSA Weight Ratio (w/w)	5, 10
Stirring Rate During Emulsion Stabilization (rpm)	800, 1200, 1500
Stirring Rate During Crosslinking (rpm)	600
Crosslinking Time (hours)	6, 12, 24

coater. The samples were then analyzed using Joel 6335F field emission microscope housed at the Particle Engineering Research Center (PERC).

Particle sizing

The dry particle size and particle size distributions of bovine serum albumin mesospheres was measured using a Coulter LS 230 particle size analyzer housed at (PERC). For each condition sample three 1% (w/v) mesosphere suspension was prepared in 3mL of acetone. The suspension was sonicated for 15-30 seconds. The suspension was added drop-wise to the chamber until obscuration read between 7% - 9% and PIDS read between 37% - 43%. Suspended mesospheres scattered light from a laser source and was detected by silicon photo-detectors. A BSA optical model translated light intensity measurements into a particle size distribution as a volume percent in discrete size blocks. The mean, median, standard deviation and particle size quartiles and other statistical data for each batch were determined using Coulter software.

Statistical analysis

Microsoft Excel was used to calculate average mean particle size, standard deviation, span average yield and percent theoretical yield. The statistical software package Sigma Stat was used to identify differences in mean particle size (n=18) and interactions between the various processing conditions. Four primary factors: protein solution concentration, suspension agent

solution concentration, crosslinker solution concentration, crosslinker/protein ratio and two secondary factors: stabilization stirring speed and crosslinking time were analyzed using a three way ANOVA. A two way ANOVA was used to find interactions between factors. The Tukey method was used for all pair wise multiple comparisons to isolate exactly which levels of each factor provided a statistical difference in mean particle size.

Results and Discussion

Results

BSA solution concentration

The processing conditions for this set of experiments are summarized in Table 3-1. Mesospheres were synthesized with varying levels of BSA concentrations, dispersion stabilization stirring rates and crosslink times while all other variables where held constant. Mean particle size data and other pertinent statistics are summarized in Table 3-2. A graphical summary of mean particle size and particle size distribution is shown in Figures 3-2 and 3-3. The statistical analysis suggests statistical differences in particle size when varying both BSA concentration ($p=0.034$) and stirring rate ($p\leq0.001$) but not in crosslinking time ($p=0.877$). When looking at the interaction of BSA concentration and stirring rate we find the dominating factor to be stirring rate. Evaluating BSA concentration within each stir rate independently no statistical

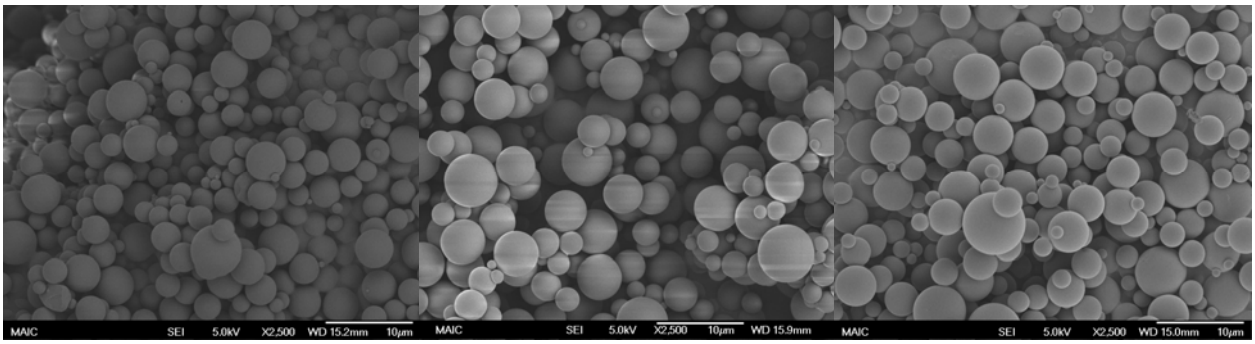

Figure 3-2. SEM micrographs of mesospheres synthesized with varying BSA concentrations A) 10% (w/w) Mean particle size 2.3µm±0.01 B) 20% (w/w) Mean particle size 2.0µm±0.01 C) 30% (w/w) Mean particle size 2.3µm±0.04

Table 3-2. Summary of BSA concentration statistics

BSA	Stir Rate (rpm)	Time (hrs)	Average Diameter (μm)	STD	% >1um	% <10um	Average Actual Yield(g)	Average % Theoretical Yield
10%	800	24	6.9	2.8	64	77	0.4	83%
10%	800	12	5.9	0.7	72	77	0.4	79%
10%	800	6	4.6	0.9	65	85	0.4	77%
10%	1200	24	2.3	0.1	70	100	0.4	83%
10%	1200	12	3.6	0.5	68	95	0.4	79%
10%	1200	6	2.7	0.2	62	98	0.4	78%
10%	1500	24	2.3	0.0	75	100	0.4	83%
10%	1500	12	3.1	0.2	84	100	0.4	73%
10%	1500	6	2.6	0.2	83	99	0.4	75%
20%	800	24	3.8	0.4	60	92	1.0	93%
20%	800	12	3.8	1.1	61	90	0.9	88%
20%	800	6	5.0	0.7	71	84	0.9	86%
20%	1200	24	2.1	0.1	52	100	0.9	86%
20%	1200	12	2.2	0.1	57	100	0.9	84%
20%	1200	6	2.8	0.6	57	97	0.9	87%
20%	1500	24	2.0	0.1	65	100	1.0	92%
20%	1500	12	2.2	0.2	70	100	0.9	84%
20%	1500	6	2.3	0.2	65	100	0.9	83%
30%	800	24	4.9	0.4	63	80	1.2	76%
30%	800	12	5.0	1.4	61	80	1.2	80%
30%	800	6	5.3	0.8	65	78	1.1	73%
30%	1200	24	3.0	0.6	55	96	1.2	78%
30%	1200	12	2.8	0.5	55	97	1.2	79%
30%	1200	6	2.9	0.2	57	97	1.1	72%
30%	1500	24	2.3	0.4	61	100	1.2	76%
30%	1500	12	2.1	0.1	54	100	1.2	80%
30%	1500	6	2.1	0.2	62	100	1.1	73%

difference was found in particle size between a 10% (w/v), 20% (w/v) or 30% (w/v) concentration. Evaluating stir rate a statistical difference was found between BSA concentration ($p=0.034$) and stirring rate ($p\leq0.001$) but not in crosslinking time ($p=0.877$). When looking at the interaction of BSA concentration and stirring rate we find the dominating factor to be stirring rate. Evaluating BSA concentration within each stir rate independently no statistical difference was found in particle size between a 10% (w/v), 20% (w/v) or 30% (w/v) concentration.

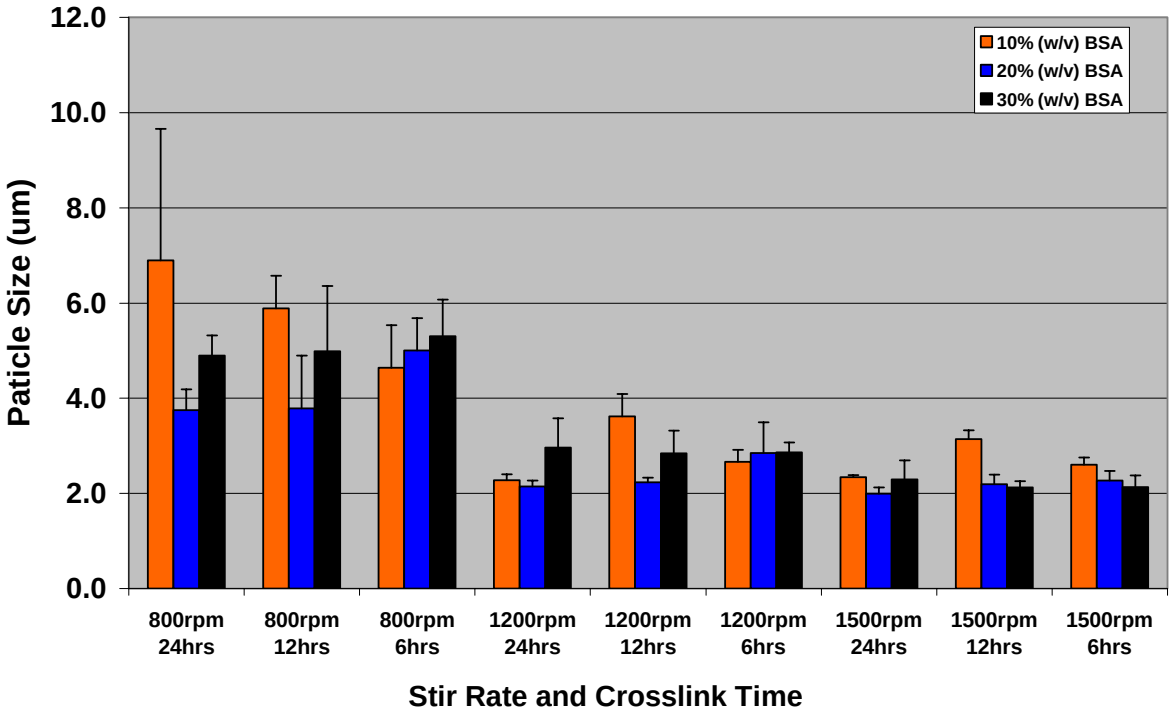

Figure 3-3. Mean particle size varying BSA concentration

Evaluating stir rate a statistical difference was found between BSA concentration ($p=0.034$) and stirring rate ($p\leq0.001$) but not in crosslinking time ($p=0.877$). When looking at the interaction of BSA concentration and stirring rate we find the dominating factor to be stirring rate. Evaluating BSA concentration within each stir rate independently no statistical difference was found in particle size between a 10% (w/v), 20% (w/v) or 30% (w/v) concentration. Evaluating stir rate a statistical difference was found between 800rpm and 1200rpm, 800rpm and 1500rpm but not between 1200rpm and 1500rpm at each BSA concentration level. We look to the size distribution graph for some explanation. The shape of the particle size distribution curve remains almost unchanged with increasing crosslink time. As dispersion stir rate increases the shape of the distribution curve moves from bimodal toward normal distribution. The mathematical representation of particle size distribution known as span is defined as the difference between the

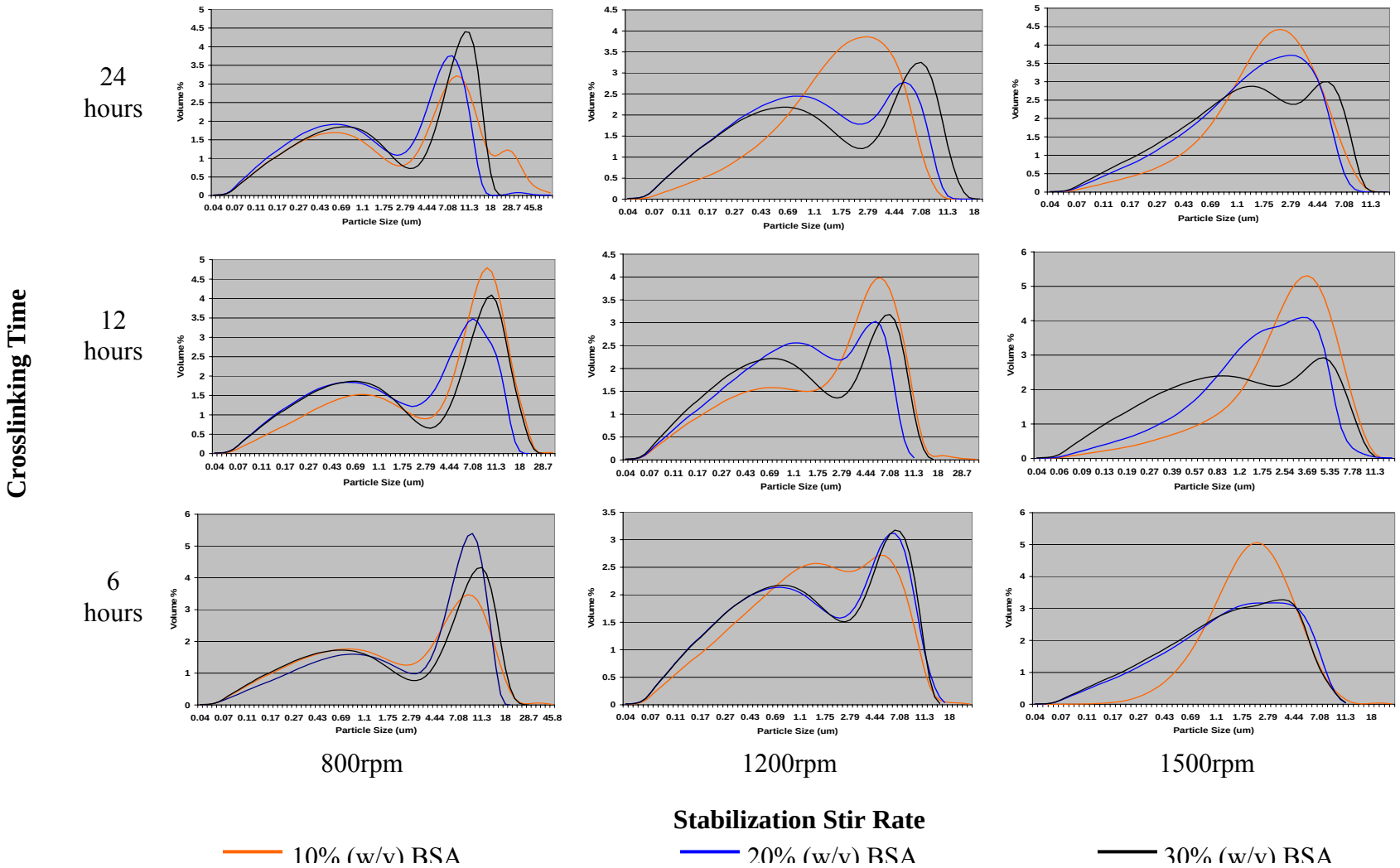

Figure 3-4. Particle size distributions varying BSA concentration

Table 3-3. Processing conditions varying CAB concentration

Processing Condition	Level
BSA Concentration (% w/v)	20
CAB Concentration (%w/v)	3, 5
Aqueous Phase Volume (mL)	5
Organic Phase Volume (mL)	45
D/C Ratio	11.1
Genipin Concentration (mg/mL)	30
GEN/BSA Weight Ratio	5, 10
Stirring Rate During Emulsion Stabilization (rpm)	800, 1200, 1500
Stirring Rate During Crosslinking (rpm)	600
Crosslinking Time (hours)	6, 12, 24

90^{th} and 10^{th} percentile diameter divided by the 50^{th} percentile diameter. Span increases with increasing BSA solution concentration, decreases with increasing stir rate, and remains almost unchanged with increasing crosslink time. As BSA solution concentration increases the actual

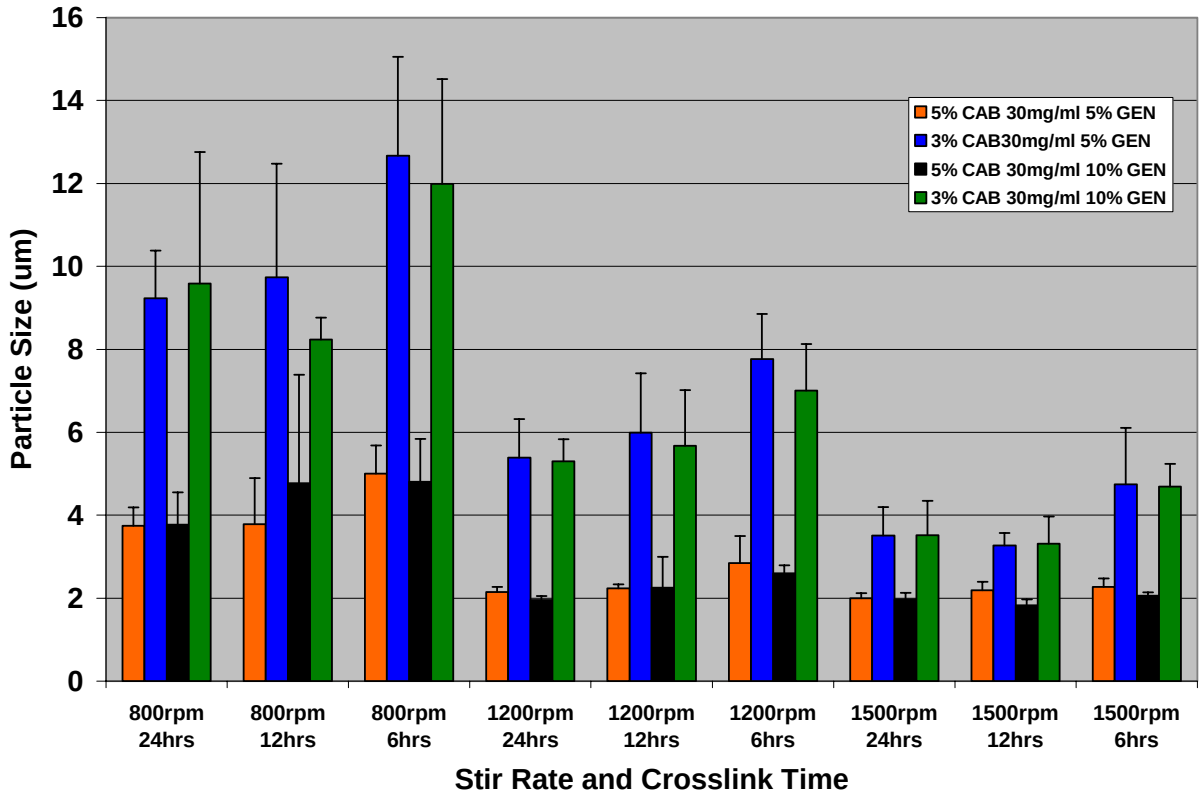

Figure 3-5. Mean particle size varying CAB concentration

product yield of mesospheres increases while percent theoretical yield appears to be a function of crosslink time increasing with increasing crosslink time. During preparations of the different solutions it was noted that the precise concentration was more difficult to achieve for a 30% (w/v) than a 10 or 20% (w/v) solution. The quantity of particles falling in the 1µm-10µm increases with increasing stir rate and increasing crosslink time.

CAB solution concentration

The process conditions of synthesized batches are summarized in Table 3.3 Mesospheres were synthesized with varying CAB concentrations, dispersion stabilization stirring rates and crosslink times while all other variables were held constant (Figure 3-5). Mean particle size data and other Figure 3-5: SEM micrograph of mesospheres synthesized with varying CAB concentrations pertinent statistics are summarized in Table 3-4. A graphical summary of mean particle size and particle size distribution is shown in Figures 3-6 and 3-7. CAB concentration is a factor that affects particle size. A statistically significant difference ($p \leq 0.001$) with statistically significant interaction factors with both secondary variables of stir rate ($p \leq 0.001$) and crosslink time ($p \leq 0.001$). As CAB solution concentration increases particle size decreases. This result is true at every level of stir rate however as the stir rate increases from 800rpm to 1500rpm the difference in mean particle size decreases, which suggest there exist a minimum stir rate where the CAB concentration/stir rate interaction will no longer effect particle size. This is confirmed in a comparison between stir rates of 1200rpm and 1500rpm with a constant 5% (w/v) CAB concentration where no statistical difference in mean particle size was produced. A similar trend of decrease in mean particle size continues as crosslink time increases from 6 to 24 hours. Particle size distribution moves from bimodal toward a normal distribution with increasing stir for mesospheres synthesized with 5% (w/v) CAB solution. The particle size distribution curve for 3% (w/v) CAB solution keeps a bimodal shape with increasing stir rate.

Table 3-4. Summary of statistics varying CAB concentration

Lot	CAB	GEN (gen/bsa) (mg/ml)	Stir Rate (rpm)	Time (hrs)	Average Diameter (μm)	STD	Span	% <10um	% >1um	Average Actual Yield(g)	Average % Theoretical Yield
1	5%	30 (5)	800	24	3.8	0.4	5.1	92	60	1.0	93%
2	5%	30 (5)	800	12	3.8	1.1	3.0	90	61	0.9	88%
3	5%	30 (5)	800	6	5.0	0.7	2.4	84	71	0.9	86%
5	5%	30 (5)	1200	24	2.1	0.1	5.3	100	52	0.9	86%
6	5%	30 (5)	1200	12	2.2	0.1	4.4	100	57	0.9	84%
7	5%	30 (5)	1200	6	2.8	0.6	4.7	97	57	0.9	87%
9	5%	30 (5)	1500	24	2.0	0.1	2.7	100	65	1.0	92%
10	5%	30 (5)	1500	12	2.2	0.2	2.4	100	70	0.9	84%
11	5%	30 (5)	1500	6	2.3	0.2	3.1	100	65	0.9	83%
49	3%	30 (5)	800	24	9.2	1.2	2.3	54	72	1.0	91%
50	3%	30 (5)	800	12	9.7	2.7	2.2	53	74	0.9	84%
51	3%	30 (5)	800	6	12.7	2.4	2.0	42	84	0.9	82%
53	3%	30 (5)	1200	24	5.4	0.9	4.0	77	68	0.9	88%
54	3%	30 (5)	1200	12	6.0	1.4	3.2	73	69	0.9	83%
55	3%	30 (5)	1200	6	7.8	1.1	2.1	64	81	0.8	81%
57	3%	30 (5)	1500	24	3.5	0.7	5.8	92	58	0.9	88%
58	3%	30 (5)	1500	12	3.3	0.3	5.2	94	59	0.9	86%
59	3%	30 (5)	1500	6	4.7	1.4	3.1	85	70	0.8	81%
13	5%	30 (10)	800	24	3.8	0.8	5.1	91	59	0.9	78%
14	5%	30 (10)	800	12	4.8	2.6	2.9	83	61	0.9	85%
15	5%	30 (10)	800	6	4.8	1.0	3.7	82	63	1.0	88%
17	5%	30 (10)	1200	24	2.0	0.1	5.0	100	51	0.8	72%
18	5%	30 (10)	1200	12	2.3	0.7	3.7	100	53	0.8	76%
19	5%	30 (10)	1200	6	2.6	0.2	5.5	99	55	0.9	84%
21	5%	30 (10)	1500	24	2.0	0.2	2.1	100	69	0.8	74%
22	5%	30 (10)	1500	12	1.8	0.1	2.0	100	67	0.8	70%
23	5%	30 (10)	1500	6	2.1	0.1	2.9	100	64	0.9	85%
61	3%	30 (10)	800	24	9.6	3.2	2.3	54	72	0.9	81%
62	3%	30 (10)	800	12	8.2	0.5	2.4	58	71	0.8	69%
63	3%	30 (10)	800	6	12.0	2.5	2.1	46	82	0.9	78%
65	3%	30 (10)	1200	24	5.3	0.5	4.4	77	64	0.9	80%
66	3%	30 (10)	1200	12	5.7	1.3	3.6	75	65	0.8	74%
67	3%	30 (10)	1200	6	7.0	1.1	2.8	68	74	0.9	80%
69	3%	30 (10)	1500	24	3.5	0.8	4.4	92	60	0.8	75%
70	3%	30 (10)	1500	12	3.3	0.7	5.8	93	58	0.8	72%
71	3%	30 (10)	1500	6	4.7	0.6	3.6	85	69	0.8	76%

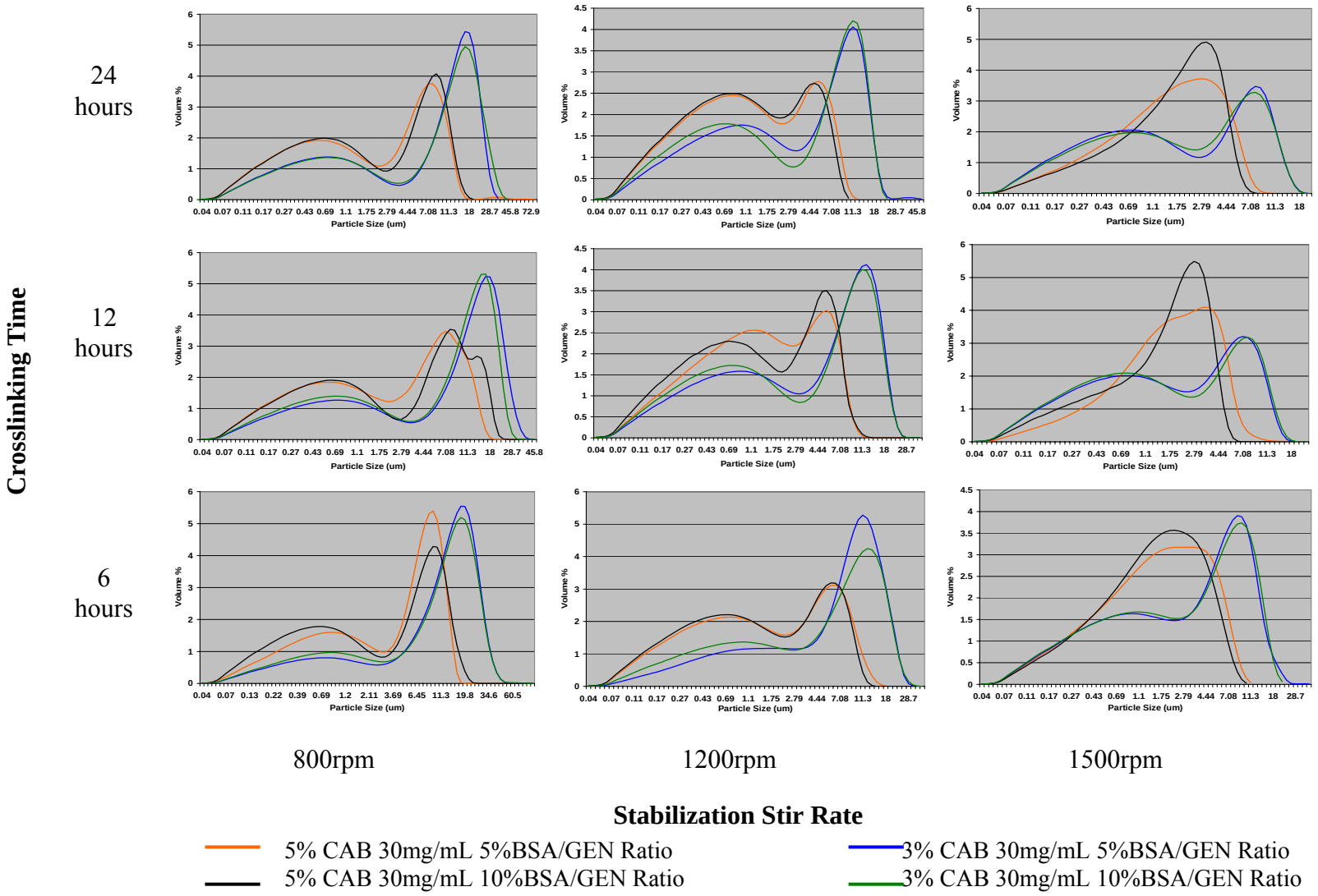

Figure 3-6. Particle size distributions varying CAB concentration

Table 3-5. Processing conditions varying genipin concentration

Processing Condition	Level
BSA Concentration (% w/v)	20
CAB Concentration (%w/v)	5
Aqueous Phase Volume (mL)	5
Organic Phase Volume (mL)	45
D/C Ratio	11.1
Genipin Concentration (mg/mL)	30, 60
GEN/BSA Weight Ratio	5, 10
Stirring Rate During Emulsion Stabilization (rpm)	800, 1200, 1500
Stirring Rate During Crosslinking (rpm)	600
Crosslinking Time (hours)	6, 12, 24

Mathematically this is shown as span decreases with increasing stir rate for 5% (w/v) CAB and increases with increasing stir rate for 3% (w/v) CAB solution. At the low level crosslink density actual product yield and percent theoretical yield are similar averaging 0.9 grams and high 80's percentage respectively. At the higher crosslink density actual product yield is greater at the high level crosslink time (24 hours) and low level CAB concentration (3% w/v) combination. The opposite is true at the low and medium crosslink time (6, 12 hours) and high level CAB concentration (5%w/v) combination. The difference in actual product yield is greater with 5% (w/v) CAB than with 3% (w/v) CAB solution.

Genipin solution concentration

The process conditions of synthesized batches are summarized in Table 3.5. Mesospheres were synthesized with varying genipin solution concentrations, dispersion stabilization stirring rates and crosslink times while all other variables were held constant (Figure 3-8). Mean particle size data and other pertinent statistics are summarized in Table 3.4. A graphical summary of mean particle size and particle size distribution is shown in Figures 3.5 and 3.6. Genipin concentration is not a factor that affects particle size. Again stir rate appears to be the primary factor effecting particle size. This set of experiments provided the most insight as to how both stabilization stir

Table 3-6. Summary of statistics for varying genipin concentration

Lot	GEN (gen/bsa) (mg/ml)	Stir Rate (rpm)	Time (hrs)	Average Diameter (μm)	STD	Span	% <10um	% >1um	Average Actual Yield(g)	Average % Theoretical Yield
1	30 (5)	800	24	3.8	0.4	5.1	92	60	1.0	93%
2	30 (5)	800	12	3.8	1.1	3.0	90	61	0.9	88%
3	30 (5)	800	6	5.0	0.7	2.4	84	71	0.9	86%
5	30 (5)	1200	24	2.1	0.1	5.3	100	52	0.9	86%
6	30 (5)	1200	12	2.2	0.1	4.4	100	57	0.9	84%
7	30 (5)	1200	6	2.8	0.6	4.7	97	57	0.9	87%
9	30 (5)	1500	24	2.0	0.1	2.7	100	65	1.0	92%
10	30 (5)	1500	12	2.2	0.2	2.4	100	70	0.9	84%
11	30 (5)	1500	6	2.3	0.2	3.1	100	65	0.9	83%
13	30 (10)	800	24	3.8	0.8	5.1	91	59	0.9	78%
14	30 (10)	800	12	4.8	2.6	2.9	83	61	0.9	85%
15	30 (10)	800	6	4.8	1.0	3.7	82	63	1.0	88%
17	30 (10)	1200	24	2.0	0.1	5.0	100	51	0.8	72%
18	30 (10)	1200	12	2.3	0.7	3.7	100	53	0.8	76%
19	30 (10)	1200	6	2.6	0.2	5.5	99	55	0.9	84%
21	30 (10)	1500	24	2.0	0.2	2.1	100	69	0.8	74%
22	30 (10)	1500	12	1.8	0.1	2.0	100	67	0.8	70%
23	30 (10)	1500	6	2.1	0.1	2.9	100	64	0.9	85%
25	60 (5)	800	24	5.1	1.1	3.3	82	65	1.0	94%
26	60 (5)	800	12	5.6	1.7	3.1	77	67	0.9	82%
27	60 (5)	800	6	6.2	2.5	2.0	77	73	0.9	87%
29	60 (5)	1200	24	2.3	0.4	5.2	99	54	0.8	77%
30	60 (5)	1200	12	2.2	0.3	4.7	99	54	0.9	82%
31	60 (5)	1200	6	2.9	0.2	4.7	98	60	0.9	82%
33	60 (5)	1500	24	2.1	0.1	2.6	100	67	0.9	81%
34	60 (5)	1500	12	2.1	0.1	2.8	100	65	0.8	74%
35	60 (5)	1500	6	2.3	0.1	2.4	100	73	0.8	80%
37	60 (10)	800	24	6.0	1.6	2.3	73	71	0.9	85%
38	60 (10)	800	12	4.0	0.5	4.7	90	60	0.9	83%
39	60 (10)	800	6	5.1	2.1	3.2	81	64	0.9	81%
41	60 (10)	1200	24	2.5	0.2	5.7	99	52	0.8	71%
42	60 (10)	1200	12	2.5	0.3	5.1	99	55	0.8	75%
43	60 (10)	1200	6	2.6	0.3	5.4	98	55	0.9	78%
45	60 (10)	1500	24	2.0	0.1	2.8	100	64	0.9	79%
46	60 (10)	1500	12	2.0	0.2	3.0	100	61	0.8	72%
47	60 (10)	1500	6	2.1	0.2	2.8	100	65	0.9	79%

rate and crosslink time affected particle size. A statistically significant difference in mean particle size ($p \leq 0.001$) was found between the three levels of stir rate. Generally particle size

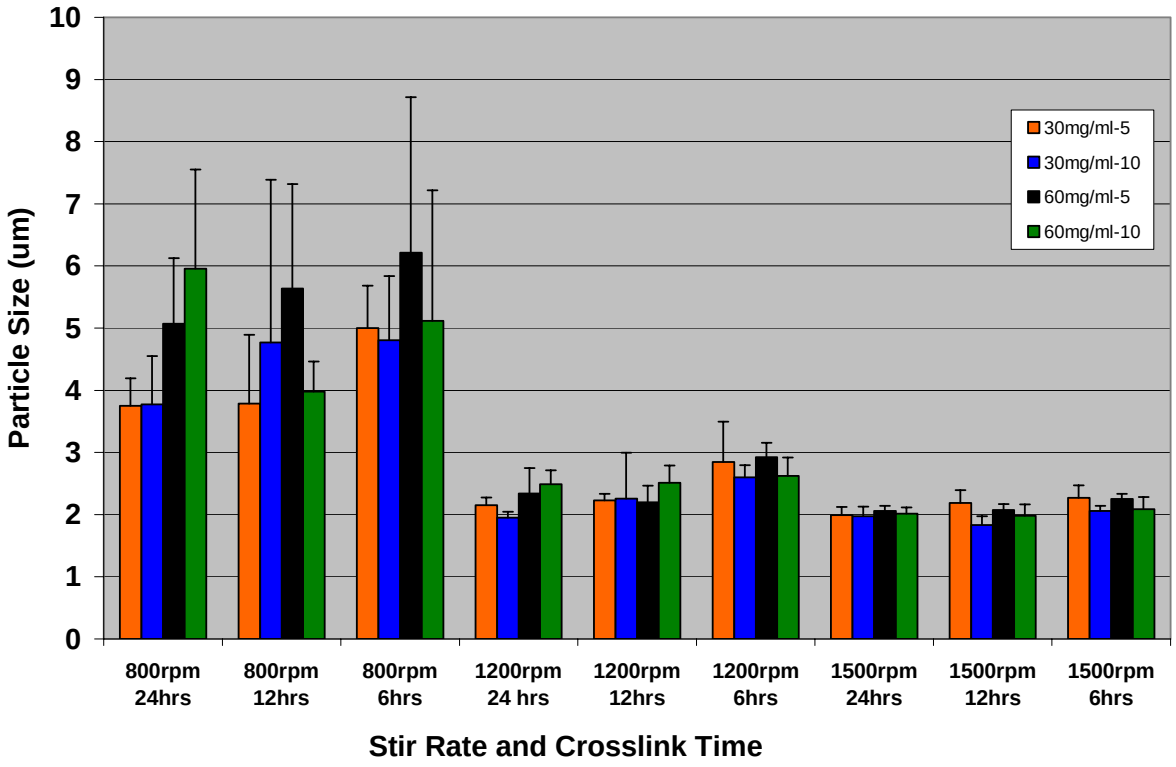

Figure 3-7. Mean particle size varying genipin concentration

decreases with increasing stir rate with statistically significant differences between stir rates of 800rpm and 1200rpm and 800rpm and 1500rpm but not between 1200rpm and 1500rpm. A statistically significant difference (p=0.028) in mean particle size was found between the three levels of crosslink time, specifically between 6 and 24 hours but not between 6 and 12 hors or 12

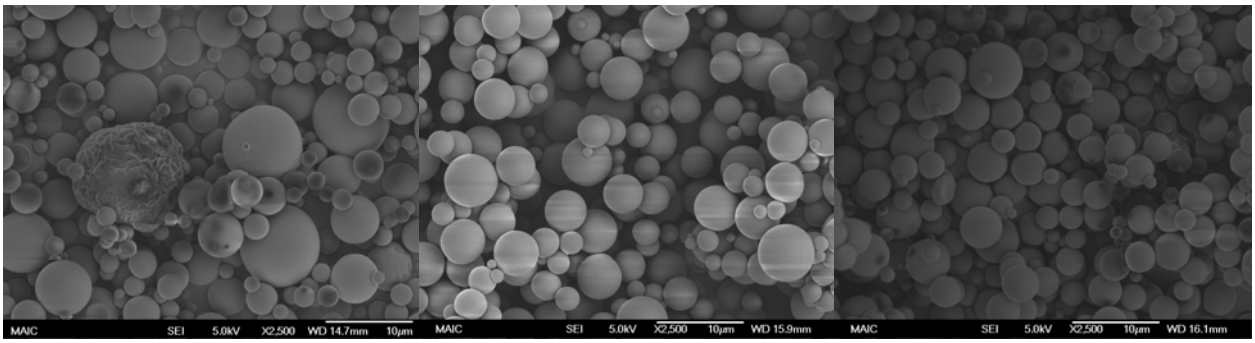

Figure 3-8. SEM micrographs of mesospheres synthesized with varying GEN/BSA ratio A) 1% (w/w) B) 5% (w/w) C) 10% (w/w)

Table 3-7. Processing conditions varying GEN/BSA ratio

Processing Condition	**Level**
BSA Concentration (% w/v)	20
CAB Concentration (%w/v)	5.0
Aqueous Phase Volume (mL)	5.0
Organic Phase Volume (mL)	45.0
D/C Ratio	11.1
Genipin Concentration (mg/mL)	30
GEN/BSA Weight Ratio	1, 5, 10
Stirring Rate During Emulsion Stabilization (rpm)	800, 1200, 1500
Stirring Rate During Crosslinking (rpm)	600
Crosslinking Time (hours)	6, 12, 24

Table 3-8. Summary of statistics varying GEN/BSA ratio

GEN (gen/bsa) (mg/ml)	Stir Rate (rpm)	Time (hrs)	Average Diameter (μm)	STD	% <10um	% >1um	Average Actual Yield(g)	Average % Theoretical Yield
30 (1)	800	24	5.3	0.9	79	66	0.8	84%
30 (1)	800	12	7.4	2.9	67	76	0.8	83%
30 (1)	800	6	8.4	3.7	63	81	0.9	86%
30 (1)	1200	24	3.2	0.9	95	57	0.9	85%
30 (1)	1200	12	2.9	0.5	97	59	0.9	86%
30 (1)	1200	6	3.4	0.6	95	65	0.8	84%
30 (1)	1500	24	2.1	0.1	100	72	0.8	79%
30 (1)	1500	12	2.3	0.0	100	70	0.9	84%
30 (1)	1500	6	2.5	0.3	100	78	0.8	82%
30 (5)	800	24	3.8	0.4	92	60	1.0	93%
30 (5)	800	12	3.8	1.1	90	61	0.9	88%
30 (5)	800	6	5.0	0.7	84	71	0.9	86%
30 (5)	1200	24	2.1	0.1	100	52	0.9	86%
30 (5)	1200	12	2.2	0.1	100	57	0.9	84%
30 (5)	1200	6	2.8	0.6	97	57	0.9	87%
30 (5)	1500	24	2.0	0.1	100	65	1.0	92%
30 (5)	1500	12	2.2	0.2	100	70	0.9	84%
30 (5)	1500	6	2.3	0.2	100	65	0.9	83%
30 (10)	800	24	3.8	0.8	91	59	0.9	78%
30 (10)	800	12	4.8	2.6	83	61	0.9	85%
30 (10)	800	6	4.8	1.0	82	63	1.0	88%
30 (10)	1200	24	2.0	0.1	100	51	0.8	72%
30 (10)	1200	12	2.3	0.7	100	53	0.8	76%
30 (10)	1200	6	2.6	0.2	99	55	0.9	84%
30 (10)	1500	24	2.0	0.2	100	69	0.8	74%
30 (10)	1500	12	1.8	0.1	100	67	0.8	70%
30 (10)	1500	6	2.1	0.1	100	64	0.9	85%

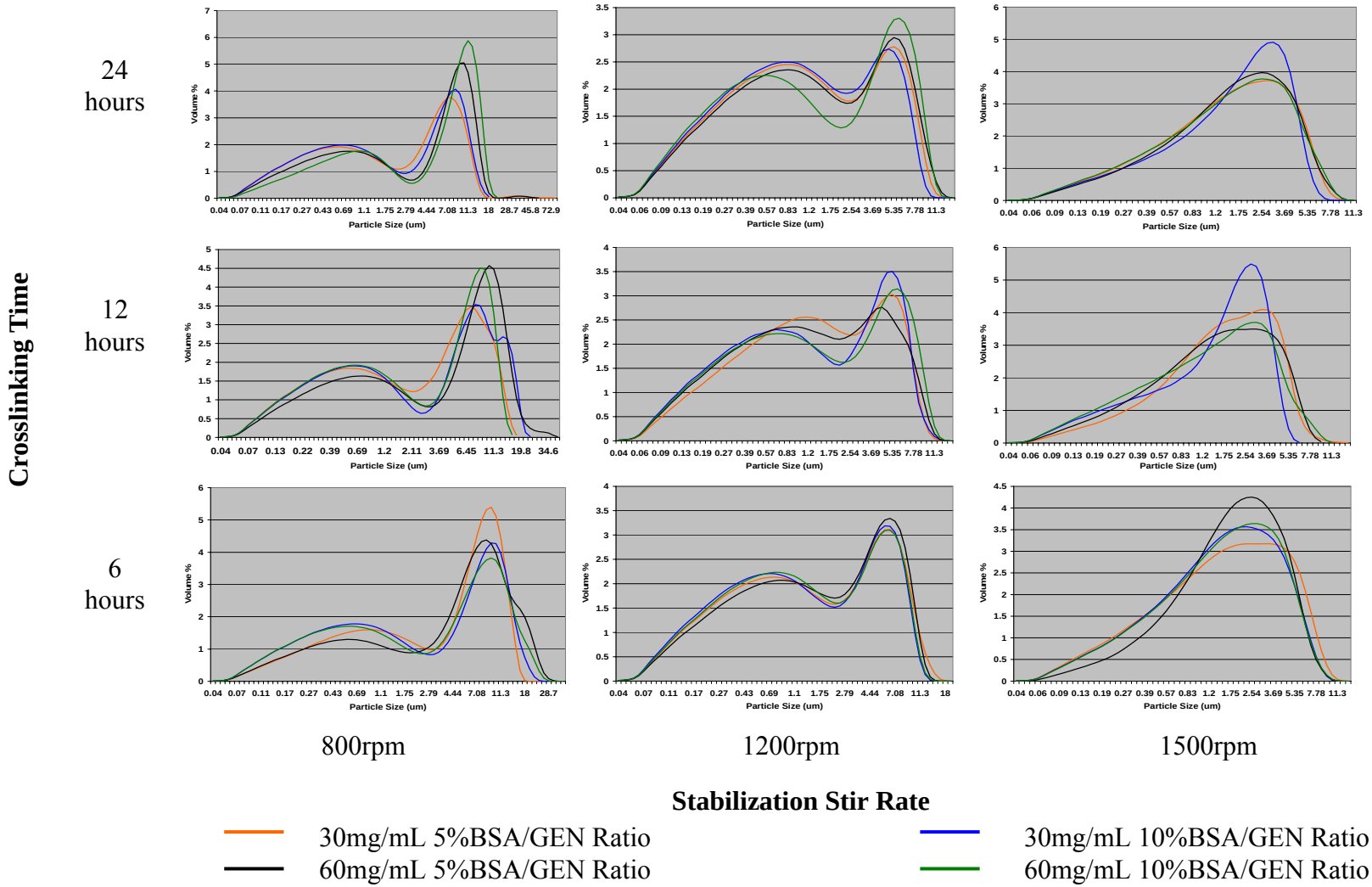

Figure 3-9. Particle size distributions varying genipin concentrations

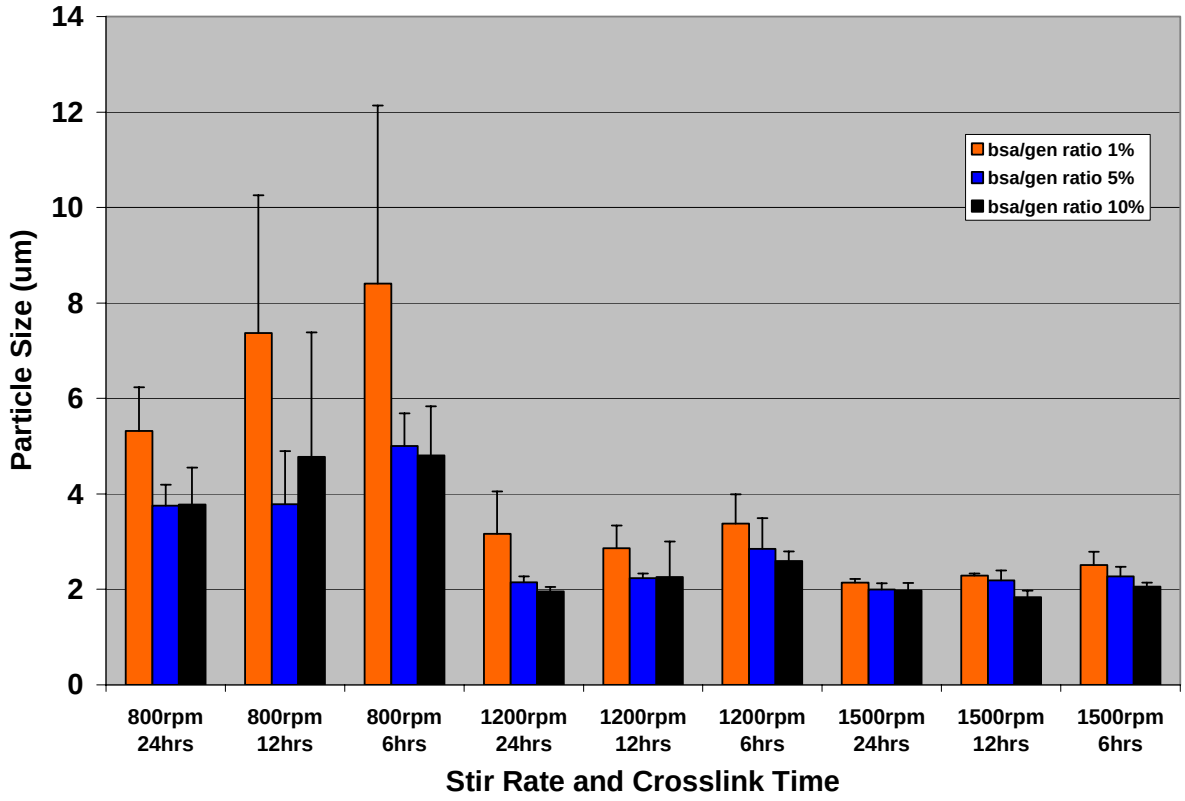

Figure 3-10 Mean particle size varying GEN/BSA ratio

and 24 hours. At the low level stir rate the shape of the particle size distribution curve becomes a more defined bimodal function with increasing crosslink time. The shape of the distribution curve at the medium stir rate level mimics that of the lower level with a higher volume percent of the two distributions. The high level stir rate produced a distribution curve resembling a more normal distribution. Span values confirm these results. Span values increase from 800rpm to 1200rpm and decrease from 1200rpm to 1500rpm. The low values of span denote a narrow particle size distribution. Actual product yield averaged 0.9 grams for each condition. Percent theoretical yield is higher for mesospheres synthesized with the 30mg/mL genipin solution than with the 60mg/mL genipin solution at each level GEN/BSA ratio. Percent theoretical yield is also higher for the lower level GEN/BSA ratio (5% w/w) for both genipin solution concentrations.

GEN/BSA ratio

The process conditions of synthesized batches are summarized in Table 3.8. The GEN/BSA ratio varied while all other variables were held constant. Mean particle size data and other pertinent statistics are summarized in Table 3.9. A graphical summary of mean particle size and particle size distribution is shown in Figures 3.7 and 3.8. A Holm-Sidak test confirms a statistical difference among the three levels of GEN/BSA ratio ($p \leq 0.001$). GEN/BSA ratio affects particle size where mean particle size decreases with increasing GEN/BSA ratio. A statistically significant difference exists when comparing GEN/BSA ratios of 1% and 5% or 1% and 10% but when comparing 5% and 10%. An interaction factor exist between stir rate and GEN/BSA ratio at the low stir rate level of 800rpm however at the middle and high stir rate level no such interaction level is apparent. As has been shown under the previous primary factors a statistical difference in mean particle size exists between stir rates of 800rpm and 1200rpm or 800rpm and 1500rpm but not between 1200rpm and 1500rpm. Again no interaction factor is apparent between crosslink time and GEN/BSA ratio. The previously described trend of span values was true for this set of experiments. Span values increase from 800rpm to 1200rpm and decrease from 1200rpm to 1500rpm. Actual product yield was highest at the medium GEN/BSA ratio (5% w/w) averaging 0.9 grams and 0.8 grams for both the low and high (1%w/w,10%w/w) GEN/BSA ratio levels. Percent theoretical yield was also highest at the 5% (w/w) GEN/BSA level averaging 87% for 5% (w/w) GEN/BSA, 84% for 1% (w/w) GEN/BSA and 79% for 10% (w/w) GEN/BSA ratio.

Discussion

We begin this discussion by defining suspension crosslinking. It is composed of three primary steps: formation of small aqueous droplets in an water-in-oil emulsion, hardening of the

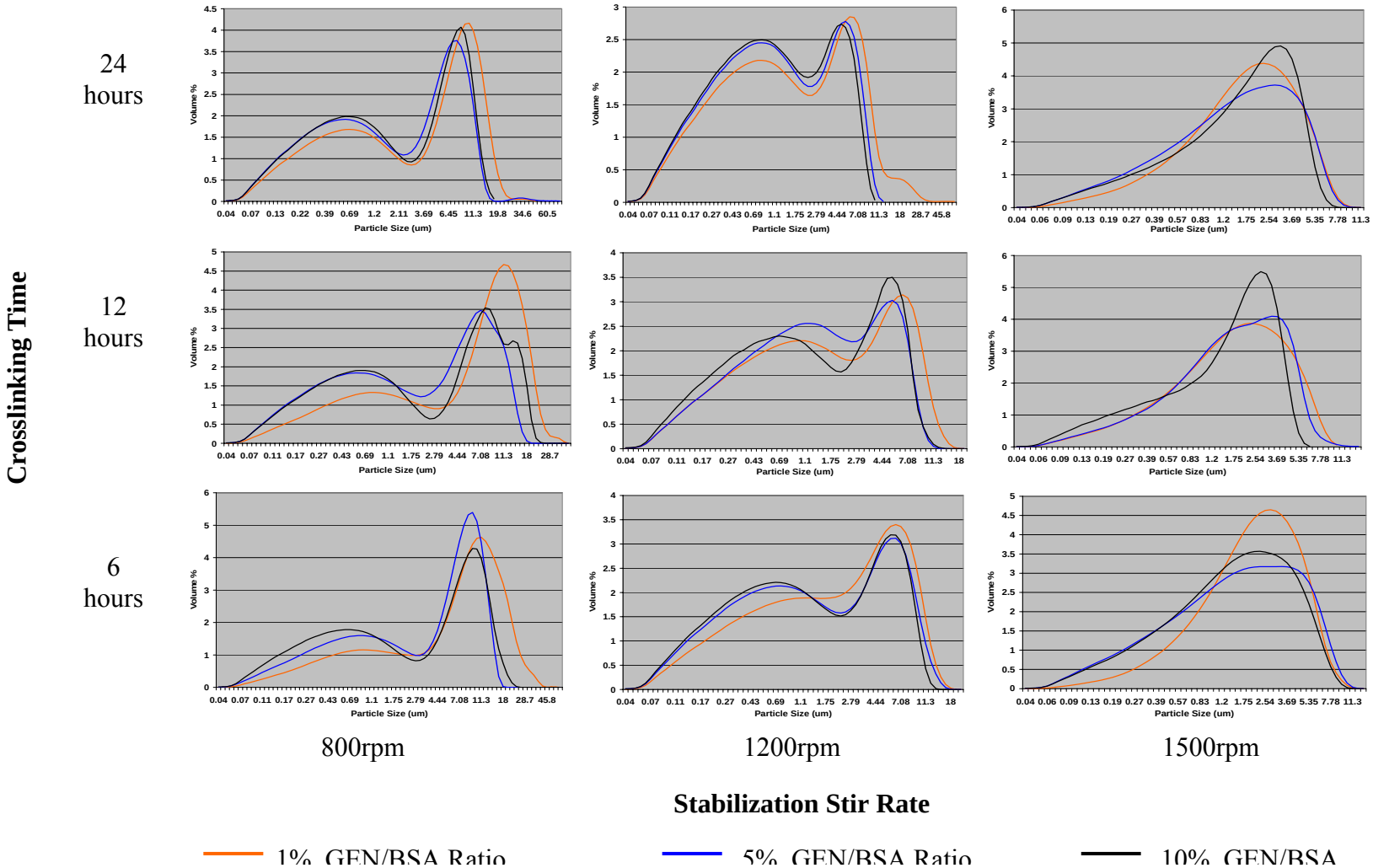

Figure 3-11. Particle size distributions varying GEN/BSA ratio

droplets through covalent crosslinking and recovery of the crosslinked particles[94]. The focus of this work was on controlling particle size and distribution of genipin crosslinked albumin mesospheres for use as controlled release drug delivery devices. We wanted to produce particles in the size range of 1μm to 10μm with a narrow size distribution so it was important to determine to what extent various processing factors affected particle size and size distribution. In a 1989 review Gupta and Hung[95] summarized the factors affecting size and size distribution of albumin microspheres Of this list we choose to investigate protein solution concentration, suspension agent solution concentration, crosslinker solution concentration, protein/crosslinker ratio, stirring speed and crosslinking time. These factors seemed particularly important based on previous work involving glutaraldehyde crosslinked BSA microspheres and genipin crosslinked gelatin microspheres.[3, 5] Bovine serum mesospheres were synthesized using dispersion suspension crosslinking. This work details both trends within each independent variable and interaction factors between the variables.

The hypotheses of decrease in mean particle size with increasing CAB solution concentration and increasing emulsion stabilization stir rate were confirm through experimentation. Longo[96] found that continuous phase concentration was important because low continuous phase concentration would be insufficient to produce spherical particles and too high a concentration resulted in a difficult time removing excess dispersant during washing. Ultimately Longo's work showed that using a concentrated polymer solution as the continuous phase produced smooth spherical particles with a wide particle size distribution. It is well documented throughout literature that within a set design apparatus increasing stir rate or dispersion energy produces smaller particles[3, 5, 10, 95-98]. This can be explained by studying and understanding the concepts of emulsions and droplet formation.

Droplet formation in a suspension system is a dynamic process balancing droplet break-up and coalescence. Average droplet size is primarily controlled by synthesis apparatus design, viscosity of the two phases and mixing speed where the size distribution is primarily controlled by uniformity of the mixing force throughout the suspension mixture. The more uniform the mixing process the more uniform the size of the droplets[94]. Emulsions are dispersions of immiscible or in some cases partially miscible liquids. Our system is further classified as a dispersed microemulsion. Emulsions are thermodynamically unstable and will break up without the addition of a surfactant or emulsifying agent. Proteins contain hydrophilic tails and hydrophobic heads and undergo weak preferential adsorption at the water-oil interface. This slight denaturing of the protein acts as self stabilization surfactant in the emulsion.[94, 97, 99] The volume fraction of the dispersed phase in our system is low which also helps to stabilize the emulsion. High viscosity of the continuous phase also contributes to the stabilization of droplets by inhibiting coalescence[96, 99].

Droplet break-up depends on the type of flow in the apparatus. Flow is described as turbulent (chaotic), laminar (well defined), or transitional (somewhere in between). Turbulent flow is found near the propeller while laminar flow is found at distances away from the propeller.[100, 101] Due to the geometry of our synthesis apparatus described earlier flow in the system is turbulent so we can use the boundary layer shear force model to describe droplet breakup. Hinze[102] was the first to establish a basis for droplet break-up in which surface and viscous forces contribute to droplet stabilization. He's theory states that viscous shear stress of the continuous phase deform the droplet and the droplet is broken when viscous shear stress of the continuous phase can overcome surface tension forces and viscous stress of the dispersed phase. In a stirred tank droplet break-up will occur in a small zone along the edge of the

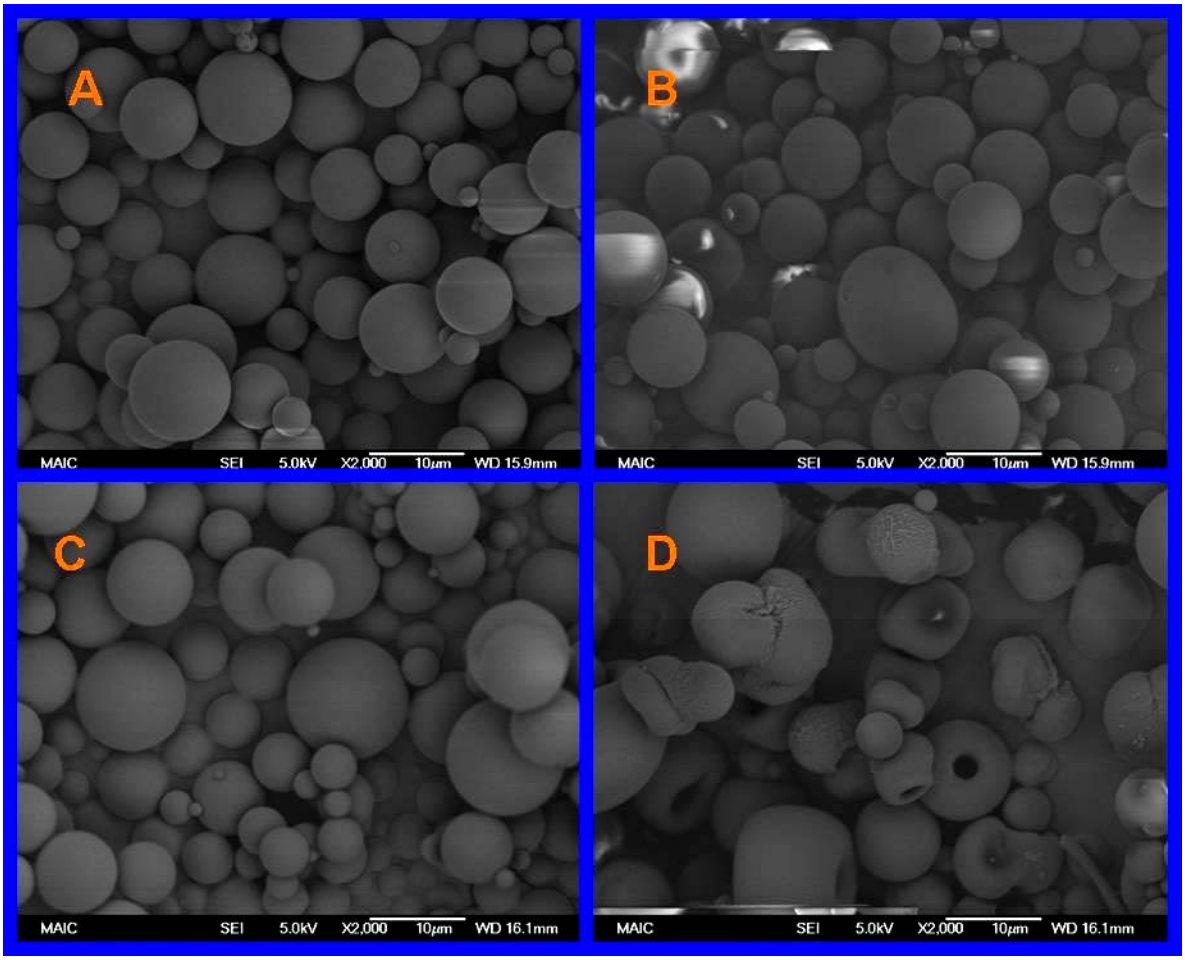

Figure 3.12. SEM micrographs (magnification 2000 X) of mesospheres at varying crosslink times A) 24 hours B) 12 hours C) 6 hours D) 3 hours

the continuous phase can overcome surface tension forces and viscous stress of the dispersed phase. In a stirred tank droplet break-up will occur in a small zone along the edge of the propeller blade where shear rate is the highest. The dynamic equilibrium between droplet breakup and coalescence will determine the size distribution of the aqueous protein droplets in the CAB solution[94, 98, 102-105]. The results presented on decrease in mean particle size with increasing stir rate and CAB solution concentration are explained very well by this theory of droplet formation and stabilization.

Microsphere particles result from a gradual hardening of the droplets formed during emulsion. To inhibit coalescence of droplets crosslinking occurs under constant stirring though

not at as high a rate as emulsion. The most important factor in crosslinking microspheres is having sufficient supply of functional groups so protein solution concentration is an important factor. Others factors such as crosslinker concentration or crosslink time will control the crosslink density of the particles. Crosslink density will ultimately control drug uptake, mesosphere degradation and drug release all of which are factors discussed in later chapters[94]. Crosslinking time was the first variable investigated. Mesosphere batches were prepared using crosslinking times of 3, 6, 12 and 24 hours. Electron microscopy showed three hours of crosslinking was insufficient to synthesis spherical mesospheres while crosslinking times of six, twelve and twenty-four hours produced spherical particles (Figure 3.10). The hypothesis that mean particle size would increase with increasing crosslink time was not confirmed. In fact for this system crosslink time seems to have little to no affect on particle size or size distribution.

Willmott et al found that increasing the glutaraldehyde/protein ratio produced larger particles. The reaction time between glutaraldehyde and albumin is only a few seconds so the rate of the reaction depends on the concentration of glutaraldehyde. At high concentrations of glutar-aldehyde the microspheres may solidify before maximal dispersion has occurred[106]. The reaction between albumin and genipin is a slow rate reaction so it is reasonable to believe that maximal dispersion is achieved before the crosslinking reaction can begin and therefore particle is governed by initial droplet formation. To add the crosslinker solution stirring of the system is stopped momentarily and the crosslinking stir rate is reduced. This may cause some coalescence resulting in a broader particle size distribution at low emulsification stabilization stir rates. Only at low GEN/BSA ratios will mean particle size become a function of GEN/BSA ratio. An important observation was the color change of the mesosphere solution during the crosslinking

reaction from white to light green to dark blue with increasing crosslink time. This color change is attributed to the reaction between genipin and amino acids[107].

The concentration of the protein solution was an important factor to investigate. El-Mahdy[108] presented work suggesting that low concentrations of albumin solutions would be insufficient in producing spherical particles and ultimately decreasing the albumin concentration produced a decrease in mean particle size. Based on previous work done by Hadba[3], Cuevas[5] and Luftensteiner[109] it was hypothesized that particle size would increase with increasing protein concentration. The general explanation being that an increase in protein concentration would increase the viscosity of the aqueous phase making it harder for droplets to break up[95]. This result was not confirmed during experimentation as protein concentration had no affect on particle size. Gallo[97] reported the opposite trend of increasing mean particle size with decreasing protein concentration. No concluding explanations can be offered at this time with respect to protein concentration and mean particle size.

CHAPTER 4
SYNTHESIS OF GENIPIN CROSSLINKED BOVINE SERUM ALBUMIN MESPHERES: FACTORS THAT AFFECT DEGRADATION

Introduction

The purpose of this research was to establish which processing conditions in the synthesis of bovine serum albumin (BSA) mesospheres controlled macroscopic degradation. We also evaluated how storage conditions of synthesized mesospheres affected degradation. Previous analysis evaluated processing conditions that controlled particle size and particle size distribution. The goal was to produce spherical bovine serum albumin (BSA) mesospheres using dispersion suspension crosslinking with dry particle size range of 1-10μm. The effects of processing factors: stirring rate, BSA concentration, CAB concentration, genipin concentration, crosslinking time and GEN/BSA ratio were investigated. Of these factors stirring rate during emulsion stabilization, CAB concentration and GEN/BSA ratio had the greatest affect on particle size. The fasted stir rate of 1500 rpm produced a normal particle distribution from 1μm to 10μm while GEN/BSA ratios of 5% or 10% (w/w) gave particles with an average mean size of 2μm. Although the remaining factors of BSA concentration and genipin concentration showed no significant affect on particle size there was some suspicions that they could affect degradation kinetics. Based on these results and assumptions we evaluated crosslinking time, GEN/BSA ratio, BSA concentration, genipin concentration and storage conditions for their affect on macroscopic degradation. The change in mean particle size from dry to wet (swollen ratio) and protein elution during enzymatic degradation were used as numeric outcome.

Materials and Methods

Materials

Bovine serum albumin (BSA) and cellulose acetate butyrate (CAB) were purchased from Sigma-Aldrich. 1, 2 Dichloroethane (DCE), Biorad® Protein Assay Kit, Tween 80 and acetone were

Table 4-1. Mesosphere formulations investigated for degradation kinetics

BSA (%)	GEN (mg/mL)	GEN/BSA Ratio% (w/w)	Crosslinking Time(hours)	Mean Particle Size (μm)	%> 1um	%< 10um
20	30	5	6	2.3	65	100
20	30	5	12	2.2	70	100
20	30	5	24	2.0	65	100
10	30	5	24	2.3	75	100
30	30	5	24	2.3	61	100
20	30	1	24	2.1	72	100
20	30	10	24	2.0	69	100
20	60	5	24	2.1	67	100
20	60	10	24	2.0	64	100

purchased from Fisher Scientific. Genipin (GEN) was produced by Wacko Company and purchased from the distributor City Chemical. Ultrapure water was prepared in the laboratory using a Barnstead NANOpure.

Methods

Solution preparation

BSA, CAB, and genipin solutions were prepared by methods described in Chapter 3.

Phosphate buffer saline solution (0.1M) was prepared by first preparing sodium phosphate monobasic and sodium phosphate dibasic counter salt solutions. 20.70g of sodium phosphate monobasic salt was dissolved in 1.5L ultrapure water to a final pH=4.6. 42.59g of sodium phosphate dibasic salt was dissolved in 3.0L of ultrapure water. In a 4L Erlenmeyer flask the two counter salts were mixed at a ratio of 1 part monobasic and 2.9 parts dibasic solution. The mixture was stirred and pH was adjusted until pH=7.4. Finally the solution was filtered using a 0.22μm cellulose acetate filter.

The enzyme digestion buffer was prepared by dissolving 720mg ethylenediame tetracetic acid (EDTA) disodium salt., 80 mg L-cysteine hydrochloride hydrate, 50 mg papaya latex papain and 50 mg bacterial protease Type VIII in 100mL sterile filtered 0.1M phosphate buffered saline solution (pH=7.4).

Mesosphere synthesis

Based on the results of the particle size data from Chapter 3 nine different mesosphere formulations were chosen to be evaluated for degradation kinetics. All mesosphere formulations synthesized with 3% (w/v) CAB were eliminated from further considerations. Formulations chosen were those that produced a normal particle size distribution with particle size range from 1μm-10μm where greater than 50% were larger than 1μm and 95% were smaller than 10μm (Table 4-1).

Scanning electron microscopy

Field emission scanning electron microscopy was used to examine the morphology of synthesized mesospheres. Dry mesospheres were mounted on carbon tape on an aluminum SEM stub. Stubs were sputter coated with carbon for two minutes using a Technix Hummer V Sputter Coater. The samples were then analyzed using Joel 6335F field emission microscope housed at the Particle Engineering Research Center (PERC) at 5KeV accelerating voltage and a working distance of 15mm.

Swelling study

The wet particle size and particle size distributions of bovine serum albumin mesospheres was measured using a Coulter LS 230 particle size analyzer housed at the Particle Engineering Research Center (PERC). For each condition sample three 1% (w/v) mesosphere suspensions was prepared in 3mL of 0.55% (v/v) Tween 80-0.1M PBS solution. Full hydration of the mesospheres was reached in 30 seconds. The suspension was sonicated for 15-30 seconds. The suspension was added drop-wise to the chamber until obscuration read between 7% - 9% and PIDS read between 37% - 43%. Suspended mesospheres scattered light from a laser source and was detected by silicon photo-detectors. A BSA optical model translated light intensity measurements into a particle size distribution as a volume percent in discrete size blocks. The

mean, median, standard deviation and particle size quartiles and other statistical data for each batch were determined using Coulter software.

Mesosphere digestion

Genipin crosslinked bovine serum albumin mesospheres were weighted in 10mg samples into a 2 mL centrifugal filter tube (Ultrafree-CL centrifugal filter device; low binding 0.1µm membrane). Digestion buffer (1.5mL) was added to the test tube and samples were incubated at 37ºC under stirred conditions. At predetermined time periods every 10minutes for the first 30 minutes then every 30 minutes up to two hours, then every two hours up to six hours, then every 12 hours up to 24 hours.

Biorad® protein assay was used to determine protein concentration. Maximum absorbance for an acidic solution of Coomassie Brilliant Blue G-250 dye shifts from 465nm to 595nm when protein binding occurs. The Coomassie blue dye binds primarily to basic and aromatic amino acid residues. The assay dye reagent concentration is a solution containing Coomassie blue dye, phosphonic acid and methanol. The dye reagent was diluted 1 part dye reagent concentrate to 4 parts distilled water and filtered with a 0.22µm cellulose acetate filter for use.

To accurately calculate BSA concentration of samples a BSA standard curve was created in the linear range for BSA (0.2 to 0.9mg/mL). The absorbance of five dilutions of a 1mg/mL BSA solution was measured. In a 1.5mL cuvette 30µL aliquot and 1.5mL of dye reagent were mixed. The solution was incubated at room temperature under constant stirring for 10 minutes. Absorbance was measured at 595nm. Measurements were taken in triplicate for each standard solution and the standard curve was accepted if the coefficient of determination (R^2) was 0.99 or greater.

Table 4-2. Processing conditions for swelling/degradation study

Processing Condition	Level
BSA Concentration (% w/v)	10, 20, 30
CAB Concentration (%w/v)	5
Aqueous Phase Volume (mL)	5
Organic Phase Volume (mL)	45
D/C Ratio	11.1
Genipin Concentration (mg/mL)	30, 60
GEN/BSA Weight Ratio	1, 5, 10
Stirring Rate During Emulsion Stabilization (rpm)	1500
Stirring Rate During Crosslinking (rpm)	600
Crosslinking Time (hours)	6, 12, 24

Statistical analysis

Microsoft Excel was used to calculate average mean particle size, standard deviation, span, average yield and percent theoretical yield. The statistical software package Sigma Stat was used to identify differences in mean particle size and interactions between the various processing conditions. Four primary factors: BSA concentration, genipin concentration, GEN/BSA ratio and crosslinking time were analyzed using a one way ANOVA was used to measure statistical differences in swollen particle size (n=18). The Holm-Sidak and Tukey methods was used for all pair wise multiple comparisons to isolate exactly which levels of each factor provided a statistical difference in mean particle size. A one way ANOVA was used to measure statistical differences in '% BSA Remaining' at each time point.

Results

Swelling study

We investigated the swollen behavior of genipin mesospheres of various processing conditions (Table 4-2): crosslink time, GEN/BSA ratio, BSA concentration, and genipin concentration. We also compared the swollen particle size of the same formulations at two time intervals (two to four weeks refrigeratored and four to six months room temperature). Generally we expected the results for swollen ratio mimicked that of the dry particle size.

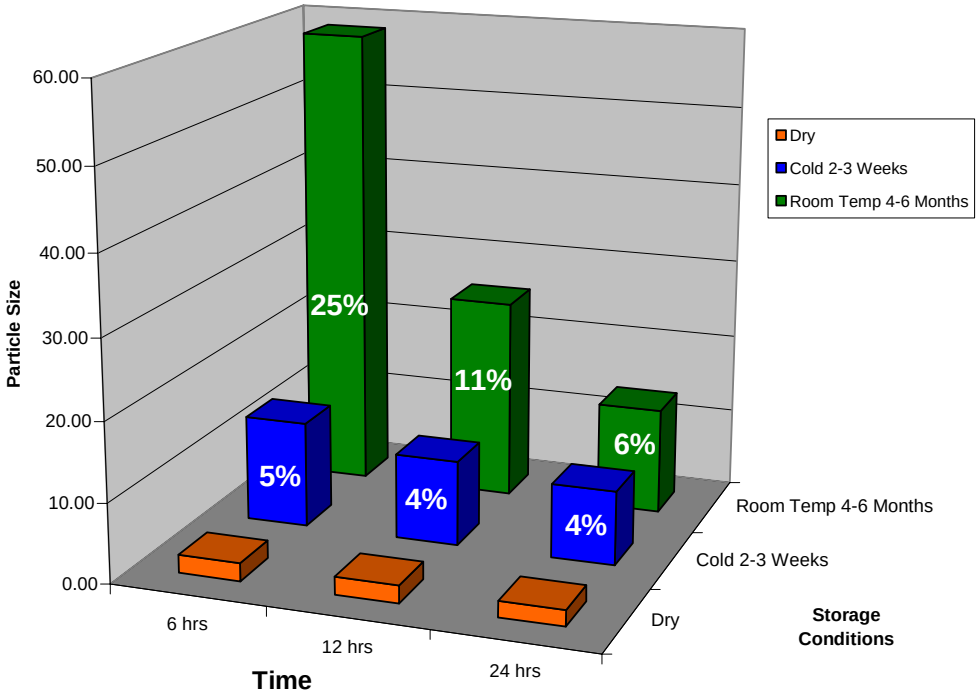

Figure 4-1. Swollen ratio at varying crosslinking times

Crosslinking time. A graphical representation of swollen ratio is found in Figure 4-1. For refrigerator stored mesospheres we find a significant difference in swollen particle size of mesospheres crosslinked for six and twenty-four hours but not between those crosslinked for six twelve or twelve and twenty-four hours. For the same mesospheres stored at room temperature for four to six months were find a significant difference in mean particle size between mesospheres crosslinked for six and twelve and six and twenty four hours but not between twelve and twenty-four hours. This was the expected result because the genipin reaction is quenched at shorter crosslinking time leaving available reactive groups unreacted in the interior of the mesosphere. Swollen ratio decreased with increasing crosslinking time for both cold stored and room temperature stored

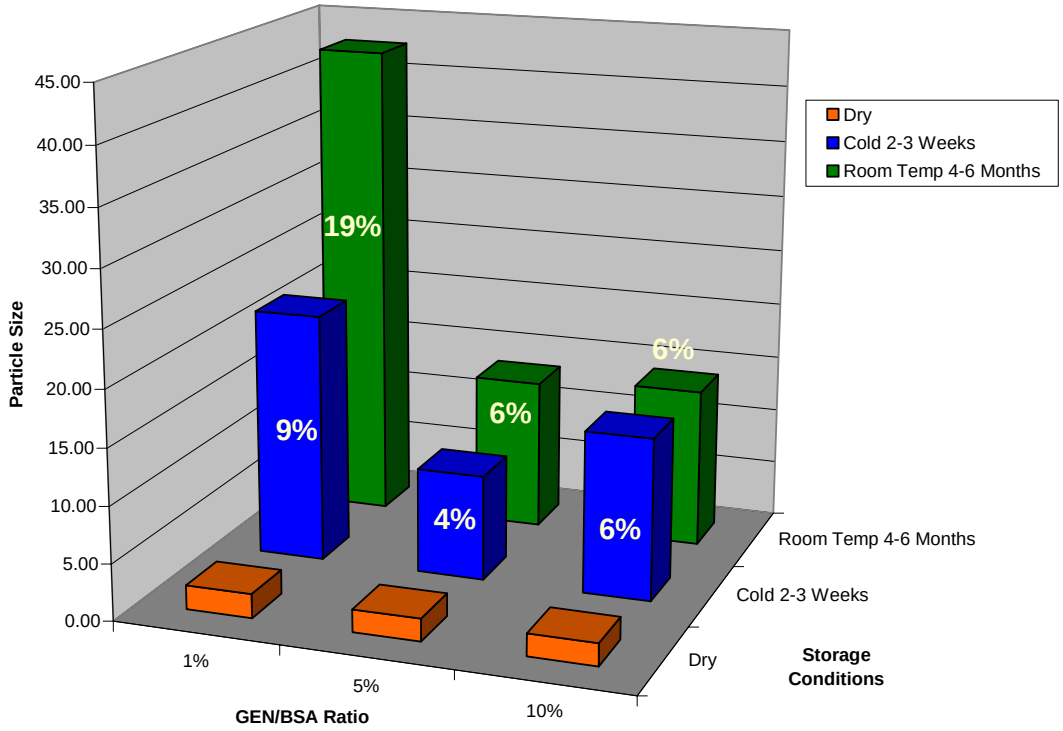

Figure 4-2. Swollen ratio with varying GEN/BSA ratios

mesospheres with a significant difference in mean swollen ratio for mesospheres crosslinked for six and twelve and six and twenty-four hours and room temperature stored. These results suggest that mesospheres with longer crosslinking times will degrade at a slower rate than those synthesized with short crosslinking times.

GEN/BSA ratio. Swollen particle size and swollen ratios of varying GEN/BSA ratios produced mixed results. For cold stored mesospheres swollen particle size showed a minimum at the medium crosslink ratio of 5% (w/w) with no statistically significant differences in mean swollen particle size. For room temperature stored mesospheres mean swollen particle size was a maximum at the minimum crosslinking ratio of 1% (w/w) with a statistically significant difference between the crosslinking ratios of 1% and 10%. Swollen ratios of both cold stored and room followed the

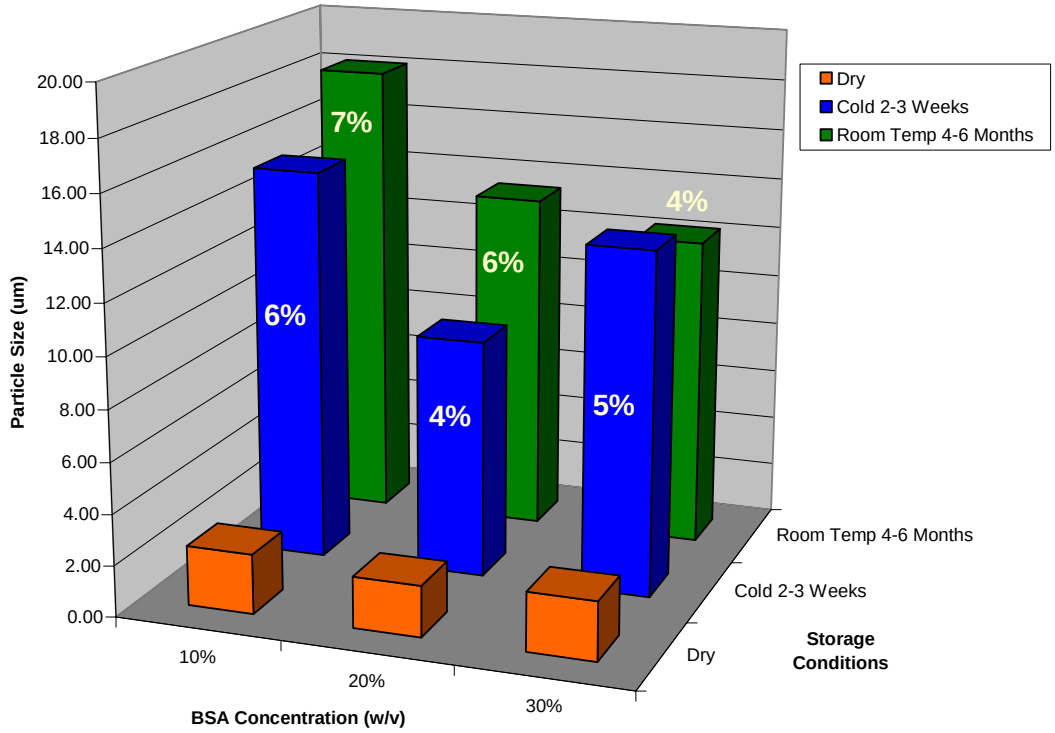

Figure 4-3. Swollen ratios at various BSA concentrations temperature stored

trend of swollen particle size producing a minimum at 5% for cold stored and a maximum at 1% for room temperature stored mesospheres. Though no statistically significant differences resulted the same difference in swollen ratio of room temperature stored mesospheres is produced between crosslinking ratios of 1% and 5% and 1% and 10%. This result along with the minimum swollen ratio produced with cold storage suggests that saturation of available reaction sites is achieved at 5% (w/w) GEN/BSA ratio.

BSA concentration. Mean swollen particle size is expected to decrease with increasing BSA concentration. Higher concentrations of albumin mean increased opportunities for secondary bonding such as hydrogen bonding that will act as crosslinks making swelling of the mesosphere more difficult.

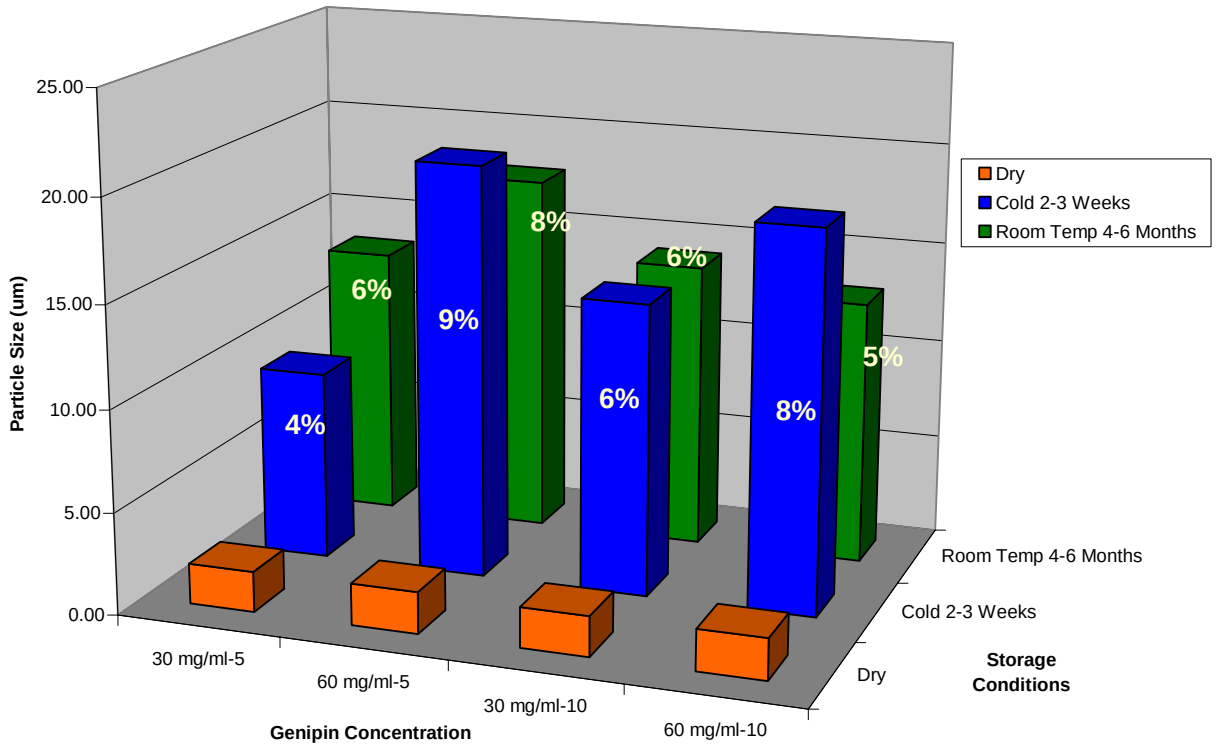

Figure 4-4. Swollen ratios at various genipin concentrations

The results of this study followed that phenomen a. Swollen ratios of both cold stored and room temperature stored mesospheres were low and no significant differences were found between any of the levels of BSA concentration. Enzymatic degradation of mesospheres should be independent of BSA concentration.

Genipin concentration. Genipin concentration was the final factor investigated. Results of swollen particle size did not mimic that of dry particle size. The higher concentration genipin solutions gave larger mean particle size and higher swollen ratios. Though the weight of genipin is the same the actual volume of genipin is lower therefore for the same volume of albumin the ability of genipin to diffuse through the mesosphere is decreased leaving a less crosslinked interior and a microstructure more susceptible to swelling for the higher concentration genipin

solution. However we did not find this to be true of this study. No statistically significant differences were found in comparing any level of particle size or swollen ratio.

Mesosphere degradation study

From the swollen ratio data we hypothesized that crosslinking time and GEN/BSA ratio would most influence enzymatic degradation. Spectrophotometric assay was used to quantify the concentration of solubilized BSA in digestion buffer. Degradation is presented as the total percentage of solubilized BSA in solution versus time.

Crosslinking time. Crosslinking time and storage conditions both affect time of enzymatic degradation Figure (4-5). Generally the longer the crosslinking time the slower the mesosphere

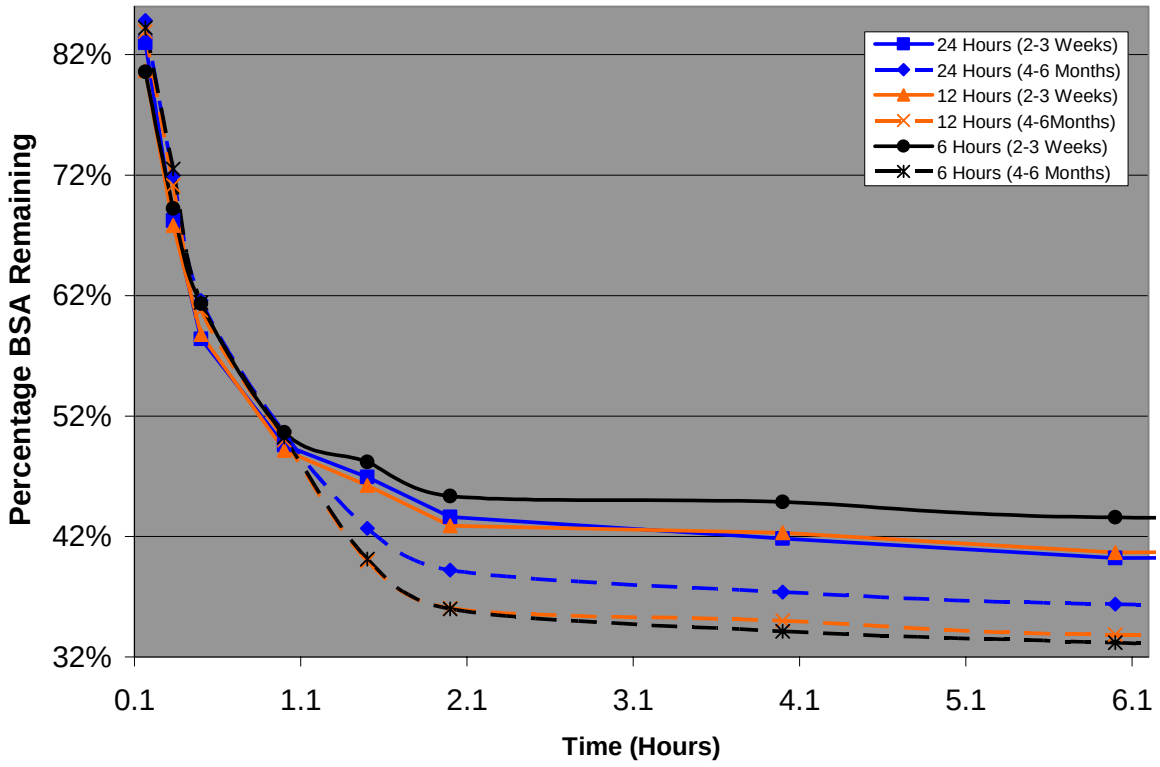

Figure 4-5. Enzymatic degradation versus time at various crosslinking times

degrades. At all levels of crosslinking time the mesospheres that had been stored at room temperature for four to six months prior were statistically different from those stored for two to three weeks with those stored for the longer period degrading to a higher extent that those stored for only two to three weeks. Initially it appears that the mesospheres that were stored for a shorter period of time before testing degrade faster than those stored for longer periods of time. Looking at each storage time independently we find that a significant difference exists in the exent of degradation for crosslinking times of twenty-four and twelve and twenty-four and six hours but between twelve and six hours. Mesospheres crosslinked for the two shorter time periods degrade to a greater extent than those crosslinked for twenty-four hours.

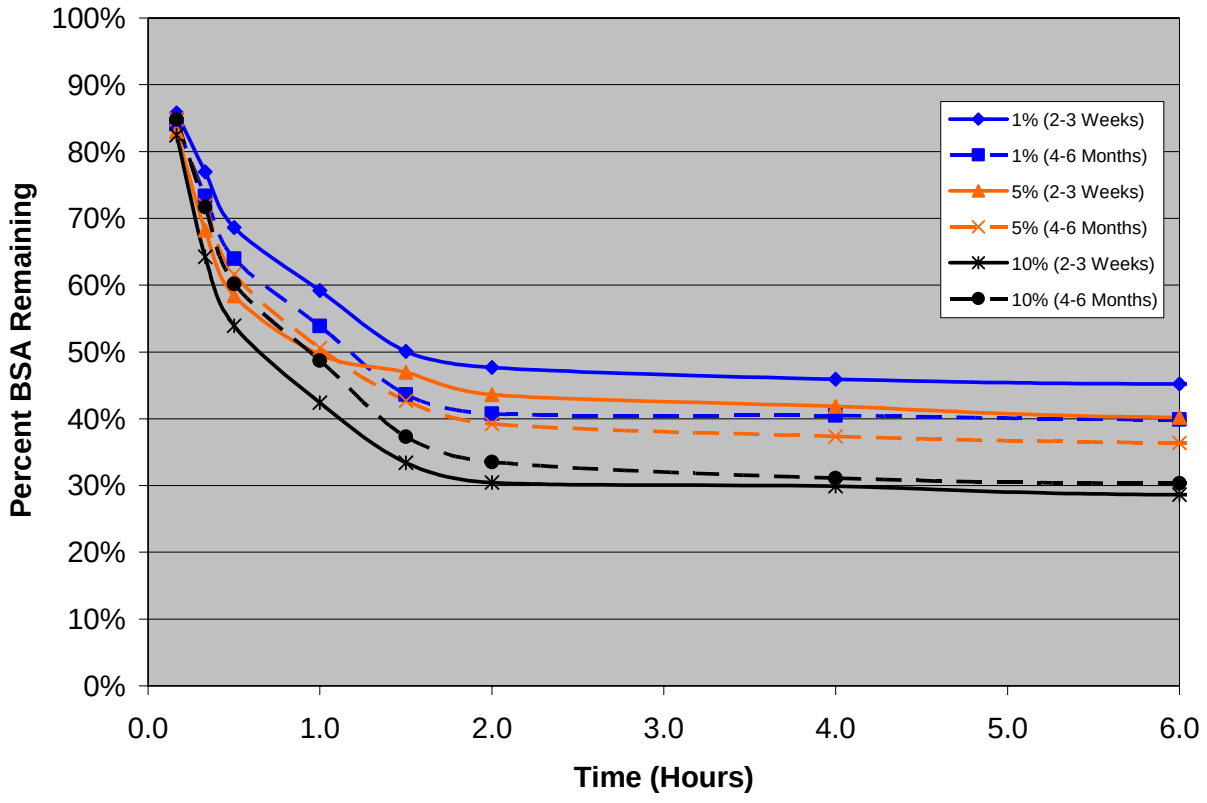

Figure 4-6. Enzymatic degradation versus time at various GEN/BSA ratios

GEN/BSA ratio. As expected GEN/BSA ration affected mesosphere degradation (Figure 4-6). Mesospheres with the short storage period of 2 to 3 weeks degradation was significantly different for GEN/BSA ratios of 1% (w/w) and 10% (w/w) and for 5% (w/w) and 10% (w/w) but not between 1%(w/w) and 5% (w/w). Mesospheres stored for 4-6 months initially degraded at the same rate. After ten minutes GEN/BSA ratios of 1% (w/w) and 5% (w/w) and 1% (w/w) and 10% (w/w) degraded at statistically significant rates. GEN/BSA ratios became statistically significant after one and a half hours of degradation. In the cases stated above the mesospheres with the higher GEN/BSA appear to degrade to a higher extent however this is misleading. One problem with the characterization of BSA is that the genipin-amino acid reaction is characterized by a blue

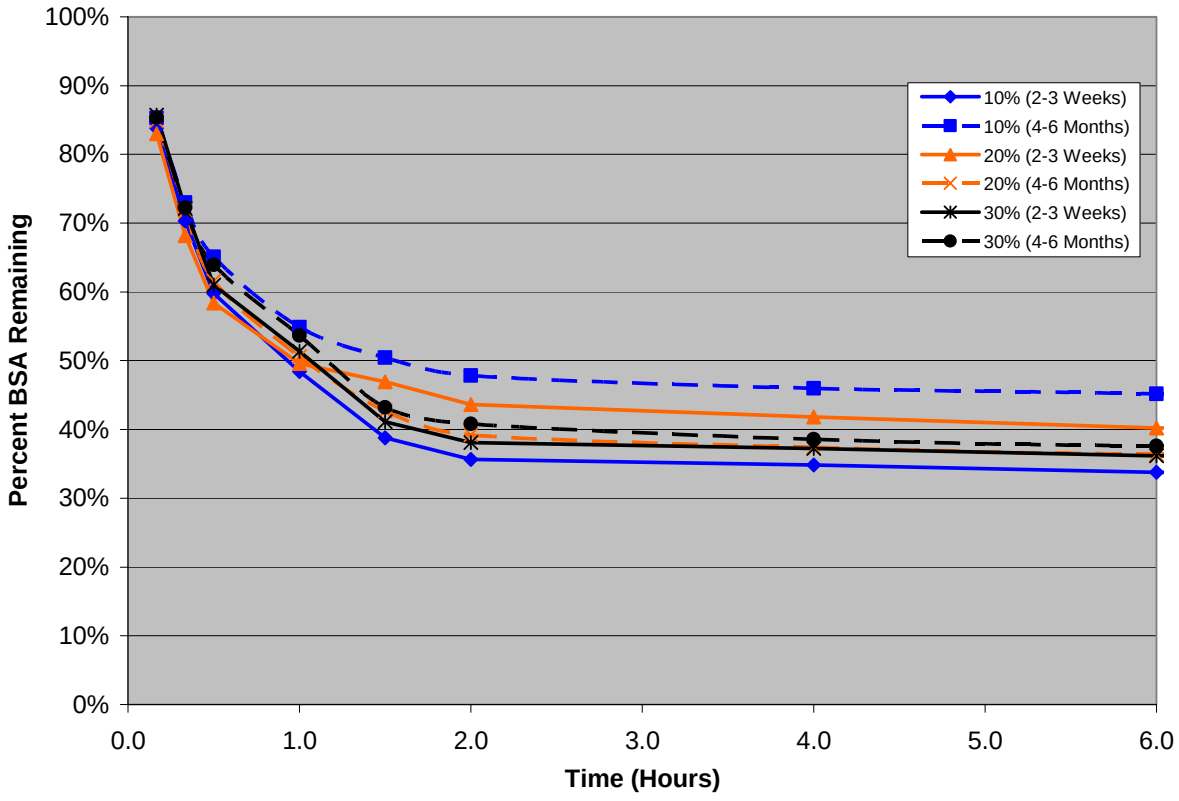

Figure 4-7. Enzymatic degradation versus time at various BSA concentrations

pigment and so is the assay used to quantify the BSA in solution. The blue color of the assay is enhanced by the blue color of the genipin amino acid group reaction and BSA volumes may be overestimated. One way to circumvent this problem would be to use a ninhydrin assay which measures free amino acid groups.

BSA concentration. Mesospheres with 20% (w/v) BSA degrade at a rate between that of 10% (w/v) and 30% (w/v) for both storage lengths (Figure 4-7). For each level of BSA concentration the longer storage length resulted in greater degradation extent. The enhancement of the assay color was also a factor in this study.

Genipin concentration. For all levels of genipin concentration the longer storage length resulted in greater degradation extent (Figure 4-8). There was a synergistic relation between

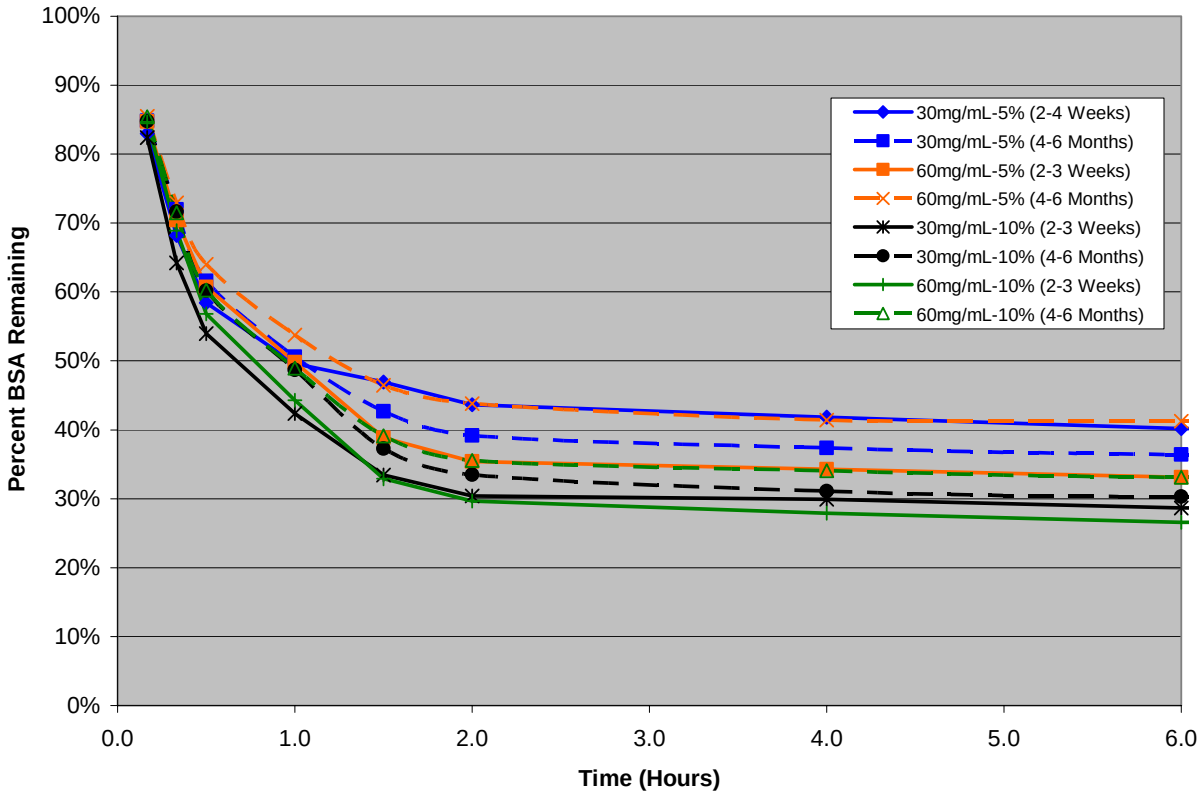

Figure 4-8. Enzymatic degradation versus time at various genipin concentrations

genipin concentration and GEN/BSA ratio. Mesospheres synthesized with the 30mg/mL genipin solution degraded at a statistically different ate than those synthesized with the 60mg/mL genipin solution. The enhancement of the assay color was also a factor for the higher genipin concentration solution in this study. Mesospheres with longer storage length had lost the blue pigment of the reaction so we evaluate degradation rates based on these values. Longer storage lengths show that the higher genipin concentration degraded at a higher rate and greater extent.

Discussion

The theory of the mechanism of crosslinking mesospheres is very simple. When genipin is added to the reaction vessel crosslinking starts at the surface of the droplets reacting with the available amino acid groups. Genipin diffuses through the interior of the mesosphere reacting with as many available amino acid groups as possible. When the genipin has penetrated the entire sphere the remaining solution diffuses out of the mesospheres, is removed during washing and the mesospheres are homogeneously crosslinked. If the concentration of genipin is lower than saturation then a case hardened mesosphere is produced where the surface is highly crosslinked where the interior is less crosslinked. We refer to the measure of case hardening or inhomogeneous. We use the measure of swollen particle size or more specifically the swollen ratio (percent change in particle size from dry to swollen) as the numeric representation of this phenomena and use the value as a predictor of degradation. Because swelling by definition is the incomplete dissolution it provides a good base to predict degradation behavior. Degradation is defined macroscopically as the destruction or dissolution of mesospheres and microscopically as the breaking of individual bonds. Since the application of these mesospheres is the delivery of a drug through degradation of the mesosphere matrix the macroscopic definition holds a higher priority. As crosslink desity increases the number of bond to break increases and degradation slows. Based on the swelling and degradation of the nine formulations of mesospheres

investigated in this study it was determined that the most suitable formulation to continue on to drug loaded was that of a 20% BSA, 5% CAB solution, 30mg/mL genipin solution, 5% GEN/BSA ratio with a dispersion stirring rate of 1500 rpm and a crosslinking period of 24 hours. This formulation resulted in minimal swelling and medium degradation rate.

CHAPTER 5
SYNTHESIS AND EVALUATION OF DRUG LOADED GENIPIN AND GLUTARALDEHDE BOVINE SERUM ALBUMIN MESOSPHERES

Introduction

The purpose of this research was to synthesize and evaluate drug loaded mesospheres formulations. Both genipin and glutaraldehyde crosslinked albumin-drug formulations were prepared. From the results of the two previous chapters the optimal blank mesosphere processing conditions were determined to be 20% BSA solution, 5% CAB solution, 30mg/mL genipin solution, 5% GEN/BSA ratio with a dispersion stirring rate of 1500 rpm and a crosslinking period of 24 hours. Blank mesospheres were synthesized using the above conditions and post loaded with drug. In situ loaded mesospheres were also prepared using the same processing parameters. Both cisplatin and cyclophosphamide were investigated as varying drug concentrations. Dry particle size of drug loaded mesospheres was compared to that of blank mesospheres. Drug loading, *in vitro* release and cytotoxicity of were investigated.

Materials and Methods

Materials

Bovine serum albumin (BSA) and cellulose acetate butyrate (CAB), cyclophosphamide (Cat # C0768), 4-(4-nitrobenzyl) pyridine, triethylamine, acetic acid (glacial), sodium acetate trihydrate, sodium bisulfite, and dimethyl sulfoxide (DMSO) were purchased from Sigma-Aldrich. 1, 2 Dichloroethane (DCE) and acetone were purchased from Fisher Scientific. Genipin (GEN) was produced by Wacko Company and purchased from City Chemical. Cisplatin was purchased from Fisher Scientific. Ultrapure water was prepared in the laboratory using a Barnstead NANOpure. Muriune Lewis lung carcinoma cells were purchased from ATCC (Cat # CRL-1642). Dulbecco's modified Eagle's media was purchased from Sigma Aldrich. CytoTox 96 Non-Radioactive Cytotoxicity Assay was purchased from Promega

Methods

Solution preparations

Drug solutions were prepared by dissolving the appropriate mass of solid drug water or 10% DMSO.

BSA solutions were prepared by dissolving the appropriate amount of solid BSA in the previously prepared drug solution. These albumin-drug solutions required further characterization after preparation because solid albumin powder is hygroscopic absorbing approximately 10% of its weight in water. The true concentration was measured. Approximately 1 ml of BSA solution was dried at 130ºC on a Mettler LJ16 Moisture Analyzer to determine the dry weight per volume percent. Concentration was adjusted until true concentration was achieved to 20.0% ± 0.5. The drug solution concentration was accounted for in this calculation. Density of the solution was determined gravimetrically and weight percent protein was used to determine the weight per volume concentration of the albumin solution.

Cellulose acetate butyrate solutions were prepared by dissolving the appropriate mass in DCE to a final concentration of 5% (w/v).

Genipin solutions were prepared by dissolving the appropriate mass in acetone to a final concentration of 30mg/ml or 60mg/ml.

Glutaraldehyde solutions were prepared by vacuum distilling 25% aqueous glutaraldehyde solution and recovering the glutaraldehyde distillate. The distillate was then dissolved in DCE to a final concentration of 40mg/ml.

0.1M phosphate buffer saline solution was prepared by first preparing sodium phosphate monobasic and sodium phosphate dibasic counter salt solutions. 20.70g of sodium phosphate monobasic salt was dissolved in 1.5L ultrapure water to a final pH=4.6. 42.59g of sodium phosphate dibasic salt was dissolved in 3.0L of ultrapure water. In a 4L Erlenmeyer flask the two

counter salts were mixed at a ratio of 1 part monobasic and 2.9 parts dibasic solution. The mixture was stirred and pH was adjusted until pH=7.4. Finally the solution was filtered using a 0.22μm cellulose acetate filter.

The enzyme digestion buffer was prepared by dissolving 720mg ethylenediame tetracetic acid (EDTA) disodium salt., 80 mg L-cysteine hydrochloride hydrate, 50 mg papaya latex papain and 50 mg bacterial protease Type VIII in 100mL sterile filtered 0.1M phosphate buffered saline solution (pH=7.4).

0.2M sodium acetate buffer (pH=4.6) was prepared by dissolving glacial acetic acid (7.0318g/L) and sodium acetate trihydrate (11.2827g/L) in ultrapure water.

NBP solution was prepared by dissolving solid 4-(4-nitrobenzyl) pyridine in acetone at a 3.3% (w/v) concentration.

Triethylamine solution was prepared by mixing triethylamine in acetone at a 10% (v/v) concentration.

Sodium bisulfite buffer was prepared by dissolving solid sodium bisulfite in sodium acetate buffer.

Mesosphere synthesis

Non drug loaded BSA mesospheres for post-loading mesospheres were prepared using the optimal formulation determined from chapters 3 and 4. Specifically 5ml of 20% (w/v) aqueous BSA solution was added to a 300mL Labonco lyophilization flask containing 45ml of 5% (w/v) CAB/DCE solution. The mixture was stirred for 20 minutes at 1500rpm on either a Lightnin (model #L1V08) high speed mixer. Genipin solution was added to the reaction vessel to stabilize the mesospheres and stirring rate reduced to 600rpm. The crosslinking reaction continued for 24 hours then 50mL of acetone was added to the reaction vessel and stirring continued for one additional hour. Particles were collected through centrifugation on a Dynac II benchtop (Clay

Adams) by transferring approximately 25mL of solution to each of four 50mL centrifuge tubes, adding acetone to the 40mL mark and centrifuging for 5 minutes at 2000 rpm. The supernant CAB/acetone mixture was decanted, the mesosphere pellet was resuspended in acetone and centrifuged for 10 minutes at 2000 rpm for three additional washes. Particles were then air dried.

Post drug loading mesosphere synthesis

Mesospheres were post-loaded using the following procedure: 100mg of mesospheres were weighted into a 10 x 75mm disposable glass culture tube. A few drops of acetone were added to insure minimal agglomeration of the mesosphere pellet and then 4mL of drug solution was added. The mixture was vortexed for 1 minute and placed on a roto-tumbler for 12 hours. The samples were recovered by centrifugation for 10 minutes at 2000 rpm using the Dynac II bench top centrifuge. The supernatant was carefully collected for analysis. The samples were washed with acetone three times. The supernatants were carefully collected in each of the washing steps. The collected supernatants were stored for spectrophotometric analysis to determine the concentration of drug remaining in the wash solutions.

Cyclophosphamide is highly water soluble so drug solutions were prepared in ultrpure water at a low concentration of 9mg/mL and a high concentration of 36mg/mL. The solubility of cisplatin in water at room temperature is 1mg/mL. To increase the solubility of cisplatin in water cisplatin solutions were heated and a concentration of 1.8mg/mL was achieved. By dissolving cisplatin in a heated 10% (v/v) DMSO a concentration of 15mg/mL was achieved.

In situ drug loading mesosphere synthesis

In situ loaded mesospheres were prepared using standard mesosphere synthesis procedures replacing the standard 20% (w/v) BSA solution with BSA-drug solution. Drug solutions of cyclophosphamide (CTX) and cisplatin (CDDP) were first prepared then the appropriate weight of BSA was dissolved in the solution to a concentration of 20% (w/v). As with all other BSA

solutions the concentration was determined by moisture analysis and the density was determined gravenemetrically. *In situ* drug loaded mesospheres were prepared using mesosphere synthesis methods described in Chapter 3.

Scanning electron microscopy

Field emission scanning electron microscopy was used to examine the morphology of synthesized mesospheres. EDS was used to confirm the presence and mapping of drug in the mesospheres. Dry mesospheres were mounted on carbon tape on an aluminum SEM stub. Stubs were sputter coated with carbon for three minutes using a Technix Hummer V Sputter Coater. The samples were then analyzed using Joel 6335F field emission microscope housed at the Particle Engineering Research Center (PERC).

Particle sizing

The dry particle size and particle size distributions of BSA mesospheres were measured using a Coulter LS 230 particle size analyzer housed at PERC. For each condition sample three 1% (w/v) mesosphere suspension was prepared in 3mL of acetone. The suspension was sonicated for 15-30 seconds. The suspension was added drop-wise to the chamber until obscuration read between 7% - 9% and PIDS read between 37% - 43%. Suspended mesospheres scattered light from a laser source and was detected by silicon photo-detectors. A BSA optical model translated light intensity measurements into a particle size distribution as a volume percent in discrete size blocks. The mean, median, standard deviation and particle size quartiles and other statistical data for each batch were determined using Coulter software.

Determination of drug loading

Drug loading was quantified by digesting 2mg of drug loaded mesospheres in 1.5 ml of enzyme digestion buffer at 37 °C for 24 hours. Solubilized protein was precipitated by addition of an equal volume of a 10 w/v % trichloroacetic acid (TCA) solution .The solution was

incubated at room temperature for 30 minutes. The suspension was centrifuged at 2000rpm for 10 minutes and the supernatant was analyzed on a Shimadzu UV-2401PC (UV-VIS) a matched matrix background. Standard albumin drug solutions were incubated under the same conditions then precipitated with TCA to account for drug degradation or loss in this process. Cisplatin was quantified by mixing equal volumes of the sample solution and sodium acetate bisulfite solution then absorbance was read at 281nm and compared to a standard curve. Cyclophosphamide was quantified by using 4, 4 –nitrobenzyl pryridine (NBP) assay. A 0.5mL aliquot (standard or sample) was added to a 15mL centrifuge tube standing in ice bath and diluted to 1.0mL with ultrapure water. 0.25mL sodium acetate buffer and 0.38mL NBP solution were added in secession, vortexed and placed in boiling water bath for 20 minutes. The centrifuge tube was cooled to room temperature and 2.0mL triethylamine solution was added and vortexed for 30 seconds then let incubate at room temperature for 5minutes absorbance wavelength 585nm and compared against a standard curve.

***In-vitro* release**

Two mg of drug loaded mesospheres were weighted into 2 ml Ultrafree-CL Centrifugal Filter Devices (low binding Duraproe PVDF membrane 0.1 um) Fisher Cat # UFC40VV25 and incubated for in 1.5mL 0.05M phosphate buffered saline (PBS). At predetermined time points the 1.5mL aliquots were collected and replaced with 1.5mL of fresh PBS. Aliquots collected were spectrophotometrically analyzed on a Shimadzu UV-2401PC UV-Vis against a matched matrix background. The release profiles are presented as the total amount of drug released versus time.

Cytotoxicity

Cytotoxicity was evaluated in vitro using Murine Lewis lung carcinoma cells and cytoxcity assay. Lewis lung is a well documented cell line used in studying the mechanism of

chemotherapeutic agents.[110] Cells were grown in a humidified chamber at 37ºC, 5% CO_2 environment for three days. Cells were then transferred to a 96 well plate and allowed to attach for a 24 hour period. Cells were subjected to free drug or mesosphere treatment and predetermined time points percent cytotoxicity was measured using Promega CytoTox 96 assay.

Cyto Tox 96 is a colorimetric assay that measures lactate dehydrogenase (LDH), a stable cytosolic enzyme released upon cell lysis. Culture supernant was mixed with the assay buffer and allowed to incubate or 30 minutes at room temperature. This results in the conversion of a tetrazolium salt (INT) into a red formazan product (Figure 5-1). The amount of color formed is proportional to the number of lysed cells. An increase in wavelength absorbance corresponds to in larger number of dead cells. Results are presented as % cytotoxicity versus time. Treatment groups consisted of cisplatin in situ loaded genipin and glutaraldehyde crosslinked mesospheres.

Results and Discussion

Post loading

Post loading of genipin and glutaraldehyde crosslinked mesospheres was attempted because swelling data suggested some diffusion loading could be achieved. Non drug loaded mesosphere standards known as 'blank' were synthesized using the same processing conditions

The general chemical reactions of the Cyto Tox 96 Assay are as follows:

LDH

$$NAD^+ + \text{lactate} \rightarrow \text{pyruvate} + NADH$$

Diaphorase

$$NADH + INT \rightarrow NAD+ + \text{formazan (red)}$$

Figure 5-1. LDH conversion to formazan (red)

Table 5-1. Drug loading and mean particle size for post loaded mesospheres

Lot	Drug Con(mg/mL)	%Loading (w/w)	ParticleSize (µm)	>1µm	<10µm
Cisplatin-Genipin	0.5	1.0	195	71	61
	1.8	1.0	311	81	34
	15	3.2	119	63	62
Cisplatin-Glutaraldehyde	0.5	0.5	4.0	50	90
	1.8	0.6	4.5	49	90
	15	2.6	1.5	37	100
Cyclophosphamide-Genipin	9	6.0	2.2	58	99
	36	8.2	3.0	54	95
Cyclophosphamide-Glutaraldehyde	9	4.0	2.4	47	96
	36	7.1	2.5	47	96

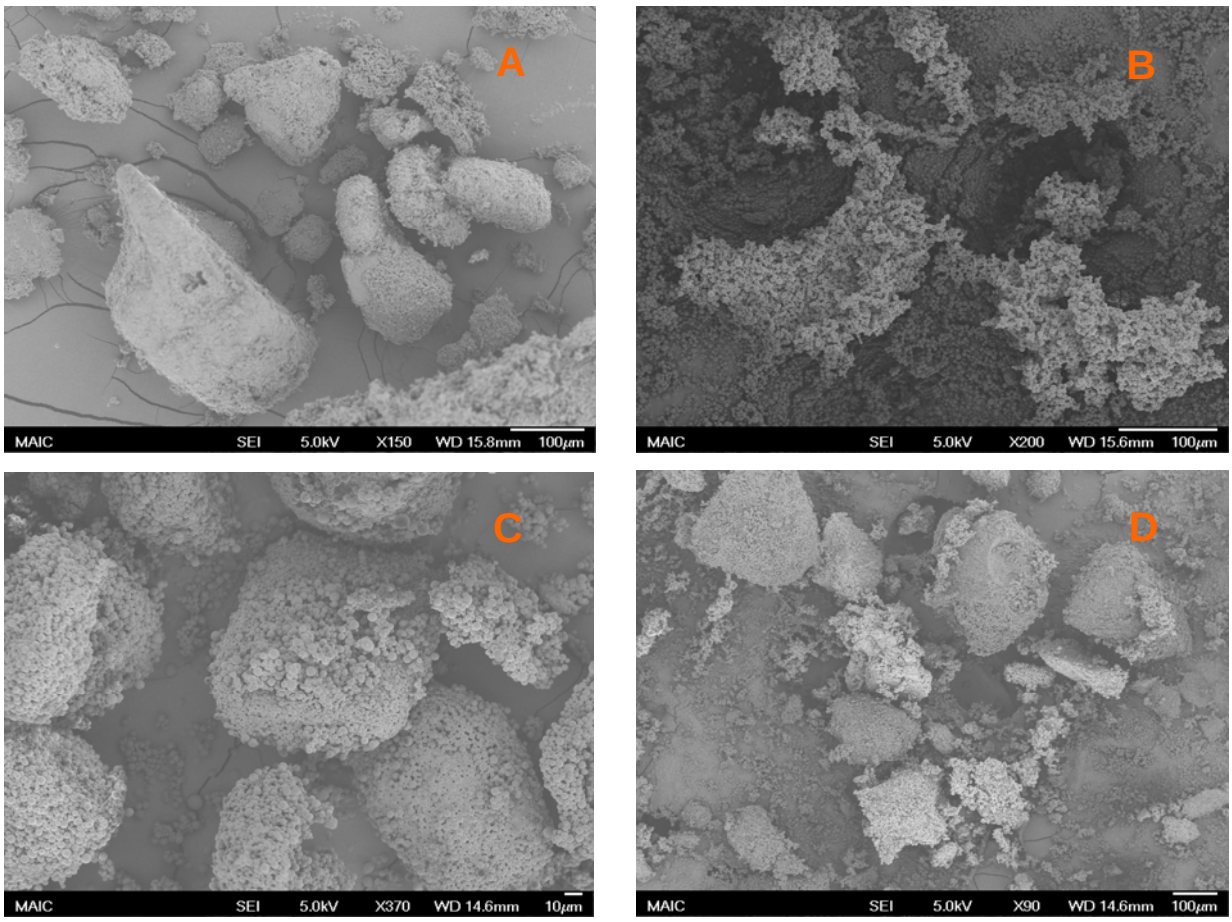

Figure 5-2. SEM micrographs of drug loaded mesospheres A) 3.2% (w/w) CDDP-genipin crosslinked B) 2.6% (w/w) CDDP glutaraldehyde crosslinked C) 8.2% (w/w) CTX-genipin crosslinked D) 7.1% (w/w) CTX-glutaraldehyde crosslinked

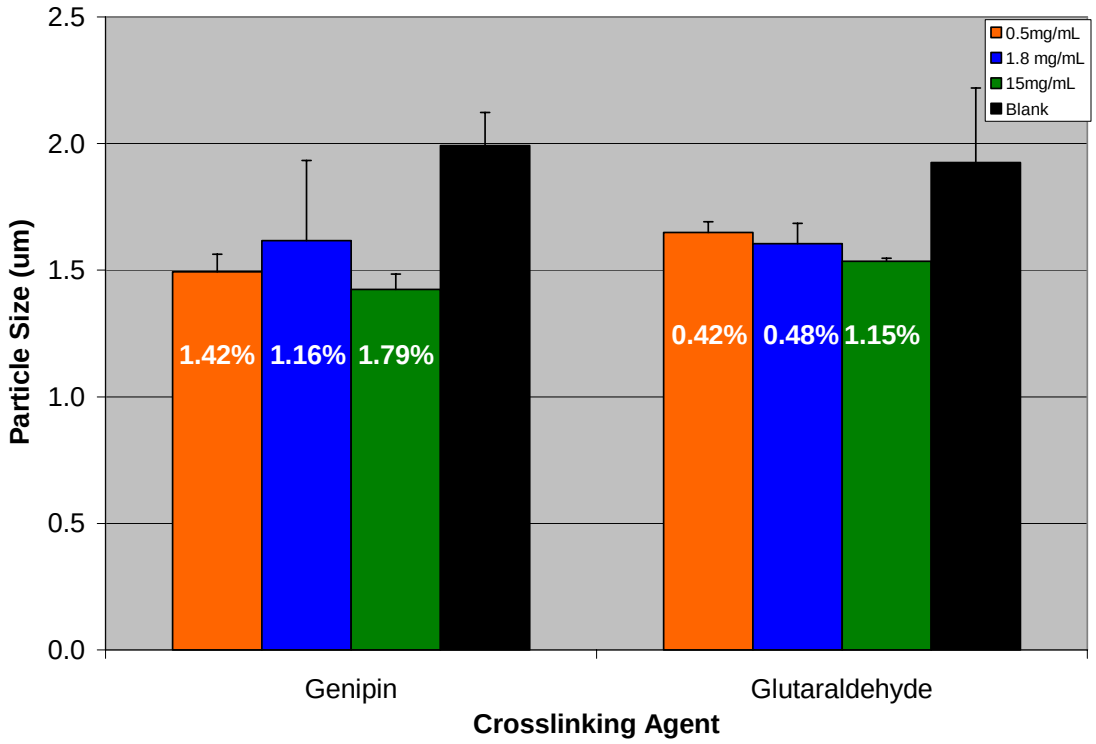

Figure 5-3. Mean particle size of in situ loaded cisplatin mesospheres

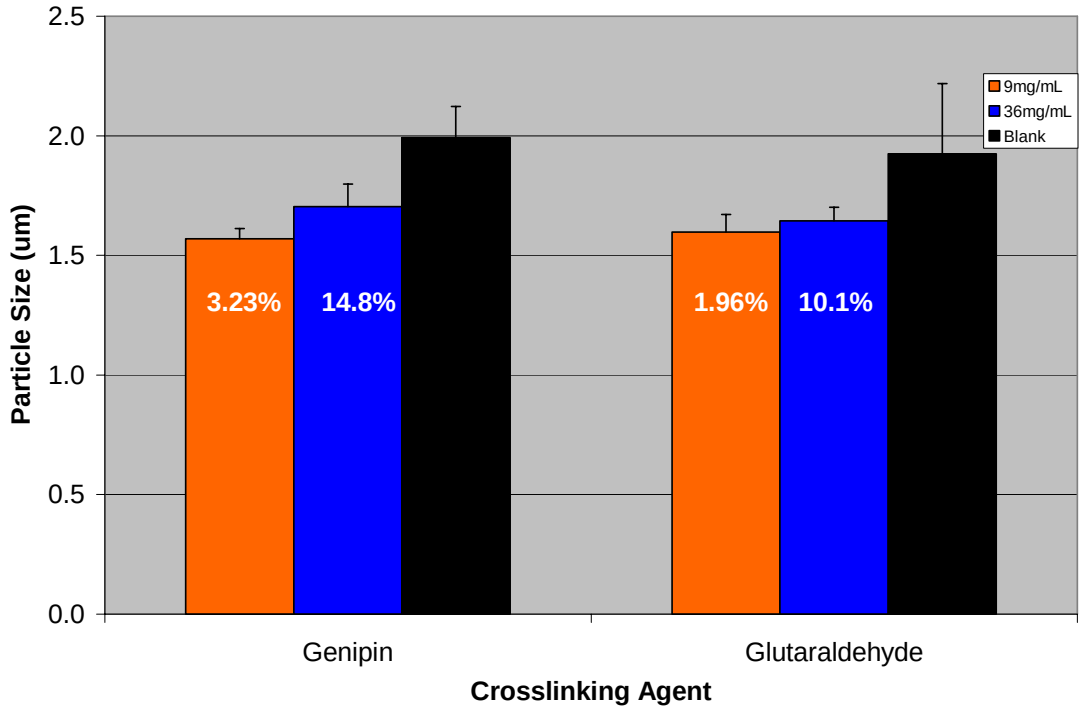

Figure 5-4. Mean particle size of in situ loaded cyclophosphamide mesospheres

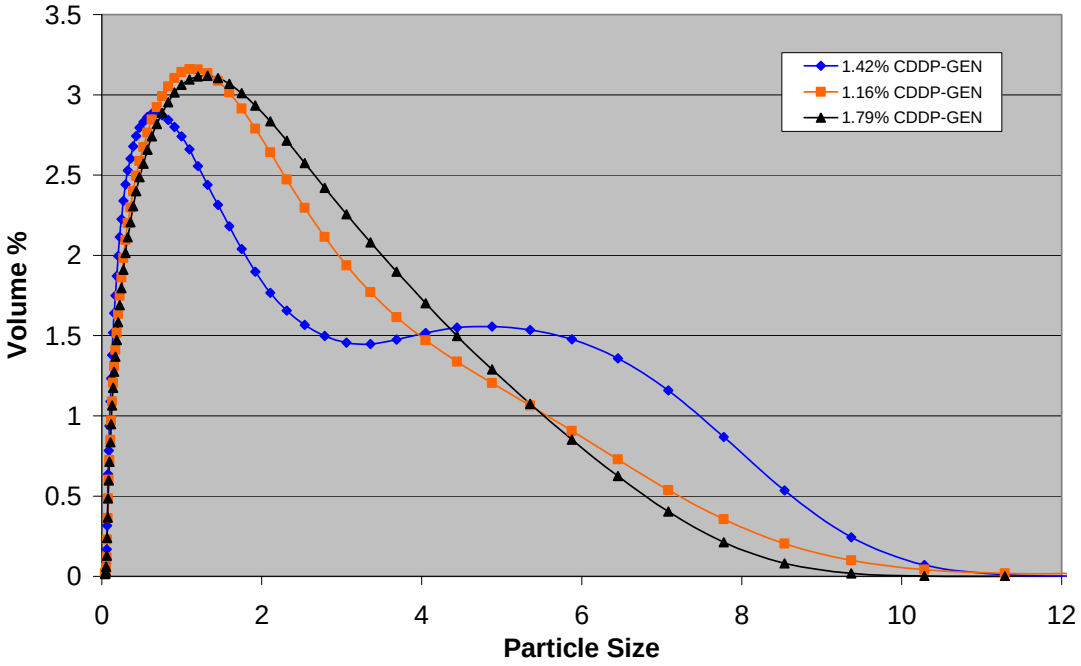

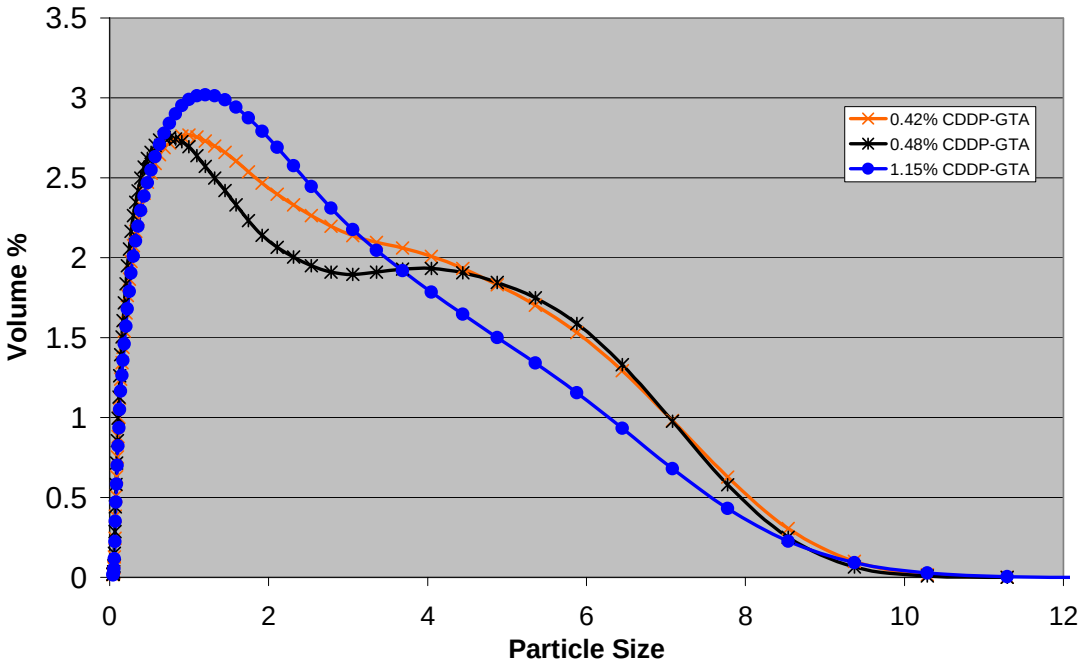

Figure 5-5. Particle size distribution of glutaraldehyde and genipin crosslinked cisplatin in situ loaded

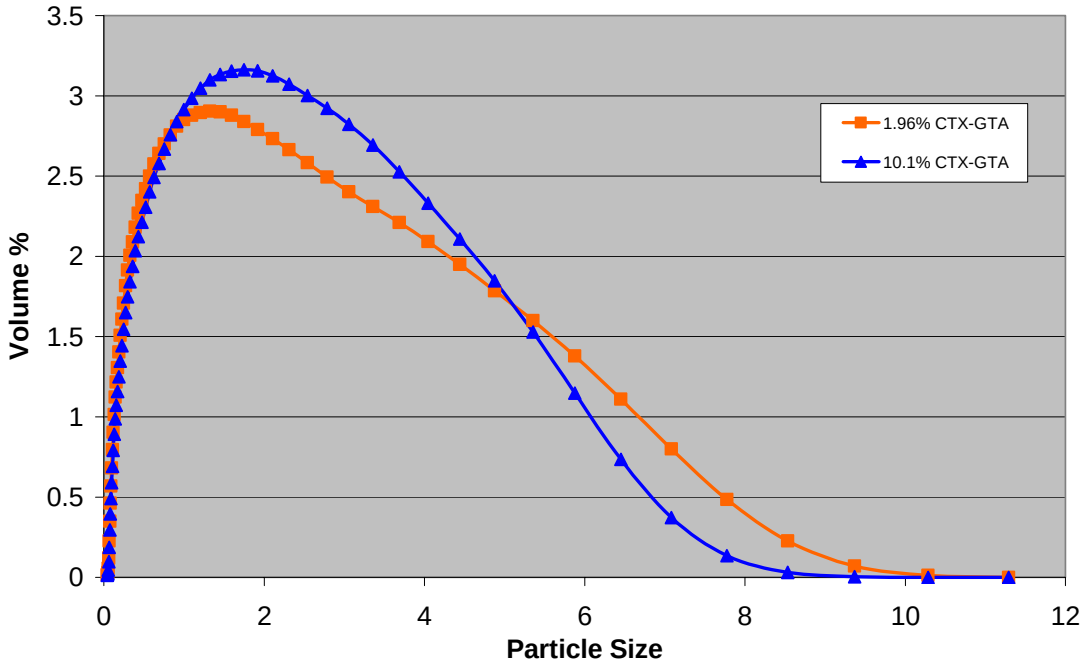

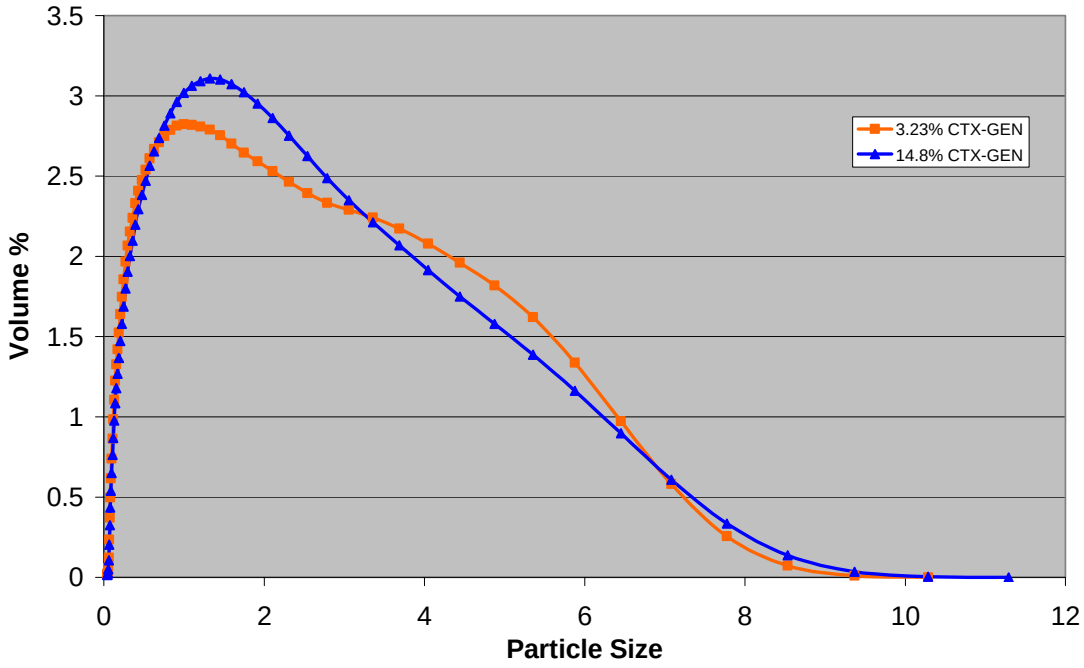

Figure 5-6. Particle size distribution of glutaraldehyde and genipin crosslinked cisplatin in situ loaded mesospheres

as the drug loaded mesospheres. Both genipin and glutaraldehyde standards were prepared. Dry particle size was obtained by suspending MS in acetone similar to methods described in chapters three and four. Particle size of both post and *in situ* loaded formulations were compared to non drug loaded standards. Table 5-1 summarizes % drug loading and mean particle size for post loaded mesospheres. Figure 5-2 displays SEM micrographs of maximum drug loaded mesospheres. Post loading mesospheres is an inefficient method of drug loading with cisplatin solutions. Genipin crosslinked mesospheres swelled during loading and remained agglomerated upon drying increasing in mean particle size from 2.3µm to over 100µm. Glutaraldehyde crosslinked mesospheres also swelled increasing in mean particle size from 2.3µm to 4.0µm. Higher drug loading was achieved with genipin crosslinked mesospheres than with glutaraldehyde crosslinked spheres. Drug loading also increased as the concentration of drug solution concentration increased. The highest drug loading achieved was 3.2% (w/w) and 2.6% (w/w) with genipin and glutaraldehyde respectively. Post loading of BSA mesospheres was more efficient with cyclophosphamide solutions. Mesospheres maintained mean particle size of approximately 2.0µm. The highest loading achieved was 8.2% (w/w) and 7.1% (w/w) with

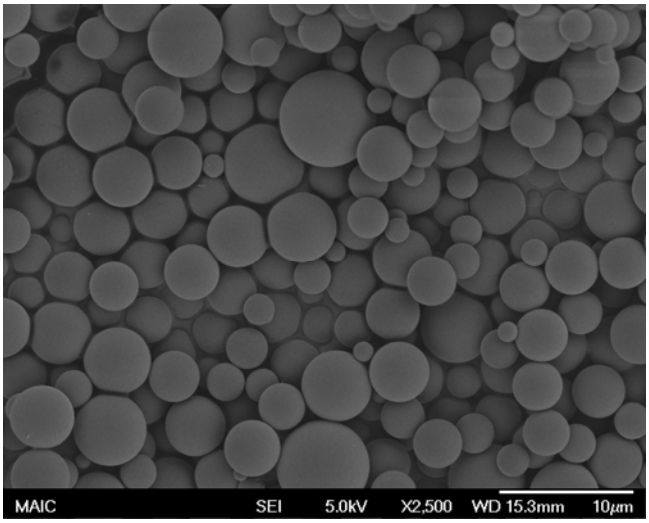

Figure 5-7. SEM micrograph of 15% (w/w) CTX-genipin crosslinked mesospheres

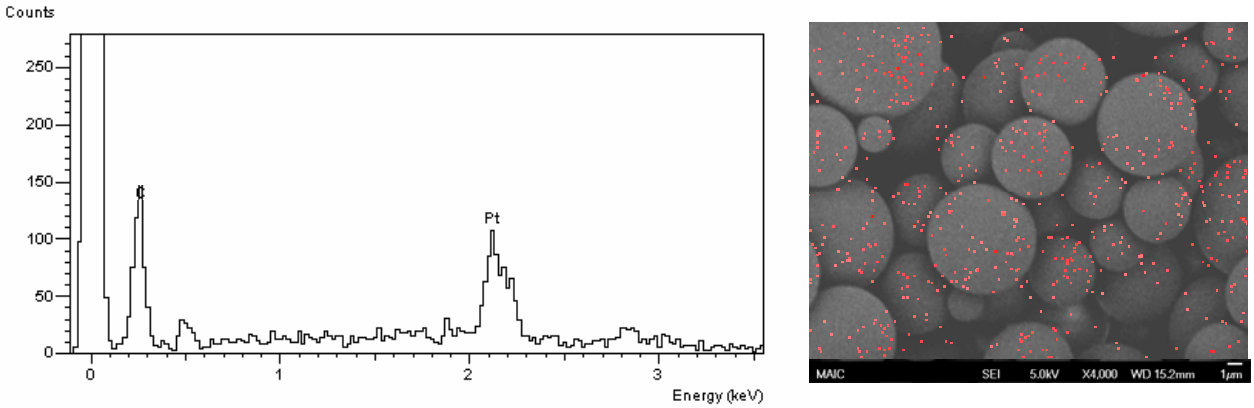

Figure 5-8. Platinum elemental mapping over 1.42% CDDP in situ loaded genipin crosslinked mesospheres

genipin and glutaraldehyde respectively.

In Situ loading.

In situ loading of cyclophosphamide was achieved using a low drug solution oncentration of 9 mg/mL resulting in a drug loading of 3.23% (w/w) and a high drug concentration solution of 36mg/mL resulting in a loading of 14.8% (w/w) for genipin crosslinked mesospheres and 1.96% (w/w) and 10.1% (w/w) for glutaraldehyde crosslinked mesospheres. In situ loading of cisplatin was achieved using low (0.5mg/mL), medium (1.8mg/mL) and high (15mg/mL) drug concentration solutions. SEM was used to confirm the presence of platinum in

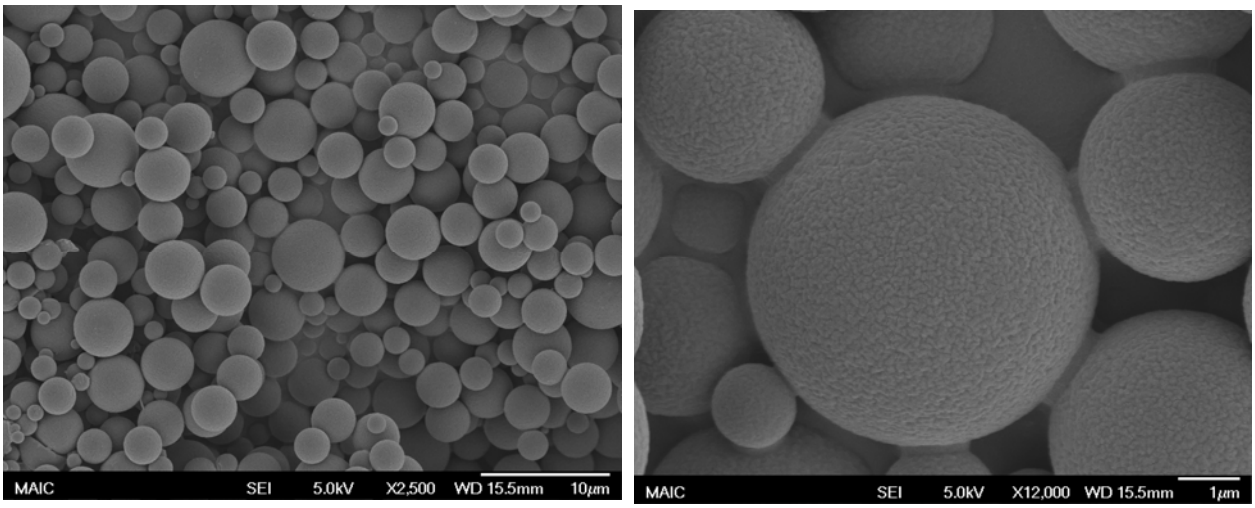

Figure 5-9. SEM micrograph of 1.8% (w/w) CDDP-genipin crosslinked mesospheres

Table 5-2. Treatments for cytotoxicity study.

Dose Level	Crosslinking Agent	% Drug Loading (w/w)
0.5 ppm	Genipin	1.2
		1.4
		1.8
	Glutaraldehyde	0.4
		0.5
		1.2
12.5 ppm	Genipin	1.2
		1.4
		1.8
	Glutaraldehyde	0.4
		0.5
		1.2
25 ppm	Genipin	1.2
		1.4
		1.8
	Glutaraldehyde	0.4
		0.5
		1.2

ciplatin loaded mesospheres (Figure 5-1). A maximum loading of 1.79% was achieved using the 15mg/mL drug solution. Graphical representations of particle size and particle size distribution of in situ loaded mesospheres are depicted in figures 5-2 through 5-5.

Cisplatin in vitro drug release

An in vitro release study was first performed in PBS to determine whether drug release would be a function of diffusion or mesosphere erosion. After seeing measurable release of cisplatin after five days it was determined that drug release would indeed be a function of mesosphere degradation. In vitro release was then carried out in protease enzyme buffer to mimic in vivo conditions. Cisplatin mesospheres released from 40% to 100% of loaded drug depending on the crosslinking agent. In both cases the greatest loading of cisplatin released the least quantity of drug. These high loading mesospheres were synthesized using a drug solution prepared with 10% DMSO. The solvent DMSO was used to increase the solubility of the drug in aqueous solution and there by increasing drug loading of mesospheres. Cisplatin is chemically stable in DMSO for

two hours. After two hours cisplatin is converted to an inactive transplatin isomer. Cisplatin is also degraded by white light.[111] Mesospheres were stored under white light which could have also contributed to low measurable drug loading. Other methods of increasing drug loading including using saline as the drug solvent or a double step in situ/post loading procedure should be investigated.

Drug is retained in mesospheres through physical entrapment of covalent bonds between amine groups on albumin or reactive aldehyde groups of genipin or glutaraldehyde. The results presented thus far are promising however they are incomplete. Cisplatin drug loading were similar to results from Mcclusky where a maximum loading of 1.5% (w/w) was achieved[10]. The measurements presented are only attempts to measure intact cisplatin. A full description requires measures of intact platinum compound, ultrafiltrable platinum and total platinum. This data is best acquired by atomic absorption spectrophotometry of high performance liquid chromatography.[89]

Diffusional drug release was first evaluated and no release was seen during day one so an enzyme release system was developed. A small volume slow flow system was used to better simulate fluid turnover in the tumor. In this model degradation of the mesosphere is the release rate limiting factor. Assume that a lack of diffusional is a result of maximum crosslinking. Release is ultimately going to be based on the type of tissue and enzyme concentrations. Others have found similar results.[83, 84]

Cisplatin microspheres have been explored delivery methods for arthritis and liver cancer.[91-93] The effect of crosslink density was consistent with other researches have found with glutaraldehyde crosslinked human serum albumin microspheres where the total drug released

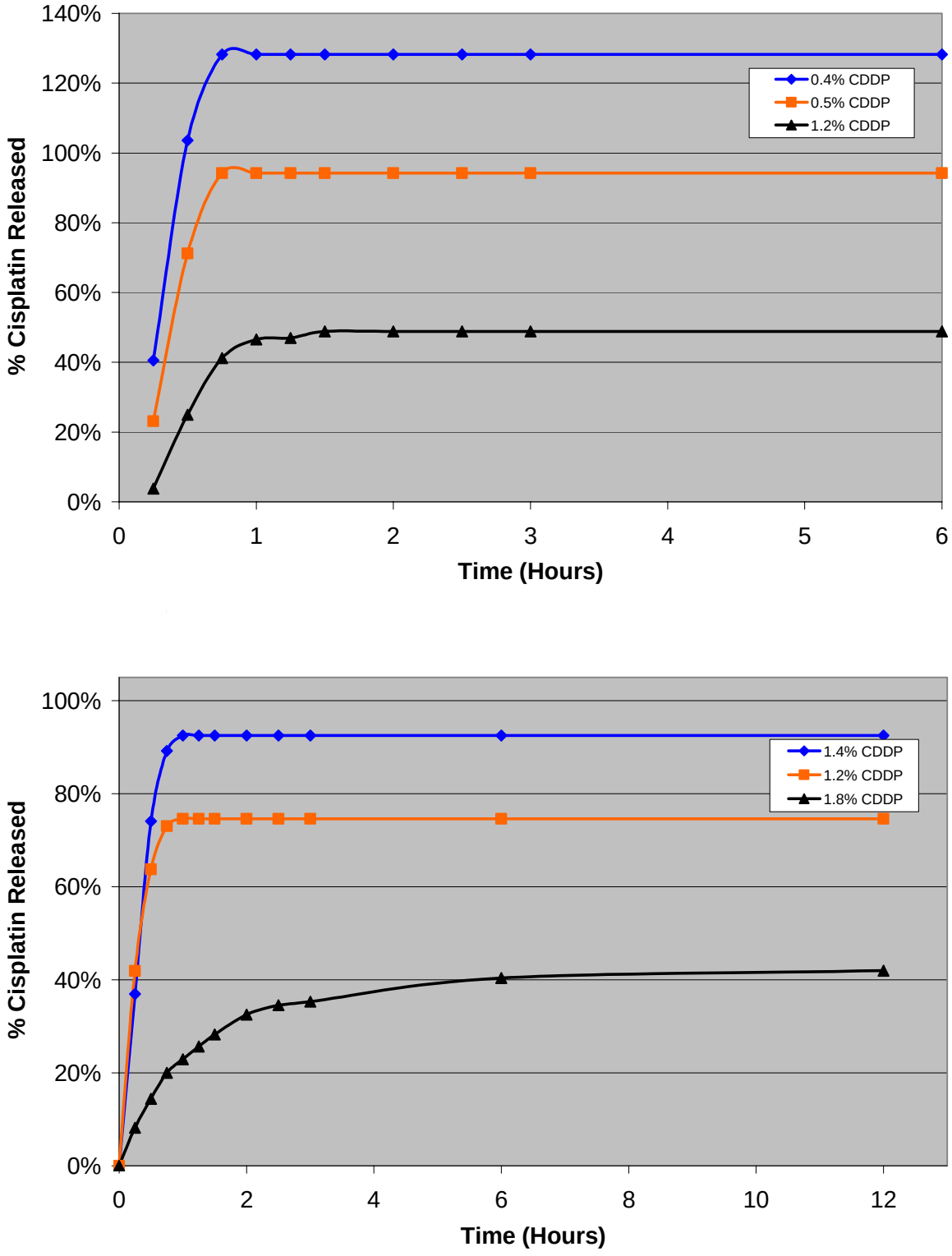

Figure 5-10. In vitro drug release profiles for glutaraldehyde and genipin crosslinked in situ loaded cisplatin mesospheres.

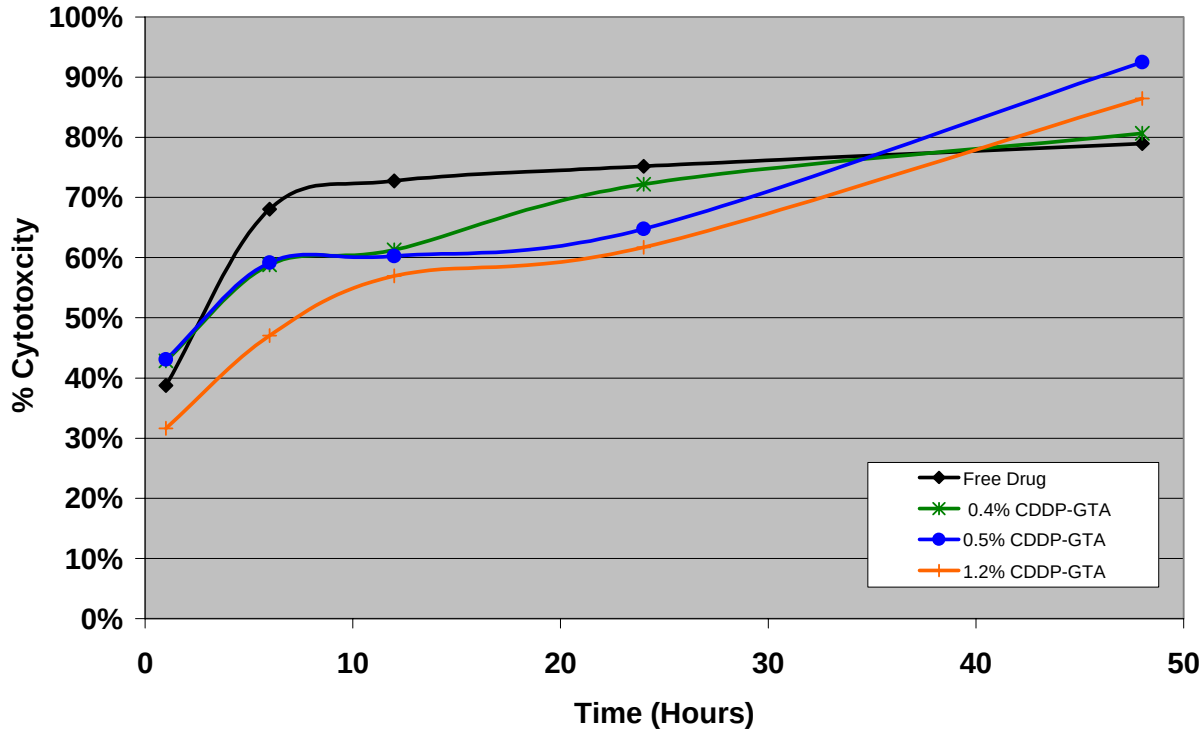

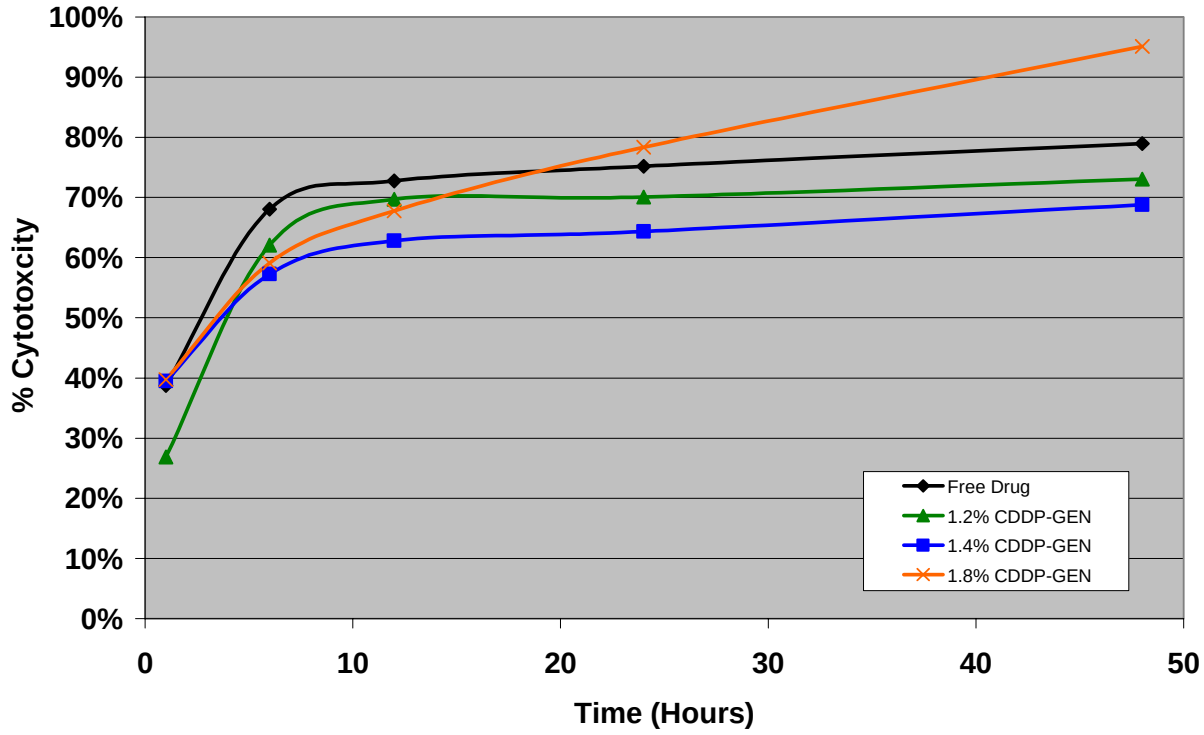

Figure 5-11. Cytotoxicity profile of genipin and glutaraldehyde crosslinked cisplatin mesospheres at 0.5ppm dose level

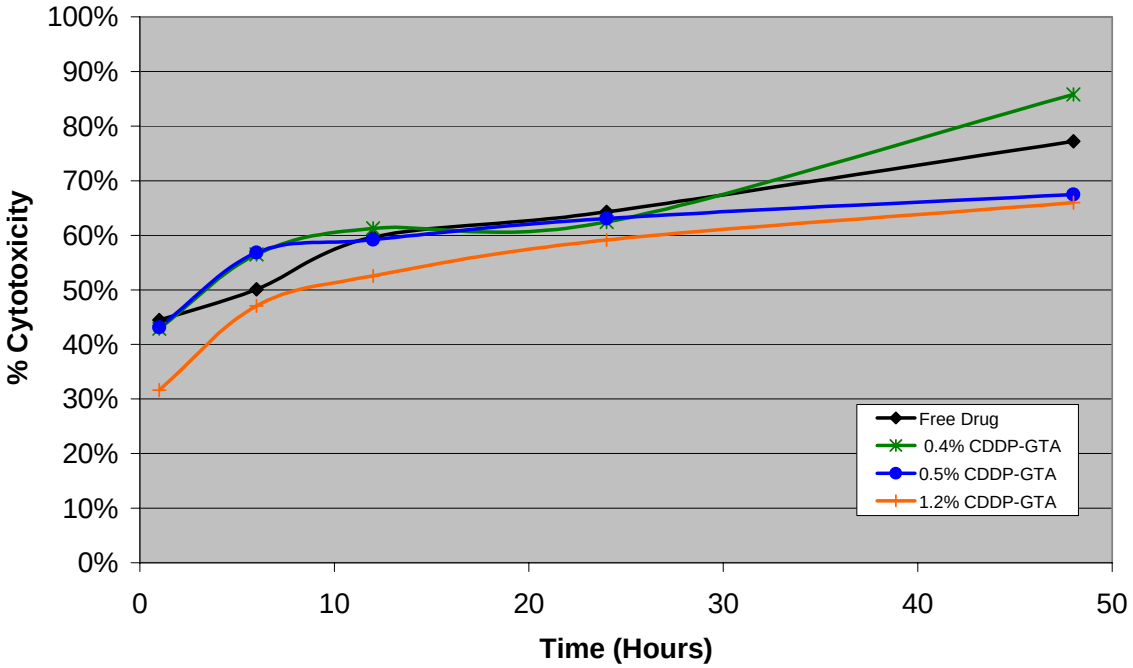

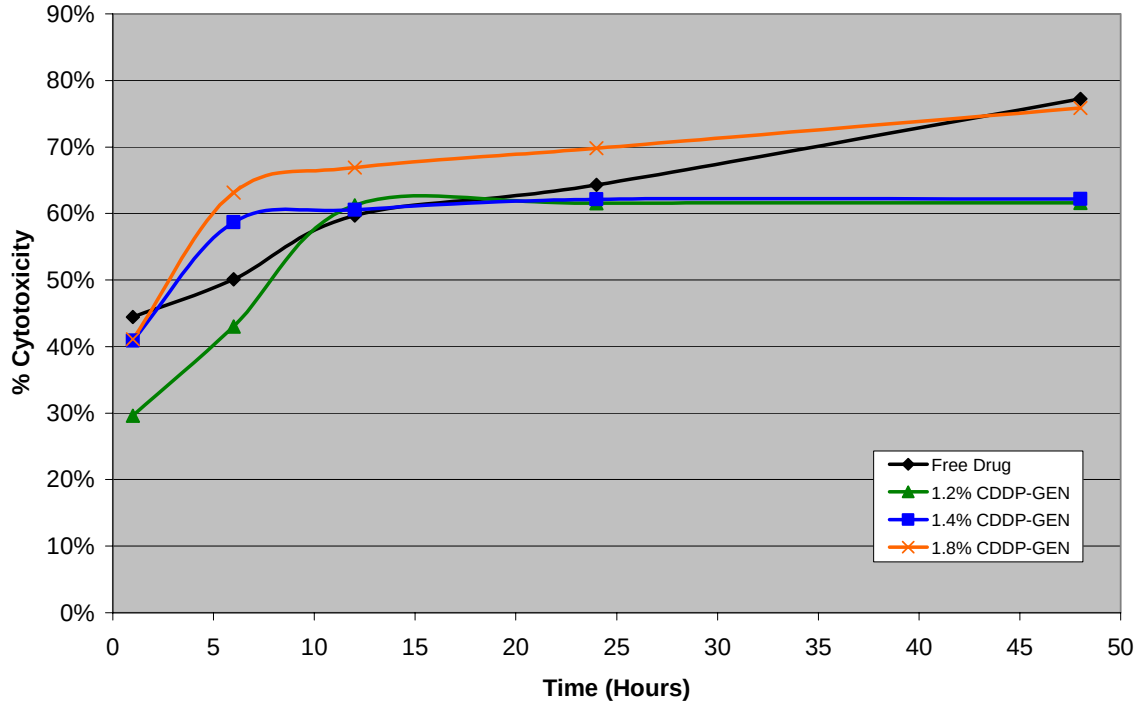

Figure 5-12. Cytotoxicity profile of genipin and glutaraldehyde crosslinked cisplatin mesospheres at 12.5ppm dose level

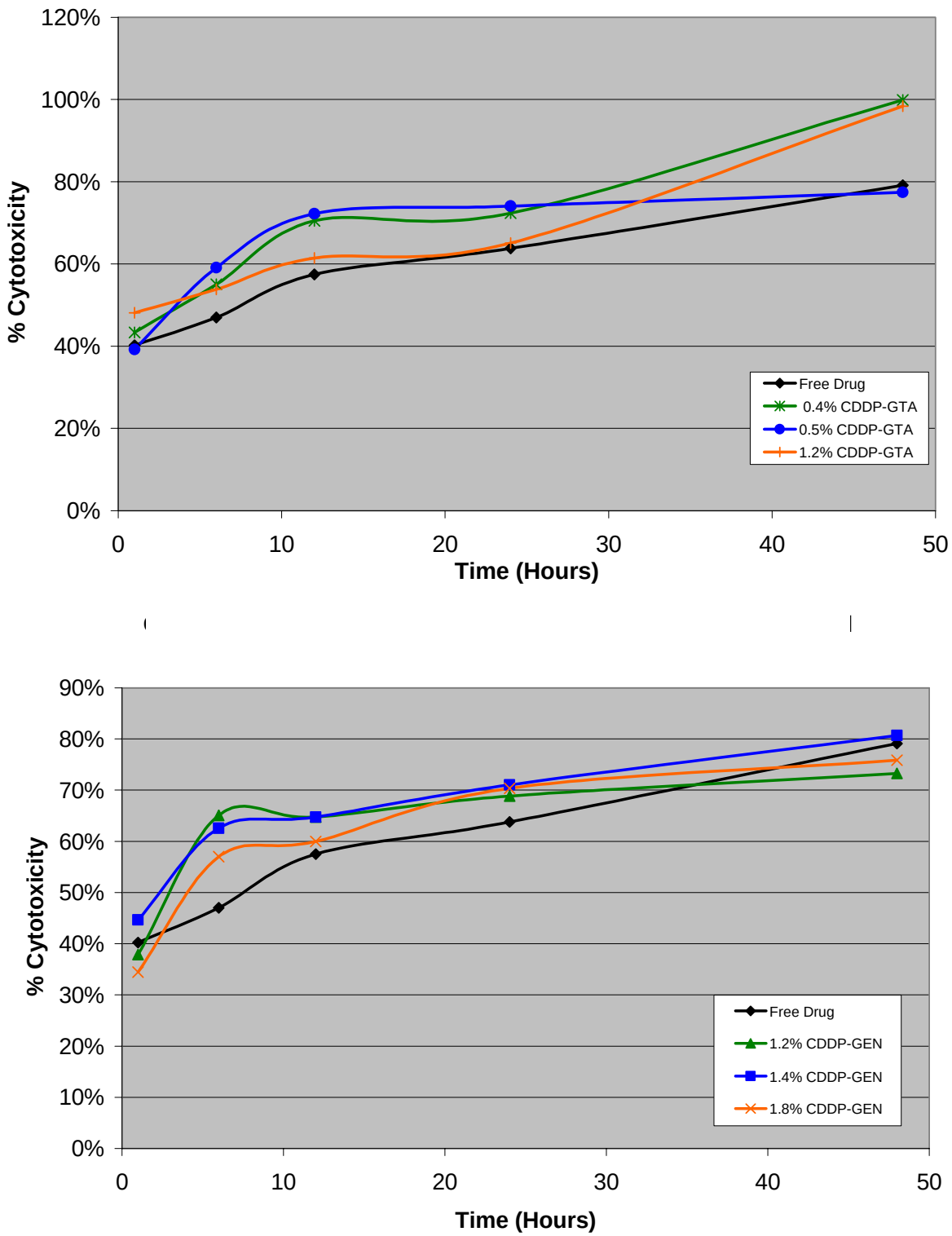

Figure 5-13. Cytotoxicity profile of genipin and glutaraldehyde crosslinked cisplatin mesospheres at 25ppm dose level

was greater with the low crosslink density.[92] Drug recovery of 40%-70% is typical and similar to the results of Nishioka who investigated albumin-chitosan microspheres.[83, 84] Since 100% of drug was not released the remaining drug was probably covalently bonded to the albumin matrix.

Cisplatin cytotoxicity

To verify that mesosphere bound drug was still chemically active cytotoxicity studies were performed. Ultimate interest was primarily in whether or not cell death resulted from treatment and secondly how does bound drug cytotoxicity compared to that of an equivalent free drug dose. Three levels of drug does were evaluated. In all instances bound cisplatin performed as well as or better than the free drug dose (Figures 5-11 through 5-13). Generally these results showed that mesospheres exhibited a cytotoxic affect. However, it can not be used as a quantitative measure of efficiency. There was no way to verify cell count in each well plate nor was it possible to verify the exact number of mesospheres in each well plate. Additionally sample size was only three so no statistical inferences can be made. To determine efficacy of using bound cisplatin *in vivo* studies should be performed.

CHAPTER 6
RELATED BIOMEDICAL POLYMER STUDIES

I. In Vivo Evaluations of Mitoxantrone Loaded Albumin Microspheres and Genipin Crosslinked Gelatin Meso/Microspheres in a Murine Mammary Adenocarcinoma Model

Local intratumoral chemotherapeutics has long been a goal within this laboratory. In vivo evaluations provide a critical link in taking mesospheres formulations from the laboratory to clinical trials. The following describes how the 16/C murine mammary adenocarcinoma tumor line was maintained in the laboratory as well as how animal studies were used to simulate chemotherapy treatment with drug loaded meso/microspheres.

Materials

Bovine serum albumin and gelatin were purchased from Sigma Chemical Company. Cellulose acetate butyrate (CAB) was purchased from Acros Organics. Glutaraldehyde solution 25% (w/w) aqueous was also purchased from Sigma Chemical Company. Genipin powder was purchased from Challenge Bioproducts Co. Ltd. Mitoxantrone (MXN) was donated by Lederle Laboratories. Ultrapure water was prepared in the laboratory using a Barnstead Nanopure Ultrapure Water System at a resistance greater than or equal to 17 MΩ-cm.

General medical and surgical supplies were purchased from the University of Florida Health Center Stores, Henry Schein or Webster Veternary Supply. All ypodermic needles were Monoject purchased from Sherwood Medical. The anesthetic Vetamine (Ketamine HCl, 100 mg/mL) and the analgesic Banamine (Fluixin Meglamine, 50mg/mL) were obtained from Schering-Plough Animal Health. Xylazine (20mg/mL) was obtained from the Butler Company. For use in experiments Ketamine was diluted to 50mg/mL, Banamine to 1mg/mL, and Xylazine to 6.67mg/mL with normal saline. Methoxyflurane (Metofane) was diluted in a 1:1 ratio with mineral oil. The 16/C murine adenocarcinoma cell line was a gift from Dr. Dietmar Seimen

(Department of Radiation Oncology, University of Florida). C3H/HeJ female mice were purchased from Jackson Laboratories.

Methods

Meso/microsphere synthesis

In a typical preparation 5ml of BSA solution was added to a 300mL Labonco lyophilization flask containing 45ml of CAB solution.(Figure 3.1) The mixture was stirred for 20 minutes at 1250rpm on either a Lightnin (model #L1V08), Caframo (model #BDC6015), or Caframo (model #BDC1850) high speed mixer. The crosslinking agent, glutaraldehyde was added to the reaction vessel and stirring rate reduced to 600rpm. The crosslinking reaction continued for 1 hour and 40 minutes after which time acetone was added to the reaction vessel and stirring continued for one additional hour. Particles were collected through centrifugation on a Dynac II benchtop (Clay Adams) by transferring approximately 25mL of solution to each of four 50mL centrifuge tubes, adding acetone to the 40mL mark and centrifuging for 5 minutes at 2000 rpm. The supernant CAB/acetone mixture was decanted; the mesosphere pellet was resuspended in acetone and centrifuged for 10 minutes at 2000 rpm for three additional washes. Particles were then air dried.

In vivo animal study protocols

All in vivo studies were conduced with the approval of the University of Florida Institutional Animal Care and Use Committee (IACUC). All scientists were trained and certified through a short course on animal handling and surgical techniques. Mice were housed in the University of Florida Animal Care Services (ACS) facilities at Shands Hospital.

The 16/C murine mammary adenocarcinoma (16/C MMAC) cell line was not viable ex vivo therefore the line was maintained in C3H/HeJ female mice. To harvest the tumor for passage mice with the tumor were euthanized with CO_2. Under aseptic conditions the tumor mas

was excised using blunt dissection and then finely minced. The tumor was resuspended in calcium free PBS at a concentration of 0.5mg tumor/mL PBS. Transplant mice were anesthetized using Metofane/mineral oil coated gauze in a 50mL centrifuge tube. Approximately 50µL of the tumor suspension was injected subcutaneously into the flank of the mouse. This type of inoculation resulted in the development of a 500mg tumor mass within 10 to 14 days post inoculation. It is important to note that since the tumor line was maintained by serial subcutaneous transplantation of primary tumor tissue and not metastatic foci the model was not expected to produce metastases.

During experimentation10 to 14 week old female C3H/HeJ mice were inoculated with 16/C MMAC tumor as described in the above paragraph. Mice were weighed and visually inspected daily for signs of tumor growth. When the tumor reached 10mm in its largest dimension mice were randomly assigned to a treatment group. To achieve high perfusion of treatment to the tumor treatment was administered through four perimeter and one in the center of the tumor. Each animal was anesthetized with Metofane and 100µL intratumoral injection was delivered through five 20µL injections. Doses were calculated based on an average mouse weight of 20 grams.

Treatment animals were monitored daily for any sign of clinical abnormalities in attitude, hydration or activity. Animal weight and tumor dimensions were recorded at least every two days for up to 60 days. Tumor weight was calculated with the equation for volume of an ellipse:

Tumor weight (g) = $(ab^2) / 2000$

where a is the largest tumor diameter and b is the diameter orthogonal to a, both measured in mm. Any animal that exhibited body weight loss of 20% of initial weight was considered to be suffering from drug toxicity and were euthanized with CO_2. Any animal with a tumor mass that

exceeded 10% of its body mass was considered a treatment failure. The animal was euthanized and the tumor excised for examination. Any animal surviving tumor free 60 days after initial treatment were considered "cured.

Results and Discussion

The mesospheres used for this study will be *in situ* loaded MXN gelatin mesospheres with a mean particle of 2μm. Gelatin mesospheres were synthesized with varying crosslinkers (GTA or Genipin) and crosslinker concentrations (0.5% GTA, 4.5% GTA, 2.3% genipin, or 20.3% genipin). The mesosphere treatment groups will receive a varying dose regiment of 14 mg/kg or 28 mg/kg of mesosphere-loaded MXN delivered in 0.1 mL 4 mg/kg MXN free drug solution. Generally, all combinations of mesosphere formulations and free drug delivery showed tumor regression. As the delivered dose increased the degree of regression increased. The most promising of all formulations were 0.5% GTA and 4.5% GTA at high delivery dose as well as 20.3% Genipin at either low or high delivery dose with approximately 25% survival 25 days post treatment. These gelatin mesospheres do com with their share of problems. Further evaluation needs to be performed to over such aspects as mesosphere swelling and suspension.

II. Preliminary Experiments for Preparation of HA and BSA/HA Blended Mesospheres

Mesospheres were prepared using suspension crosslinking. 3ml of Sepracoat, BSA, or Sepracoat/BSA blend was added a 300mL Labonco lyophilization flask containing 47ml 5% (w/v) cellulose acetate butyrate (CAB), 1, 2 dichloroethane (DCE) solution. The mixture was sheared for 20 minutes at 1250rpm, then 3ml of 0.1 M $CrK(SO_4)_2$, 0.1 M $GdCl_3$ 0.05 M $GdCl_3$, or 5%(w/v) GEN was added and shear rate was reduced to 600rpm. The reaction continued for an additional 1 hour and 40 minutes. At the two hour mark 50mL of acetone was added and the reaction continued for one additional hour. Particles were collected by centrifugation. Approximately 25mL of solution was transferred to four 50mL centrifuge tubes. Acetone was

added to the 40mL mark and centrifuged for 5 minutes at 2000 rpm. Particles were resuspended in acetone and centrifuged for 5 minutes at 2000 rpm for three additional washes. Particles were air dried overnight.

III. Preliminary Experiments for Preparation of Gadolinium Crosslinked BSA Mesospheres

Gadolinium was investigated as a viable crosslinking agent for bovine serum albumin mesospheres. The effect of gadolinium solution concentration, ion saturation and stirring speed on particle was analyzed.

Materials

Bovine serum albumin (BSA) and cellulose acetate butyrate (CAB) were purchased from Sigma-Aldrich. 1, 2 Dichloroethane (DCE) and acetone were purchased from Fisher Scientific. Genipin (GEN) was produced by Wacko Company and purchased from City Chemical. Ultrapure water was prepared in the laboratory using a Barnstead NANOpure.

Methods

Solution preparations

Bovine serum albumin is water soluble so BSA solutions were prepared in ultrapure water. The appropriate mass of BSA was weighted out in a 50ml centrifuge tube and dissolved in water. The true concentration was measured gravimetrically and the density of the solution was

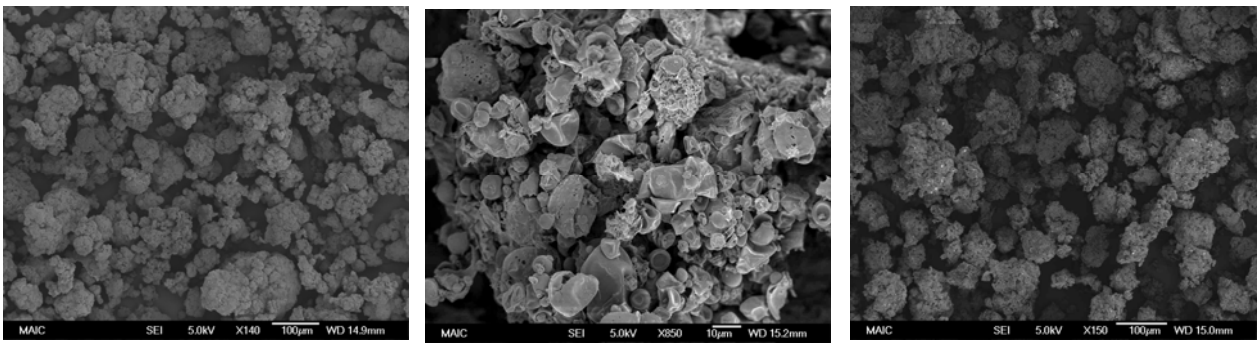

Figure 6-1. 0.1 M CrK(SO4)2 crosslinking of a) Sepracoat b) 5% BSA c. 2.5% BSA/Sepracoat blend

determined. Approximately 1 ml of BSA solution was dried at 130ºC on a Mettler LJ16 Moisture Analyzer to determine the dry weight per volume percent. Concentration was adjusted until true concentration was achieved within 0.5%

Cellulose acetate butyrate solutions were prepared by dissolving the appropriate mass in DCE to a final concentration of 3% (w/v) or 5% (w/v).

Glutaraldehyde solutions were prepared by vacuum distilling 25% aqueous glutaraldehyde solution and recovering the glutaraldehyde distillate. The distillate was then dissolved in DCE to a final concentration of 40mg/ml.

Genipin solutions were prepared by dissolving the appropriate mass in acetone to a final concentration of 30mg/ml or 60mg/ml.

Mesosphere synthesis

A multiparameter study was designed to investigate the affect of BSA concentration, genipin concentration, CAB concentration and BSA/GEN ratio on genipin crosslinked BSA mesospheres. Mesospheres were prepared using suspension crosslinking. In a typical preparation 5ml of BSA was added to a 300mL Labonco lyophilization flask containing 45ml 5% (w/v) CAB

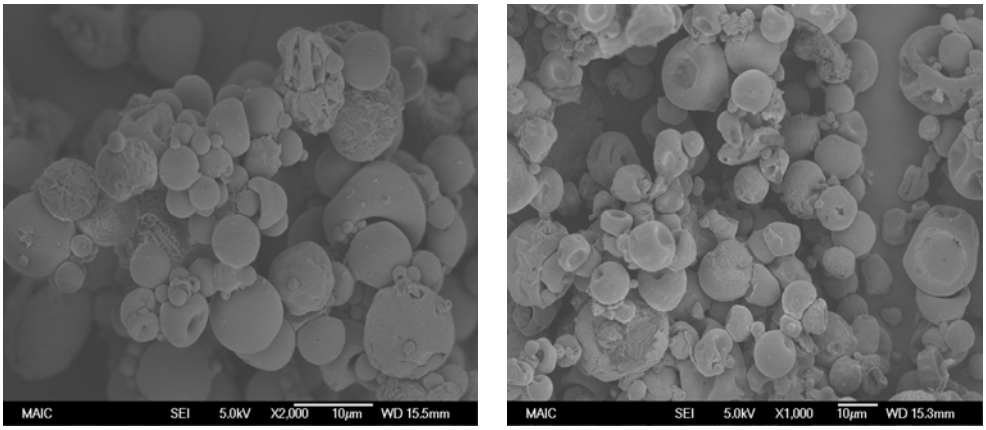

Figure 6-2. Genipin crosslinked BSA/HA mesospheres

solution. The mixture was stirred for 20 minutes at 1200rpm at which point the crosslinking agent, genipin was added and stirring rate reduced to 600rpm. The crosslinking reaction continued for some additional time after which acetone was added and the reaction continued for one additional hour. Particles were collected through centrifugation by transferring approximately 25mL of solution to each of four 50mL centrifuge tubes, adding acetone to the 40mL mark and centrifuging for 5 minutes at 2000 rpm. Particles were resuspended in acetone and centrifuged for 10 minutes at 2000 rpm for three additional washes. Particles were then air dried for 24 hours.

Scanning electron microscopy

Field emission scanning electron microscopy was used to examine the morphology of synthesized mesospheres. Dry mesospheres were mounted on carbon tape on an aluminum SEM stub. Stubs were then coated with a gold/palladium alloy for three to five minutes using a Technix Hummer V sputter Coater. The samples were then analyzed using Joel 6335F field emission microscope at 5KeV accelerating voltage and a working distance of 15mm.

Particle sizing

The dry particle size and particle size distributions of bovine serum albumin mesospheres was measured using a Coulter LS 230 particle size analyzer housed at the Particle Engineering Research Center. For each condition sample three 1% mesosphere suspension was prepared in 3mL of acetone. The suspension was sonicated for 15-30 seconds. The suspension was added drop-wise to the chamber until obscuration read between 7% - 9% and PIDS read between 37% - 43%. The BSA optical model was used to calculate particle size. The mean, median, standard deviation and particle size quartiles were determined using Coulter software.

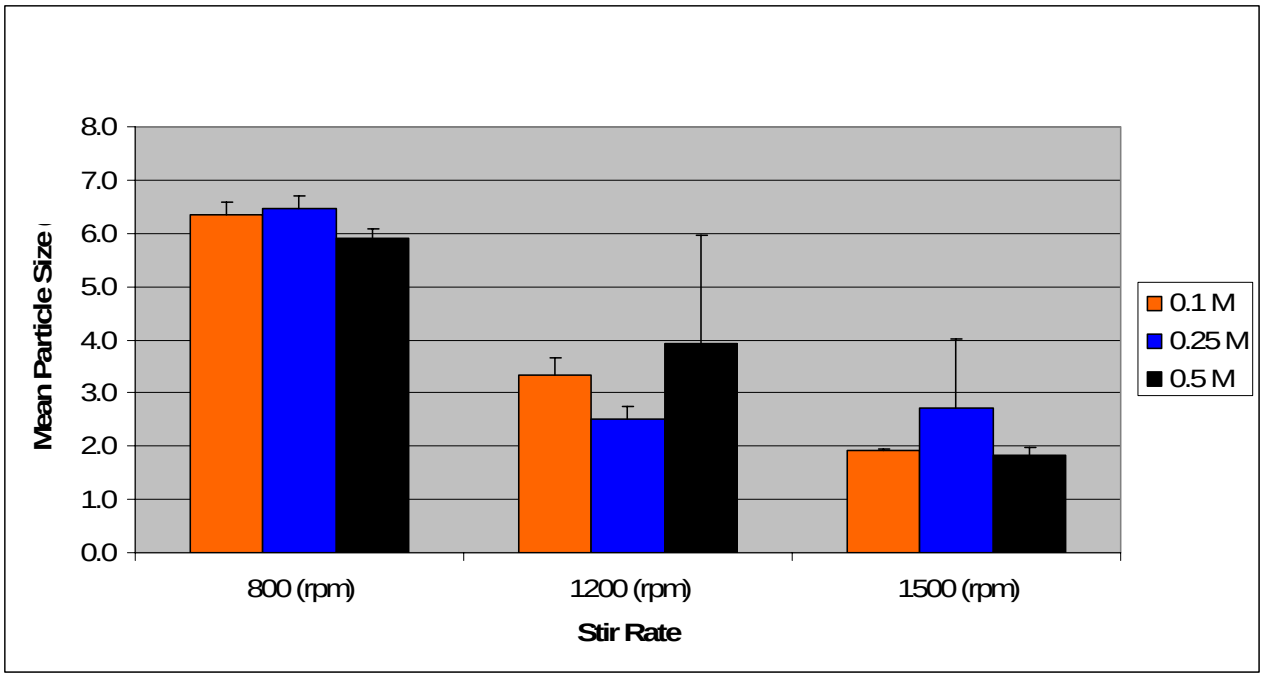

Figure 6-3. Mean particle size for gadolinium crosslinked BSA mesospheres.

Statistical analysis

The statistical software package Sigma Stat was used to identify differences in mean particle size and interactions between the various processing conditions. Three primary factors: protein solution concentration, suspension agent solution concentration, crosslinker solution concentration, protein/crosslinker ratio and two secondary factors: stirring speed and crosslinking time were analyzed using a three way ANOVA. A two way ANOVA was used to find interactions between factors. The Tukey method was used for all pair wise multiple comparisons to isolate exactly which levels of each factor provided a statistical difference in mean particle size.

Smooth spherical particles were produced (Figure 6-4) where increasing the stirring rate during the dispersion phase gave a smaller particle size. No trend was developed for the saturation of available crosslinking sites and concentration of gadolinium solution.[112]

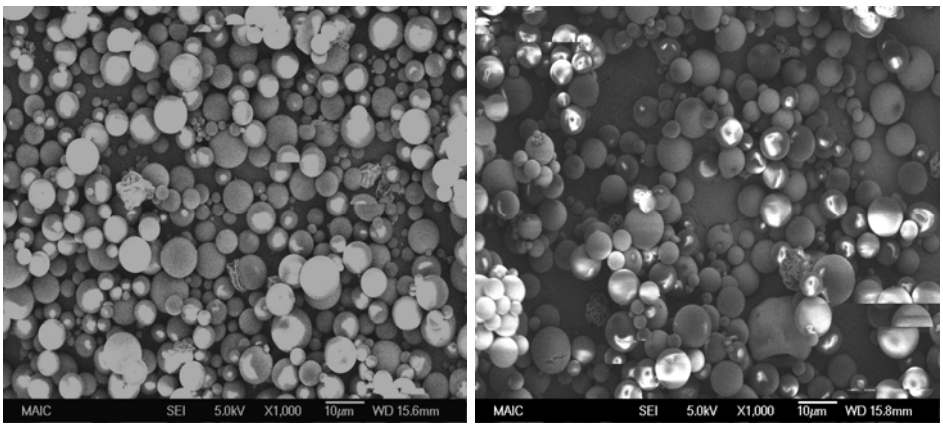

Figure 6-4. SEM micrographs of gadolinium crosslinked BSA mesospheres.

CHAPTER 7
CONCLUSIONS

The ultimate goal of this research was to synthesize and evaluate new bovine serum albumin (BSA) mesospheres crosslinked with glutaraldehyde and a novel natural crosslinking agent genipin and to evaluate properties of drug loaded mesospheres for intratumoral cancer chemotherapy.

1. Smooth spherical bovine serum albumin mesospheres crosslinked with glutaraldehyde and genipin were synthesized in a dry particle size range of 1μm to 10μm using a steric stabilization dispersion crosslinking process.

2. A multi-parameter statistical analysis of process parameters: BSA concentration, CAB concentration, crosslinker concentration, crosslinked to protein ratio, stabilization stirring rate and crosslinking time were investigated for genipin crosslinked mesospheres using particle size and size distribution as quantitative outcome:

    a. Increasing stabilization dispersion stir rate from 800rpm to 1500rpm produced mesospheres with a smaller mean particle size and a normal particle size distribution curve.

    b. Increasing crosslinking time from 3 hours to 24 hours did not affect mean particle size nor particle size distribution.

    c. Increasing GEN/BSA ration from 1% to 10% (w/w) produced the smallest particle sizes 2.4μm with narrow particle size distributions (0.4μm-10μm).

    d. Neither BSA concentration nor genipin concentration had an affect on the mean particle size.

3. Genipin crosslinked mesosphere degradation was evaluated using enzymatic degradation and protein assay to quantify the amount of unbound BSA. Increasing crosslinking time, GEN/BSA ratio, BSA concentrations, genipin concentrations slowed time of enzymatic degradation Spectrometric analysis overestimated the concentration of BSA in high genipin concentration solutions because the blue pigment formed by genipin reacting with amino acid groups enhanced the blue pigment of the assay. Particles which may be genipin-albumin oligomers formed and added to the analysis. Time of storage also affects degradation. The longer the period of storage the faster mesospheres will degrade.

4. A post synthesis drug loading method was developed for genipin and glutaraldehyde crosslinked mesospheres. A maximum loading of cisplatin was 3.2% (w/w) and 2.6% (w/w) for genipin and glutaraldehyde respectively, while no measurable loading was achieved for cyclophosphamide.

5. An *in situ* drug loading method was developed for genipin and glutaraldehyde crosslinked mesospheres. A maximum loading of cisplatin was 1.79% (w/w) and 1.15% (w/w) for genipin and glutaraldehyde respectively. A maximum loading of 14.8% (w/w) was achieved for cyclophosphamide genipin crosslinked and 10.1% (w/w) mesospheres.

6. Cisplatin drug release was dependent on the drug loading. Higher drug loadings resulted in higher drug release. Cyclophosphamide drug release was not measurable using the assay techniques available.

7. Both genipin and glutaraldehyde crosslinked cisplatin mesospheres proved to be cytotoxic over a 48 hour period. Cell death continued to increase even as cells continued to duplicate.

8. In vivo showed that intratumoral chemotherapy with free drug, albumin and gelatin bound mitoxantrone meso-microspheres as a promising treatment modality of solid tumors. The most effective treatment was mitoxantrone loaded albumin microspheres delivered in a mitoxantrone free drug solution over a scheduled regimen.

9. Hyaluronic acid and BSA/HA mesospheres crosslinked with genipin and gadolinium show potential as controlled release drug carriers and should be investigated further.

CHAPTER 8
FUTURE WORK

The focus of this research was the development of genipin crosslinked albumin mesospheres compositions for localized intratumoral delivery of chemotherapy agents. The following lists research interests to be considered for future studies:

1. **Synthesis and characterization of hyaluronic acid (HA) mesospheres.** Hyaluronic acid is currently used in treatment of ophthalmic conditions and surgical adhesions. There is also an interest in using HA in the treatment of arthritis. Drug loaded HA mesospheres offer a novel approach. It would necessary to investigate crosslinking with glutaraldehyde, genipin and gadolinium.

2. **Synthesis and characterization of blended matrix mesospheres.** Preliminary studies presented in Chapter 6 illustrated the possibility of dual matrix BSA and HA mesospheres. In addition to BSA/HA compositions it would be important to investigate BSA/gelatin and BSA/DNA compositions crosslinked with glutaraldehyde, genipin and gadolinium. Hydrated particle size, drug loading and drug release would be the major factors of interest.

3. **Protocol development for double crosslinking.** Double crosslinking of polysaccharide matrixes could offer novel degradation models as well as enhance drug loading and drug release.

4. **Develop viable degradation model through the use of focused ion beam (FIB)/Amria software and GPC/HPLC.** Little research focus has been shown on understanding how the drug, protein and crosslinking agent interact upon breakdown. FIB technology could enhance imagery traditionally obtained through TEM.

5. **Evaluation of mesosphere microstructure and crystallinity through x-ray diffraction and FTIR.** Now that research has achieved a point to where mesosphere synthesis is readily understood it is time to explore in more detail the crosslinking agent protein interaction. X-ray diffraction and FTIR provide information that can not be achived through a simple degradation study.

6. ***In vitro* evaluations of genipin crosslinked mesospheres.** *In vivo* studies should be conducted using either 16/C murine mammary adenocarcinoma cell or Lewis lung models previously developed in the Biomaterials Center to determine the *in vivo* efficacy of cisplatin loaded mesospheres. Studies should be conducted using similar methods described in Chapter 6.

7. **Develop and evaluate methods of product sterilization and storage.** Sterilization and storage evaluation are the next step to bringing a product from laboratory to market. The results presented in Chapter 4 provide a small window into how storage will affect the function and efficacy of a product. Much more investigation needs to be done in this area before mesospheres can be become a viable commercial product.

8. **Drug loading of Tamoxifen (antiestrogen) or Anastrazole in albumin mesospheres.** Hormone therapies are the newest frontier of cancer treatment. Delivery through albumin mesospheres offers the same sustained controlled release benefit as does traditional chemotherapy agents delivered in this manner.

9. **Combination drug loaded mesospheres.** Cancer is conquered through a cocktail of anticancer drugs. The ability to delivery multiple drugs through one vessel is an interesting concept to explore.

LIST OF REFERENCES

1. Goldberg, E., et al., Intratumoral cancer chemotherapy and immunotherapy: opportunities for nonsystemic preoperative drug delivery. Journal of Pharmacy and Pharmacology, 2002. **54**: p. 159-180.

2. Kumar, M.N.V.R., Nano and microparticles as controlled drug delivery devices. Journal of Pharmacy and Pharmaceutical Science, 2000. **3**(2): p. 234-258.

3. Hadba, A.R., Synthesis, Properties and In Vivo Evaluations of Sustaned Release Albumin-Mitoxantrone Microsphere Formulations for Nonsystemic Treament of Breast Cancer and Other High Mortality Cancers, in Materials Science and Engineering. 2001, University of Florida: Gainesville, FL.

4. Almond, B., Mitoxantrone-Loaded Albumin Microspheres for Localized Intratumoral Chemotherapy of Breast Cancer, in Materials Science and Engineering. 2002, University of Florida: Gainesville, FL.

5. Cuevas, B., Synthesis and Properties of Protein Micro/Mesospheres-Drug Compositions Designed for Intratumoral Cancer Therapy, in Materials Science and Engineering. 2003, University of Florida: Gainesville, FL.

6. AmericanCancerSociety, Cancer Facts and Figures 2006. 2006, American Cancer Society, Inc: Atlanta.

7. Allison, M., Sarraf, Catherine, Understanding Cancer: From Basic Science to Clinical Practice. 1997, Cambridge University Press: Cambridge.

8. Kleinsmith, L., Principles of Cancer Biology. 2006, Pearson Education Inc: San Francisco.

9. Kruh, G. and K. Tew, Basic Science of Cancer. 2000, Current Medicine Inc: Philadelphia.

10. McClusky, R.A., Synthesis and Properties of Submicron Albumin Spheres, in College of Pharmacy. 1987, University of Florida: Gainesville, FL. p. 124.

11. Salmon, S., ed. Adjuvant Therapy of Cancer VIII. Preceding of the Eight International Conference on the Adjuvant Therapy of Cancer. 1997, Lippincott-Raven Publishers: Philadelphia.

12. Gupta, P.K. and C.T. Hung, Albumin microspheres I: physico-chemical characteristics. Journal of Microencapsulation, 1989. **6**(4): p. 427-462.

13. Gupta, P.K. and C.T. Hung, Albumin microspheres II: applications in drug delivery. Journal of Microencapsulation, 1989. **6**(4): p. 463-472.

14. Jayakrishnan, A. and S. Jameela, Glutaraldehdye as a fixative in bioprostheses and drug delivery matrices. Biomaterials, 1996. **17**: p. 471-484.

15. Ueda, S., Y. Iwahashi, and H. Tokuda, Production of anti-tumor-promoting iridoid glucosides in Genipa americana and its cell cultures. Journal of Natural Products, 1991. **54**(6): p. 1677-1680.

16. Ono, M., et al., Iridoid glucosides from the fruit of Genipa americana. Chemical & Pharmaceutical Bulletin, 2005. **53**(10): p. 1342-1344.

17. Hamerski, L., et al., Iridoid glucosides from randia spinosa (rubiaceae). Phytochemistry, 2003. **63**: p. 397-400.

18. Djerassi, C., J. Gray, and F. Kincl, Naturally occurring oxygen heterocyclics.IX. Isolation and characterization of genipin. Journal of Organic Chemistry, 1960. **25**: p. 2174-2177.

19. Sheu, S.-J. and W.-C. Hsin, HPLC separation of the major constituents of gardeniae fructus. Journal of High Resolution Chromatography, 1998. **21**(9): p. 523-526.

20. Tsai, T.-H., et al., Idenification and determination of geniposide, genipin, gardenoside and geniposidic acid from herbs by HPLC/photodiode-array detection. Journal of Liquid Chromatography, 1994. **17**(10): p. 2199-2205.

21. Endo, T. and H. Taguchi, The constituents of gardenia jasminoides: geniposide and genipin-gentiobioside. Chemical & Pharmaceutical Bulletin, 1973. **21**(12): p. 2684-2688.

22. Bringmann, G., et al., Gardenamide A from rothmannia urcelliformis (rubiaceae) - Isolation, absolute stereostructure and biomimetic synthesis from genipine. European Journal of Organic Chemistry, 2001: p. 1983-1987.

23. Akao, T., K. Kobashi, and M. Aburada, Enzymic studies on the animal and intestinal bacterial metabolism of geniposide. Biological and Pharmaceutical Bulletin, 1994. **17**(12): p. 1573-1576.

24. Miyagoshi, M., S. Amagaya, and Y. Ogihara, The structural transformation of gardenoside and its related iridoid compounds by acid and b-glucosidase. Planta Medica, 1987: p. 462-464.

25. Fujikawa, S., et al., The continuous hydrolysis of geniposide to genipin using immobilized B-glucosodase on calcium alginate gel. Biotechnology Letters, 1987. **9**(10): p. 697-702.

26. Buechi, G., et al., Total synthesis of racemic genipin. Journal of the American Chemical Society, 1967. **89**(11): p. 2776-2777.

27. Djerassi, C., et al., Terpenoids.XLVII. The structure of genipin. Journal of Organic Chemistry, 1961. **26**: p. 1192-1206.

28. Paik, Y.-S., et al., Physical stability of the blue pigments formed from geniposide of gardenia fruits: effects of pH, temperature and light. Journal of Agricultural Food Chemistry, 2001. **49**: p. 430-432.

29. Touyama, R., et al., Studies on the blue pigments produced from genipin and methylamine II. On the formation mechanisms of brownish-red intermediates leading to the blue pigment formation. Chemical & Pharmaceutical Bulletin, 1994. **42**(8): p. 1571-1578.

30. Park, J.-E., et al., Isolation and characterization of water-soluble intermediates of blue pigments transformed from geniposide of gardenia jasminoides. Journal of Agricultural Food Chemistry, 2002. **50**: p. 6511-6514.

31. Fujikawa, S., S. Nakamura, and K. Koga, Genipin, a new type of protein crosslinking reagent from gardenia fruits. Agricultural and Biological Chemistry, 1988. **52**(3): p. 869-870.

32. Fujikawa, S., et al., Continuous blue pigment formation by gardenia fruit using immobilized growing cells. Journal of Fermentation Technology, 1987. **65**(6): p. 711-715.

33. Touyama, R., et al., Studies on the blue pigments produced from genipin and methylamine I. Structures of the brownish-red intermediates leading to the blue pigment formation. Chemical & Pharmaceutical Bulletin, 1994. **42**(3): p. 668-673.

34. Koo, H.-J., et al., Anti-inflammatory evaluation of gardenia extract, geniposide and genipin. Journal of Ethnopharmacology, 2006. **103**: p. 496-500.

35. Koo, H.-J., et al., Antiinflammatory effects of genipin, an active principle of gardenia. European Journal of Pharmacology, 2004. **495**: p. 201-208.

36. Suzuki, Y., et al., Antithrombotic effect of geniposide and genipin in the mouse thrombosis model. Planta Medicine, 2001. **67**: p. 807-810.

37. Yamazaki, M. and K. Chiba, Neurotrophic effects of genipin on Neuro2a cells. Journal of Health Science, 2005. **51**(6): p. 687-692.

38. Hsu, H.-Y., et al., Comparisons of geniposidic acid and geniposide on antitumor and radioprotection after sublethal irradiation. Cancer Letters, 1997. **113**: p. 31-37.

39. Isiguro, K., et al., Studies on iridoid related compounds. IV Antitumor activity of iridoid aglycones. Chemical & Pharmaceutical Bulletin, 1986. **34**(6): p. 2375-2379.

40. Chang, W.-L., et al., Immunosuppressive iridoids from the fruits of Gardenia jasminoides. Journal of Natural Products, 2005. **68**: p. 1683-1685.

41. Lee, S.-W., et al., Colorimetric determination of amino acids using genipin from Gardenia Jasminoises. Analytica Chimica Acta, 2003. **480**: p. 267-274.

42. Almog, J., et al., Genipin: A novel fingerprint reagent with colorimetric and fluorogenic activity. Journal of Forensic Science, 2004. **49**(2): p. 255-257.

43. Speer, D., et al., Biological effects of residual glutaraldehyde in glutaraldehyde-tanned collagen biomaterials. Journal of Biomedical Materials Research, 1980. **14**: p. 753-764.

44. Sung, H.-W., et al., Gelatin derived bioadhesives for closing skin wounds: an in vivo study. Journal of Biomaterials Science Polymer Edition, 1999. **10**(7): p. 751-771.

45. Huang, L., et al., Biocompatibility study of a biological tissue fixed with a naturally occurring crosslinking agent. Journal of Biomedical Materials Research, 1998. **42**: p. 568-576.

46. Chang, Y., et al., In vivo evaluation of cellular and acellular bovine pericardia fixed with a naturally occurring crosslinking agent (genipin). Biomaterials, 2002. **23**: p. 2447-2457.

47. Chang, Y., et al., Acellular bovine pericardia with distinct porous structures fixed with genipin as an extracellular matrix. Tissue Engineering, 2004. **10**(5/6): p. 881-892.

48. Chang, Y., et al., Cell-free xenogenic vascular grafts fixed with glutaraldehyde or genipin: in vitro and in vivo studies. Journal of Biotechnology, 2005. **120**: p. 207-219.

49. Sung, H.-W., et al., Mechanical properties of a porcine aortic fixed with a naturally occurring crosslinking agent. Biomaterials, 1999. **20**: p. 1759-1772.

50. Sung, H.-W., et al., Crosslinking characteristics and mechanical properties of a bovine pericardium fixed with a naturally occurring crosslinking agent. Journal of Biomedical Materials Research, 1999. **47**: p. 116-126.

51. Sung, H.-W., et al., Feasibility study of a natural crosslinking reagent for biological tissue fixation. Journal of Biomedical Materials Research, 1998. **42**: p. 560-567.

52. Sung, H.-W., et al., Stability of a biological tissue fixed with a naturally occurring crosslinking agent (genipin). Journal of Biomedical Materials Research, 2001. **55**: p. 538-546.

53. Sung, H.-W., et al., In vitro surface characterization of a biological patch fixed with a naturally occurring crosslinking agent. Biomaterials, 2000. **21**: p. 1353-1362.

54. Tsai, C.-C., et al., In vitro evaluation of the genotoxcity of a naturally occurring crosslinking agent (genipin) for biologic tissue fixation. Journal of Biomedical Materials Research, 2000. **52**: p. 58-65.

55. Liang, H.-C., et al., Effects of crosslinking degree of an acellular biological tissue on its tissue regeneration pattern. Biomaterials, 2004. **25**: p. 3541-3552.

56. Lai, P.-H., et al., Peritoneal regeneration induced by an acellular bovine pericardial patch in the repair of abdominal wall defects. Journal of Surgical Research, 2005. **127**: p. 85-92.

57. Chang, Y., et al., Reconstruction of the right ventricular outflow tract with a bovine jugular vein graft fixed with a naturally occurring crosslinking agent (genipin) in a canine model. The Journal of Thoracic and Cardiovascular Surgery, 2001. **122**: p. 1208-1218.

58. Liu, B.-S., et al., In vitro evaluation of degradation and cytotoxicity of a novel composite as a bone substitute. Journal of Biomedical Materials Research, 2003. **67A**: p. 1163-1169.

59. Sung, H.-W., et al., In vitro evaluation of cytotoxicity of a naturally occurring crosslinking reagent for biological tissue fixation. Journal of Biomaterials Science Polymer Edition, 1999. **10**(1): p. 63-78.

60. DeFail, A., et al., Controlled release of bioactiveTGF-B_1 from microspheres embedded within biodegradable hydrogels. Biomaterials, 2006. **27**: p. 1579-1585.

61. Moffat, K. and K. Marra, Biodegradable poly (ethylene glycol) hydrogels crosslinked with genipin for tissue engineering applications. Journal of Biomedical Materials Research Part B: Applied Biomaterials, 2004. **71B**: p. 181-187.

62. Mi, F.-L., et al., In vitro evaluation of a chitosan membrane crosslinked with genipin. Journal of Biomaterials Science Polymer Edition, 2001. **12**(8): p. 835-850.

63. Mi, F.-L., et al., In vivo biocompatibility and degradability of a novel injectable chitosan based implant. Biomaterials, 2002. **23**: p. 181-191.

64. Mi, F.-L., H.-W. Sung, and S.-S. Shyu, Synthesis and characterization of a novel chitosan based network prepared using naturally occurring crosslinker. Journal of Polymer Science: Part A: Polymer Chemistry, 2000. **38**: p. 2804-2814.

65. Jin, J., M. Song, and D. Hourston, Novel chitosan based films crosslinked by genipin with improved physical properties. Biomacromolecules, 2004. **5**: p. 162-168.

66. Khurma, J., D. Rohindra, and A. Nand, Synthesis and properties of hydrogels based on chitosan and poly (vinyl alcohol) crosslinked by genipin. Journal of Macromolecular Science Part A: Pure and Applied Chemistry, 2005. **43**: p. 749-758.

67. Khurma, J., D. Rohindra, and A. Nand, Swelling and thermal characteristics of genipin crosslinked chitosan and poly (vinyl pyrrolidone) hydrogels. Polymer Bulletin, 2005. **54**: p. 195-204.

68. Mi, F.-L., et al., pH-sensitive behavior of two component hydrogels composed of N,O-carboxymethyl chitosan and alginate. Journal of Biomaterials Science Polymer Edition, 2005. **16**(11): p. 1333-1345.

69. Chen, S.-C., et al., A novel pH-sensitive hydrogel composed of N,O-carboxymethyl chitosan and alginate crosslinked by genipin for protein drug delivery. Journal of Controlled Release, 2004. **96**: p. 285-300.

70. Fujikawa, S., T. Yokota, and K. Koga, Immobilized of B-glucosodase in calcium alginate gel using genipin as a new type of crosslinking reagent of natural origin. Applied Microbiology and Biotechnology, 1988. **28**: p. 440-441.

71. Bigi, A., et al., Stabilization of gelatin films by crosslinking with genipin. Biomaterials, 2002. **23**: p. 4827-4832.

72. Chen, H., et al., Reaction of chitosan with genipin and its fluorogenic attributes for potential microcapsule membrane characterization. Journal of Biomedical Materials Research, 2005. **75A**: p. 917-927.

73. Yao, C.-H., et al., Preparation of networks of gelatin and genipin as degradable biomaterials. Materials Chemistry and Physics, 2004. **83**: p. 204-208.

74. Sung, H.-W., et al., Evaluation of gelatin hydrogel crosslinked with various crosslinking agents as bioadhesives: in vitro study. Journal of Biomedical Materials Research, 1999. **46**: p. 520-530.

75. Nickerson, M., et al., Some physical and microstructural properties of genipin crosslinked gelatin maltodextrin hydrogels. Biological Macromolecules, 2006. **38**: p. 40-44.

76. Liang, H.-C., et al., Genipin-crosslinked gelatin microspheres as a drug carrier for intramuscular administration: in vitro and in vivo studies. Journal of Biomedical Materials Research, 2003. **65A**: p. 271-282.

77. Chang, W.-H., et al., A genipin crosslinked gelatin membrane as wound dressing material: in vitro and in vivo studies. Journal of Biomaterials Science Polymer Edition, 2003. **14**(5): p. 481-495.

78. Butler, M., Y.-F. Ng, and P. Pudney, Mechanism and kinetics of the crosslinking reaction between biopolymers containing primary amine groups and genipin. Journal of Polymer Science: Part A: Polymer Chemistry, 2003. **41**: p. 3941-3953.

79. Mi, F.-L., S.-S. Shyu, and C.-K. Peng, Characterization of ring opening polymerization of genipin and pH-dependent cross-linking reactions between chitosan and genipin. Journal of Polymer Science: Part A: Polymer Chemistry, 2005. **43**: p. 1985-2000.

80. Fischer, D., M.T. Knobf, and H. Durvage, The chemotherapy handbook. 5th ed. 1997, St. Louis: Mosby-Year Book.

81. Kelland, L. and N. Farrell, Platinum-Based Drugs in Cancer Therapy. Cancer Drug Discovery and Development, ed. B. Teicher. 2000, Totowa: Humana Press.

82. Li, C., et al., Formation and characterization of cisplatin-loaded poly(benzyl l-glutamate) microspheres for chemoemobolization. Pharmaceutical Research, 1994. **11**(12): p. 1792-1799.

83. Nishioka, Y., et al., Preparation and release characteristics of cisplatin albumin microspheres containing chitin and treated with chitosan. Chemical &Pharmaceutical Bulletin, 1989. **37**(11): p. 3074-3077.

84. Nishioka, Y., et al., Preparation and evaluation of albumin microspheres and microcapsules containing cisplatin. Chemical &Pharmaceutical Bulletin, 1989. **37**(5): p. 1399-1400.

85. Wang, Y.M., et al., Optimization of the formulation design of chitosan microspheres containing cisplatin. Journal of Pharmaceutical Sciences, 1996. **85**(11): p. 1204-1210.

86. Akbuga, J. and N. Bergisadi, Effect of formulation variables on cisplatin loaded chitosan microsphere properties. Journal of Microencapsulation, 1999. **16**(6): p. 697-703.

87. Matsumoto, A., et al., The polymer-alloys method as a new preparation method of biodegradable microspheres: principle and application to cisplatin-loaded microspheres. Journal of Controlled Release, 1997. **48**: p. 19-27.

88. Huo, D., et al., Studies on the poly(lactic-co-glycolic) acid microspheres of cisplatin for lung-targeting. International Journal of Pharmaceutics, 2005. **289**(63-67).

89. Workman, P. and M.A. Graham, Pharmacokinetics and Cancer Chemotherapy. Cancer Surveys, ed. E. Sidebottom. Vol. 17. 1993, Plainview: Cold Spring Harbor Laboratory Press.

90. Salgueiro, A., et al., Cyclophosphamide-loaded nanospheres: analysis of the matrix structure by thermal and spectroscopic methods. Journal of Microencapsulation, 2002. **19**(3): p. 305-310.

91. Vural, I., et al., Cyclophosphamide loaded albumin microspheres III. Intra-articular delivery and retention in knee joints of rabits. Drug Targeting and Delivery, 1992. **1**: p. 263-268.

92. Vural, I., et al., Cyclophosphamide loaded albumin microspheres II. Release characteristics. Journal of Microencapsulation, 1990. **7**(4): p. 511-516.

93. Vural, I., et al., Cyclophosphamide loaded albumin microspheres: Liver entrapment and fate in mice. Drug Development and Industrial Pharmacy, 1990. **16**(11): p. 1781-1789.

94. Arshady R., Albumin microspheres and microcapsules: methodology of manufacturing techniques. Journal of Controlled Release, 1990. **14**: p. 111-131.

95. Gupta P.K. Hung C.T., Albumin microspheres I: physico-chemical characteristics. Journal of Microencapsulation, 1989. **6**(4): p. 427-462.

96. Longo W. Iwata H. Lindheimer T. Goldberg E., Preparation of hydrophilic albumin microspheres using polymeric dispersing agent. Journal of Pharmaceutical Science, 1982. **71**(12): p. 1323-1328.

97. Gallo J.M. Hung C.T. Perrier D.G., Analysis of albumin microsphere preparation. International Journal of Pharmaceutics, 1984. **22**: p. 63-74.

98. Bahukudumbi P. Carson K.H. Rice-Ficht A. Andrews M., On the diameter and size distribution of bovine serum albumin (BSA) based microspheres. Journal of Microencapsulation, 2004. **21**(7): p. 787-803.

99. Hamley I, 3.13 Emulsions, in Introduction to soft matter. 2000, John Wiley & Sons: Chichester. p. 170-179.

100. Groenweg F. van Dieren F. Agterof W.G.M., Droplet break-up in a stirred water-in-oil emulsion in the presence of emulsifiers. Colloids and Surfaces A: Physicochemical and Engineering Aspects, 1994. **91**: p. 207-214.

101. Tjaberinga W. Boon A. Chesters A., Model experiments and numerical simulations on emulsification under turbulent conditions. Chemical Engineering Science, 1993. **48**(2): p. 285-293.

102. Hinze J.O., Fundamentals of the hydrodynamic mechanism of splitting in dispersion processes. American Institute of Chemical Engineers Journal, 1955. **1**(3): p. 289-295.

103. Shimizu K. Minekawa K. Hirose T. Kawase., Drop breakage in stirred tanks with Newtonian and non-Newtonian fluid systems. Chemical Engineering Journal, 1999. **72**: p. 117-124.

104. Zhou G. Kresta S., Correlation of mean drop size and minimum drop size with the turbulence energy dissipation and the flow in an agitated tank. Chemical Engineering Science, 1998. **53**(11): p. 2063-2079.

105. Ishizaka T. Endo K. Koishi M., Preparation of egg albumin microcapsules and microspheres. Journal of Pharmaceutical Science, 1981. **70**(4): p. 358-363.

106. Willmott N. Cummings J. Stuart J. Florence A., Adriamycin-loaded albumin microspheres: preparation, in vivo distribution and release in the rat. Biopharmaceutics & Drug Disposition, 1985. **6**: p. 91-104.

107. Young-Sook, P.C.-M., Lee; Man-Ho Cho and Tae-Ryong Hahn, Physical Stablity of the Blue Pigments Formed from Geniposide of Gardenia Fruits: Effects of pH, temperature and light. Journal of Agricultural Food Chemistry, 2001(49): p. 430-432.

108. El-Mahdy M., I.E.-S., Safwat S., El-Sayed A., Ohshima H., Mankino K., Muramatsu N., and Kondo T., Effects of preparation conditions on the monodispersity of albumin microspheres. Journal of Microencapsulation, 1998. **15**(5): p. 661-673.

109. Luftensteiner C. Viernstein H., Statistical experimental design based studies on placebo and mitoxantrone-loaded albumin microspheres. International Journal of Pharmaceutics, 1998. **171**: p. 87-99.

110. Bertram, J., CRL-1642 Product Description. 2007, ATCC The Global Bioresource Center.

111. Zieske, P., et al., Chracterization of cisplatin degradation as affected by pH and light. American Journal of Hospital Pharmacists, 1991. **48**: p. 1500-1506.

112. McDonald, M. and K. Watkin, Small particulate gadolinium oxide and gadolinium oxide albumin microspheres as multimodal contrast and therapeutic agents. Investigative Radiology, 2003. **38**: p. 305-310.

BIOGRAPHICAL SKETCH

Shema Taian Freeman was born on February 1979. She was raised in Orange Park, Florida, a suburb of Jacksonville. In 1997 she graduated in the top 10% of her class at Orange Park High School. After graduation Shema enrolled at the University of Florida and participated in the STEP-UP Program, a program run College of Engineering Office of Student Affairs, aimed at increasing minority student retention rates. She would continue to be actively involved in the program serving as a mentor and tutor for two years. Throughout her undergraduate career she participated in research programs at the Particle Engineering Research Center and conducted her senior research under the advisement of Dr. Eugene Goldberg. After graduating in 2001 she continued her work with Dr. Goldberg as a PhD student researching protein mesosphere formulations for localized intratumoral chemotherapy. In 2005, while continuing PhD studies Shema received a Master of Science degree in management through the University of Florida, Warrington School of Business. She received her Doctor of Philosophy degree in materials science and engineering in May 2008. Shema served in a wide variety of student leadership roles including vice president of the Society of Biomaterials Student Chapter, vice chairman of the Student Senate Budget and Appropriations committee and president of the Benton Engineering Council. Service to both the College of Engineering and the University of Florida was rewarded through memberships in Epsilon Lambda Chi and Florida Blue Key, the college's and university's most prestigious leadership honorary societies.